RELATIONS OF THE FACTORS IN SPRAY DRYING

RELATIONS OF THE FACTORS IN SPRAY DRYING

A

THESIS

BY

FRED H. KNELMAN B.A.Sc.

CHEMICAL ENGINEERING LABORATORIES - McGILL UNIVERSITY

Under Supervision of Dr. Wm. Gauvin

Submitted to the Faculty of Graduate studies

and Research of McGill University in partial

fulfillment of the requirements for the degree

of Master of Engineering

McGill University

Montreal, Canada

April 21, 1950

ACKNOWLEDGEMENTS

The author wishes to express his thanks to all those who, in various ways, have contributed to this work.

To members of the Chemical Engineering Department for their willing contribution.

To Mr. D. R. Abbey, for his generous assistance with the particle size determinations, and spray dryer operation.

To McGill University, without whose financial support this project would not have been possible.

TABLE OF CONTENTS

Table of Contents (cont'd.)

Table of Contents (cont'd.)

LIST OF TABLES

List of Tables (cont'd.)

List of Illustrations (cont'd.)

M. ENG. CHEMICAL ENGINEERING

ABSTRACT

F. H. KNELMAN

"RELATIONS OF THE FACTORS IN SPRAY DRYING"

The effects on the capacity and thermal efficiency of spray drying equipment resulting from variations in rate of inlet air, inlet air temperature, feed temperature, nozzle location and degree of atomization, were investigated in a down-flow, vertical spray drying chamber, 6 feet high and 4 feet in internal diameter. A two-fluid atomizing nozzle was used. The results obtained during the evaporation of water alone were compared with the drying of an actual solution under similar operating conditions. Results showed that capacity and efficiency passed through a sharp maximum at optimum values of the operating conditions and that the latter had pronounced effects on the physical properties and particle size distribution of the dried material. The effects observed can be explained in the light of the fundamental principles of drying and mass transfer in turbulent gas streams.

HISTORICAL REVIEW

INTRODUCTION

The purpose of this historical review is essentially to record and interpret the results of experimental investigations into the operation of spray dryers.

It is no easy task to present a clear, comprehensive and well-organized discussion of the published data because of the number and complex inter-relationships of the variables involved, especially since these relationships have not proven amenable to any general mathematical formulation. As a rule, each investigation has been restricted to the study of one or two variables over a comparatively narrow range of experimental conditions, and as a result, many of the published papers are restricted in scope and frequently conflicting. This scarcity of fundamental data and lack of uniformity of presentation makes a comparative study of the experimental evidence very difficult

It has been one of the tasks of this research project to present new relationships for efficiency and performance which will make such comparative studies possible.

In a broader sense, however, it must be recognized that spray drying is a complex unit operation involving problems in mass transfer, heat transfer and fluid flow. Investigations have so far been restricted mainly to the first of these fields and, as a result, a complete understanding of their inter-relationships has not been attained. In recent years, however, it has become increasingly clear that the three processes

are intimately related, and that a sound knowledge of turbulence and flow conditions near phase boundaries may be expected ultimately to provide a firm basis for the development of a theory of spray drying as a single subject involving simultaneous transfer of momentum, heat and material. An attempt, therefore, has been made to present all relevant material necessary to provide a unifying approach to this problem.

SPRAY DRYING AS A COMPLEX UNIT OPERATION

DEFINITION

Spray Drying is the drying of a sprayed solution or slurry in contact with a stream of hot gases under conditions permitting the recovery of the dried product. Most drying processes producing finely divided materials usually employ three separate operations, namely: bulk evaporation, drying, and grinding. In spray drying, however, we have a direct conversion of the sprayed liquor into a powdered product immediately suitable for packaging without further handling or grinding.

Spray drying should be distinguished from two other somewhat similar operations: Flash Drying and Spray Cooling or Crystallization. Flash Drying as defined by Gordon (65) is the practically instantaneous removal of moisture from solid materials by the application of heat in a turbulent stream of hot air. This operation may or may not be accompanied by simultaneous disintegration or grinding of the material. Spray Cooling or Crystallization involves the atomization of a hot concentrated solution into a cold medium to produce tiny crystals.

Spray drying is characterized by extremely high drying rates, which render it particularly adaptable to the drying of heat-sensitive materials. High drying rates are made possible by the intimate and direct contact between the spray droplets and the drying medium, as well as by the high specific surface of the sprayed material. As long as the moisture content is above the equilibrium value, the temperature of the

material will not rise appreciably above the wet-bulb temperature, regardless of the dry bulb of the drying medium. Of course, prolonged contact of the dried material with the drying medium will cause its temperature to approach that of the medium, but sound design of the unit should provide for immediate separation of the product.

The spray drying operation may be considered as composed of three entirely distinct component parts: atomization of the liquid to be dried into finely dispersed droplets; drying of these droplets in contact with the drying medium; collection of the product which involves its separation from the drying medium in which it is being conveyed.

I ATOMIZATION

(i) Historical Development

In the early history of spray drying, the question of the atomization of the liquid feed posed a difficult problem (135). The existing designs of spray nozzles were not adequate since they provided neither uniform nor sufficient atomization. Out of the needs of spray drying operations, new designs of atomizers and nozzles were developed.

The earliest type of spray nozzles consisted essentially of a disk of hard metal containing a minute orifice through which the liquid was forced at pressures of 2000 psi. This type of nozzle was open to many objections, most important of which was the nature of the spray pattern. As the jet left the nozzle in a solid cone, penetration by the drying gases was made very difficult, thus preventing intimate contact between the two phases. Besides this, the small disk aperture was liable to obstruction and variation in size, making spraying intermit-

tent and non-uniform. All this led to the development of special nozzles involving new principles of atomization.

(ii) General Principles

In all types of nozzles, a film or filament of liquid emerging from the nozzle, is broken up into micro-fragments due to the difference in velocity between the liquid and the surrounding medium. The energy of formation of the spray must obviously be supplied by the spray mechanism. This energy is composed mainly of three parts (88):

(a) Energy required for surface formation, which is simply the product of the surface tension and the total area developed by the spray. This energy can be easily calculated knowing the average drop size in the atomized spray, and the physical properties of the liquid. Thus, Edeling (44) has calculated that, for an average drop size of 150 microns, the total surface developed in a spray cloud of water will be 63 square meters per litre. The energy of formation will, therefore, amount to only 4.6 joules or slightly over one calorie per litre. It is evident that finer sprays will require a higher energy output, but the total energy requirements are quite small.

(b) Considerably greater in magnitude but much more difficult to assess is the energy required to deform the liquid prior to droplet formation. Since the time during which droplet formation usually takes place is of the order of a few micro-seconds, the rate of deformation is very high and the viscous forces required become very large.

(c) Finally, there is a loss of energy due to nozzle inefficiency. This last factor will obviously depend on the nozzle design.

(iii) Types of Nozzles

Fogler and Kleinschmidt, in an extensive study of atomizing nozzles (57), have adopted a classification based on the fundamental nature of spray formation. They distinguish two main types, depending on whether thin flat sheets or films are initially formed, or whether the jet issues from the nozzle in the form of filaments or threads. Both forms are unstable and under the common action of a number of factors such as surface tension, viscosity, impact, etc., break up into a mist of fine droplets. These authors further subdivide the film or sheet forming nozzles into four main types. Three of these are pressure nozzles, in which the energy for atomization is applied directly to the liquid through pressure, while the fourth is the rotating disk or centrifugal nozzle, which was designed specially to meet the needs of spray drying operations (135). Of the three pressure types, the first contains a whirl chamber through which the liquid is fed under pressures up to 2500 psi. and emerges in the form of a thin hollow conical sheet which then breaks up into drops; the other two may be designated as impact nozzles, one being an impinging nozzle and the other a double jet nozzle. In the former a jet of fluid under pressure is made to strike a fixed surface while in the latter the jet of fluid strikes a second jet. This latter type is used in the Milkal plant. From these two latter types, it is possible to obtain hollow cone, fan or disk-shaped fluid sheets (80). In the centrifugal nozzle, a sheet of fluid is thrown from the rapidly revolving edge of a spinning cup or disk. Speeds above 3600 and up to 20,000 R.P.M. are used. Rotating nozzles are among the most popular and are used in the Kestner, Krause, Ravo-

Rapid and Peebles drying plants (130). All these atomizers are capable, under certain conditions, of producing hollow spherical droplets.

The second main class of nozzles, which depends on the initial formation of thin filaments or threads, comprises one type only, the gas-atomizing or two-fluid nozzle. The liquid is torn into this jet pattern by impingement with a high velocity jet of compressed air, steam or other gases. The impingement may take place internally or externally. The Dickerson tower type spray dryer (57) and all Bowen equipment use this type of nozzle.

A simpler and more common classification of spray nozzles is based upon the mechanical device responsible for atomization, rather than on the physical principle of spray formation. According to this division, there are three types of nozzles: Pressure Nozzles, Centrifugal Nozzles, and Gas-Atomizing and Two-Fluid Nozzles, all of which have already been described.

(iv) Materials Handled

Fogler and Kleinschmidt have supplied data indicating that the energy imparted to a pound of liquid by pressure alone is small compared to the energy available in a high velocity jet of compressed air or steam (57). Thus, the use of pressure nozzles is limited to materials of relatively high fluidity which may be easily broken up, i.e. to solutions of low viscosity and finely divided colloids. On the other hand, the gas-atomizing nozzle can spray almost any fluid that can be pumped. Rotating nozzles are also useful for spraying viscous liquids and slurries.

(v) Drop Size and Size Distribution

In the field of spray drying, the question of drop size and size distribution in the atomized liquid is one of tremendous importance.

Both the size of the dried particle and the rate of drying are largely dependent upon these two factors. Generally, drop size and size distribution are a function of the amount of energy which is imparted to the fluid. This, in turn, will depend on the type of nozzles and on the physical properties of the liquid.

The gas-atomizing nozzle gives the finest atomization of any of the spray drying nozzles. According to Fogler and Kleinschmidt, however, these nozzles exhibit a marked tendency towards non-uniform particle formation, resulting from continually varying atomization conditions (57). These authors maintain that high frequency vibrations due to the rush of air from such nozzles tend to liberate dissolved gases in the form of fine bubbles distributed throughout the material. There is also evidence of pulsations which are noticeable on an ordinary pressure gauge, which again leads to non-uniform spraying action. Furthermore, there is a large reduction in the temperature of the drops emerging from such nozzles which may be estimated by the well-known equation for isentropic flow of an ideal gas:

$$T_2 = T_1 \left(\frac{P_2}{P_1}\right)^{\frac{k-1}{k}} \qquad (1)$$

It must be remembered, however, that for nozzles of this type, P_2 cannot be less than the critical pressure, i.e. .53 P_1 for air and .58 P_1 for steam. Values for the temperature of air or steam following expansion have been tabulated (57).

The views of Fogler and Kleinschmidt regarding the lack of uniformity of drop size distribution from gas-atomizing nozzles are not supported by theoretical considerations or by the experimental evidence given by Houghton, in which he clearly shows that a narrower

distribution is obtained for a two-fluid nozzle than for a pressure atomizer of the same capacity (80).

Nukiyama and Tanasawa (120, 121, 122, 123, 124) have developed empirical equations for average drop size and size distribution from small two-fluid nozzles, which, although not even dimensionally consistent, appear nevertheless to fit the published experimental data with reasonable accuracy. The first of these equations gives the average drop diameter in terms of the operating variables, as follows:

$$D_o = \frac{585\sqrt{\sigma}}{v\sqrt{\rho}} + 597\left(\frac{\mu}{\sqrt{\sigma\rho}}\right)^{0.45}\left(\frac{1000\,Q_l}{Q_a}\right)^{1.5} \qquad (2)$$

where D_o = diameter of a single drop with the same ratio of surface to volume as the total sum of drops in microns

v = relative velocity between the air stream and the liquid stream, metres/sec.

Q_l/Q_a = ratio of volume flow rate of liquid to volume flow rate of air at the 'vena contracta'

ρ = liquid density, gm./cc.

μ = liquid viscosity, poises

σ = liquid surface tension, dynes/cm.

v_a, the absolute velocity of the air at the throat, may be calculated from the well-established equation for the isentropic flow of an ideal gas:

$$v_a = \sqrt{\frac{2gkP_1v_1}{k-1}\left[1-\left(\frac{P_2}{P_1}\right)^{\frac{k-1}{k}}\right]} \qquad (3)$$

where g = the acceleration of gravity, ft./sec./sec.

k = ratio of specific heats $\frac{c_p}{c_v}$

P_1 = inlet absolute pressure, lb/sq.ft.

v_1 = specific volume at inlet, cu.ft./lb.

P_2 = absolute pressure at the throat, lb./sq.ft.

A further equation by the above authors expresses the data on distribution of drop sizes in liquid sprays, as follows:

$$\frac{dn}{dx} = ax^p e^{-bx^q} \qquad (4)$$

where x = diameter of an individual drop, microns

n = number of drops with diameters between zero and x in the total sample

a, b, q, p = constants

Nukiyama and Tanasawa found that the value of p was always 2 in the cases they studied. The value of q in most cases must be determined experimentally (101). Taking p as 2, and knowing the value of q, analysis of experimental data on liquid atomization is easily made by converting equation (4) into a log form:

$$\log_{10}\left(\frac{1}{x^2}\frac{dn}{dx}\right) = \log_{10} a - \frac{bx^q}{2.3} \qquad (5)$$

A plot of $\log_{10}\left(\frac{1}{x^2}\frac{dn}{dx}\right)$ against x^q should yield a straight line with slope equal to $\frac{b}{2.3}$. D_o can then be calculated by the use of tables which have been published (101).

The validity of equations (2), (4) and (5) has been extensively tested by L. W. Smith and co-workers, who have successfully applied them to the results of Sauter (141), Houghton (80) and Lee (97), and to experimental work of their own (101), and have thus definitely proved their usefulness.

It is interesting to note that equation (2) establishes that a definite minimum value for average droplet size is dictated by the critical velocity at the throat of the nozzle, corresponding to the speed of sound. Since under these conditions the value of the $\frac{Q_a}{Q_l}$ ratio is very large for low liquid rates, the second term in equation (2) becomes negligible, and v, in the denominator of the first term approximates 336 meters per second. Thus, for water, D_o would be equal to 15 microns, under normal conditions. Sauter has experimentally confirmed that as the relative velocity between the liquid and the air increases, the average drop diameter decreases until a constant diameter is approached (140). Micrographic studies have definitely established that as the relative velocity increases, more and more droplets of the minimum size are formed (120, 121). Finally, Edeling in a very interesting paper, (44) has determined, purely from theoretical considerations, the relation between the factors which influence the drop size and size distribution for two-fluid nozzles, which fully agree with the above discussion.

In considering the practical applications of equation (2), it must be noted that D_o is an average diameter and does not represent the minimum droplet diameter that will be formed in a spray, nor is it associated with the degree of uniformity of drop sizes. However, the existence of such a minimum drop diameter has been clearly established by Edeling and Sauter. The latter author (142) experimentally determined the minimum water drop size from a gas-atomizing nozzle to be 6 microns.

Information regarding the degree of uniformity of drop size

is given by the value of the constant "q" in equation (4). If the mass distribution of the drops is concentrated within a relatively narrow range of drop sizes, the value of q is high. On the other hand, low values of q represent a wide variation in drop sizes.

A further implication of the above considerations suggests that, beyond a certain optimum value of the relative velocity of the two fluids, all additional power expenditures for atomization are simply wasted (141).

It should be recognized that the accuracy of the expressions discussed in the preceding pages is definitely limited by a number of complicating factors, the effects of which are difficult to assess; heat transfer between the two fluids in the nozzle, possible evaporation of the liquid in the nozzle chambers, difficulty of estimating the physical properties of the two fluids under the conditions prevailing at the throat or at the vena contracta, all contribute to the complexity of the fundamental mechanisms.

The previous discussion of drop size and size distribution applies strictly to two-fluid atomizing nozzles. Considerably less work has been published on pressure and centrifugal nozzles. It is well established, however, that these two types of nozzles give similar drop size distributions, and are, as a matter of fact, quite similar as far as the mechanism of spray formation is concerned. It has been proposed that for pressure nozzles the average drop size should be inversely proportional to the density and to the square root of the pressure and surface tension, and directly proportional to the square root of the viscosity (80). More recently, however,

Smith and co-workers (101) have successfully modified the Nukiyama and Tanasawa equations to apply to pressure nozzles as well. Extension of this equation has not been made to apply to centrifugal nozzles. For the latter it is known that high rotational speeds, low viscosity and low discharge rates tend to reduce particle size (80). Very recent articles furnish information of a theoretical nature regarding drop size distribution in these nozzles (77, 152). In closing this discussion it might be useful to indicate the range of average drop diameters met in actual installations; for two-fluid nozzles, a range of 'D_o' from 15 to 70 microns is most frequently reported. Pressure and centrifugal nozzles give larger values ranging from 50 to 300 microns (88, 101).

(vi) Relative Performance

The centrifugal nozzle is the most expensive. Power costs to operate a nozzle rotating at speeds above 3600 R.P.M. are high. On the other hand, replacement and shut-down due to clogging are infrequent. However, a heavy coating on the rotary disk will unbalance it and cause non-uniform operation. Two-fluid nozzles cost little to operate and, with proper handling, clogging and replacement are infrequent. Operating costs of pressure nozzles are intermediate but they plug easily and require frequent replacement. Besides this, they have relatively lower capacities than both centrifugal and gas-atomizing nozzles.

II DRYING AND THE SPRAY CHAMBER PROCESSES

Spray Drying differs from other forms of drying in one respect only: the atomized condition of the feed. However, this dif-

ference is so unique and far-reaching that it completely dominates virtually every aspect of this operation: heat and mass transfer rates, size of equipment, design of collector, physical properties of product, etc. To the traditional problems of heat and mass transfer commonly met in the older methods of drying, atomization of the feed now adds an even more difficult one: the problem of flow conditions and turbulence, and its effect on inter-phase transfer.

In its overall aspect, spray drying is clearly a crystallization process. As such, it will involve both evaporation in the initial stages, followed by drying when the water content of the solid formed upon crystallization becomes sufficiently low. But no sharp distinction is made between these two stages, nor is one needed, since the rate of evaporation from a wholly wet solid does not depend on its water content, and is, in fact, the same as that from a free liquid surface. It should be pointed out here that this statement is strictly true only if a colloidal solution or suspension is being evaporated. It is not strictly applicable for true solutions, because as the concentrations of the latter increase, the partial pressure of the water at the temperature of the droplet will decrease, thus decreasing the driving force of the evaporation process and hence its rate. This in turn affects both heat and mass transfer and greatly complicates the problem. However, since the majority of spray drying applications deal with suspensions and colloidal solutions, this added complexity will not be considered in the following treatment, and the vapor pressure of the droplet or of the wet solid will be considered as that of pure water at that temperature. The reservation that this vapor pressure will be

less when dealing with soluble materials must always be kept in mind.

Although it is not feasible at the present time to develop a mathematical treatment from an analysis of the behaviour of a single droplet, such an analysis, nevertheless, throws considerable light on the complex processes taking place in a spray chamber.

(i) Droplet Path

Droplets emerging from nozzles possess very high initial relative velocities, of the order of several hundred feet per second. The emerging velocity is slightly smaller for two-fluid nozzles than for the other types, but increases to a maximum at a distance of approximately 6 inches from the mouth of the nozzle. For all three types of nozzles, this initial velocity rapidly decreases and is no longer measurable for particles 100 microns in diameter, approximately 0.03 second following emergence, and after a travel of about 2 feet (44). Smaller droplets will travel even shorter distances, while large particles of the order of 300 microns may cover as much as 6 feet in approximately 0.1 second (44). D. A. Smith (145) takes a travel of 12 inches from the nozzle as a fair average value of the distance covered by the droplet in commercial installations, corresponding to a flight of approximately 0.01 second. The bulk motion of the drying gases in the chamber has no effect on the path of the spray until its initial velocity is practically spent, and Edeling believes that no significant evaporation can possibly take place during so brief a period. When the terminal velocity is reached, the droplet now falls under the influence of the gas stream, which, in practically all spray drying installations, follows a circular path, with maximum tangential velocity of from 4 to 20 feet per second near the

walls, steadily decreasing in value as it nears the vertical axis of the chamber. The velocity of the gas stream right at the walls is, of course, zero. The laws of particle motion, which would permit calculation of the droplet velocity and of its path, are unfortunately not strictly applicable, owing principally to turbulence and the presence of eddy currents, and to the fact that the diameter of the droplet continually changes with time. In its simplest aspects, the system of forces influencing the motion of the particle may be reduced to three: the gravitational force, due to its own weight, the frictional force applied by the bulk motion of the gases, and directly responsible for the tangential velocity of the droplet in its circular path, and the centrifugal force which tends to pull it towards the wall. The magnitude of these three forces can be calculated from the well-known equations:

$$\text{gravitational force:} \quad F_g = \pi g D^3(\rho_s - \rho)/6 \tag{6}$$

$$\text{frictional force:} \quad F_f = \pi C u^2 D^2/8 \tag{7}$$

$$\text{centrifugal force:} \quad F_c = \pi D^3(\rho_s - \rho)u^2/6r \tag{8}$$

where:

D = droplet diameter, cm.

ρ_s = actual droplet density, gm/cu.cm.

ρ = gas density, gm./cu.cm.

C = dimensionless drag coefficient, function of Re

u = relative tangential velocity between droplet and gas stream, cm./sec.

r = radius of curvature, cm.

The capacity of a given chamber is mainly determined by the requirement that no droplet or partially wet particle shall hit the

walls to any appreciable extent under continuous operating conditions. Analysed in the light of the above equations, this undesirable behaviour will develop principally under the following circumstances: a) a large droplet in the spray will hit the wall before it has reached its terminal velocity; b) a large droplet, torn away from its normal trajectory in the spray under the influence of eddies in the gas stream, while still possessing a high velocity, will briefly assume a short radius path which will impose a high centrifugal separation force upon it and cause it to fly to the wall; c) a large droplet, having reached its terminal velocity and assumed a circular path motion in the bulk of the gases, dries at such a slow rate that centrifugal action eventually causes it to hit the wall. It is thus seen that the capacity of the dryer is governed by the time required to dry the largest of the drops formed. If these are well dried, the smaller drops will also be well dried. The capacity of a given dryer will, therefore, be increased if the average droplet diameter is kept small and the size distribution narrow.

Finally, it may be remarked that the diameter of a droplet changes continually as it progresses along its path in the chamber. Whether initially hollow or solid, its diameter will steadily decrease as evaporation proceeds. When the conventional stage of drying has been reached, however, the wet solid particle may now either remain constant in diameter, expand or shrink, depending on the drying action.

(ii) Drying

Throughout the evaporation stage and as long as the surface of the solid particle formed remains completely wetted, evaporation or drying proceeds at a constant rate which is limited by the rate of

diffusion of the water vapor through the stagnant air film at the surface. At steady state, the surface temperature of the particle assumes the wet bulb temperature of the gas. This constant-rate period is then followed by the falling-rate period, where the diffusion of the vapor through the air film is no longer controlling. D. A. Smith believes that the "unsaturated surface" stage from a partially wetted surface, which, in normal drying processes, usually precedes the "internal diffusion" stage during the falling-rate period, does not apply to spray-drying (145). However, the existence of the internal diffusion period is proven by the formation of punctured or fragmented hollow spheres, so commonly found in micrographic studies of spray dried materials. This phenomenon can be explained if the mechanism of evaporation responsible for the internal diffusion period is reviewed. The rate of diffusion of water to the surface having decreased to the point where it now controls the rate of evaporation, the latter presently takes place from a continually receding spherical surface. With a great many substances, the dried surface layer becomes relatively impervious to the diffusion of the vapors formed. Since the conduction of heat through a solid is relatively high, the rate of heat input to the droplet increases, causing expansion of the trapped air if the droplet was originally hollow, or generation of steam within solid particles. This results first in expansion of the particle if some plasticity is left, and more generally in disruption and bursting of the particle (57). Instead of expanding, dried particles may often exhibit marked shrinkage effects, or surface checking, which will also develop during the internal diffusion period.

Although of paramount importance for design purposes, data on actual drying times are very meager. Authors do not seem to agree, and the values reported for the overall duration of the process including collection, which give little information, have been variously reported as from 20 seconds (57) to 45 seconds (69). Edeling is the only author to report actual drying times, ranging from 3.0 seconds for 100-micron to 6.3 seconds for 300-micron particles. Corresponding lengths of path covered during drying were approximately 3 feet and 16 feet, respectively. The material was not specifically named, but contained 80% water initially, and did not shrink upon drying. When shrinking occurred, Edeling reported a 25% increase in both drying times and distance covered (44).

Depending on the quality of the insulation, spray driers will approach more or less adiabatic operation, that is, the relation between decrease in temperature and increase in humidity of the gas medium will follow approximately the adiabatic cooling lines on a humidity chart, and maximum utilization of the heat input will take place when the spent gases leave the chamber saturated, or at the wet bulb temperature.

(iii) Mass and Heat Transfer

The rate of evaporation and of drying during the constant rate period is controlled by the relatively slow process of molecular diffusion across the film surrounding the droplet. It has been common practice to express mass transfer data in such systems in terms of a transfer coefficient K_G, gm.moles/(sec.)(sq.cm.)(atm.), or K_C, gm.moles/(sec.)(sq.cm.)(gm.mole/cu.cm.) where $K_C = K_G RT$. Chilton and Colburn (33) first suggested that data be correlated in terms of the dimensionless group j_D, where:

$$j_D = K_C P_{BM} (\mu/PD_v)^{2/3} \Big/ u_o P = \text{Fcn.}(Re) \qquad (9)$$

where P_{BM} = log mean pressure of inert gas, atmospheres

μ = gas viscosity, poises

P = total pressure, atmospheres

D_v = diffusion coefficient or diffusivity, cm.^{2}/sec.

u_o = average velocity of the gas stream, cm./sec.

Re represents the Reynolds number, and the group in the first bracket is the Schmidt number, Sc. For heat transfer a similar dimensionless group, j_H, has been defined:

$$j_H = h(c\mu/k)^{2/3} \Big/ cu_o\rho \qquad (10)$$

where h = heat transfer coefficient, gm.cal./(sec.)(sq.cm.)(^oC)

c = specific heat of the fluid, gm.cal./(gm.)(^oC)

k = thermal conductivity, gm.cal./(sec.)(sq.cm.)(^oC/cm.)

ρ = gas density, gm./cu.cm.

Maisel and Sherwood (108), in a recent unpublished paper, review the experimental evidence, and point out the remarkable correlation that, for a great many results, $j_H = j_D = f/2$, the last equality applying if the friction factor, f, represents only that portion of total drag due to skin friction at the wall. From experimental investigation, they show further, that for single spheres, the correlation is obtained:

$$j_D = j_H = 0.43\ Re^{-0.44} \qquad (11)$$

Their work was done on spheres 3.48 and 2.55 cm. in diameter, but agreed extremely well with an identical correlation offered by Williams (153) on liquid drops. Correlation with the friction factor, f, could not be made because data for skin friction on spheres were not available.

It is, therefore, strongly indicated that similar correlations must apply to spray-drying, although no attempt to establish them has so far been made. It is possible that some slight modifications will have to be introduced to account for the fact that the relations were developed specifically for constant drying or evaporation rates, and will, therefore, not hold strictly for the comparatively short falling-rate period.

It is interesting to note that the volume of vapor formed upon removal of 1% of the water content of a droplet will be approximately 17 times the volume of the particle. The heat supplied for evaporation causes a rapid cooling of the surrounding gas, and it has been estimated that the 1% of water evaporated will surround the droplet - if suspended in still air - with a layer of cool gases equal to about five times the drop radius. However, the motion of the particle through the gas will provide eddy diffusion of this layer, but a stagnant or laminar film, through which molecular diffusion of the vapor must take place, will still surround the particle. The thickness of the film will decrease, as the relative velocity of the drop with respect to the gas stream increases.

Johnstone and co-workers (84), in treating the heat transfer problem involved in falling cloud particles, have developed the following mathematical relation:

$$h = 0.714\sqrt{Pe} \qquad (12)$$

and Pe = Peclet number $\frac{D_p v \rho_G c}{k}$

where h = the individual coefficient of heat transfer, gm.cal./(hr.)(sq.cm.)(°C)

D_p = diameter of particle, cm.

k = thermal conductivity of the fluid, gm.cal./(hr.)(sq.cm.)(^{o}C/cm.)

c = specific heat of gas, gm.cal./(gm.)(^{o}C)

ρ_G = gas density, gm./cu.cm.

v = particle velocity, in cm./hr.

This relation is similar to the known heat exchange relations for natural gas convection. Edeling (44) supplies a relationship which permits the calculation of 'h' during the free fall of small spherical droplets:

$$h = 0.22W \tag{13}$$

where h = individual coefficient of heat transfer, Kilocalories/(hr.)(sq.m.)(^{o}C)

W = water evaporated, Kg./(hr.)(sq.m.)

This author points out that values of 'h' given in equation (13) are from 4 to 10 times higher than those observed under similar conditions of natural gas convection. Edeling believes that this is explained by the fact that drying proceeds faster from spherical surfaces than from flat surfaces having similar film thicknesses and under similar conditions. Although the high drying rates involved in spray drying are admittedly considerably larger than those observed in other evaporation processes, it is certain that these increased rates are due to the vastly greater area of transfer, and certainly not to larger values of h. The values of h calculated from equation (13) are probably 100 to 1000 times too large. As far as the effect of curvature on vapor pressure and the evaporation rate is concerned, this will not begin to operate until drops less than 10^{-2} microns are encountered.

(iv) Mixing and Turbulence

In the preceding section considerations have been limited to molecular diffusion across the stagnant layer surrounding the droplet. Once the water vapor has diffused through this layer, its transfer across the turbulent gas stream is mainly by eddy diffusion, which is very rapid as compared with molecular diffusion. Maisel and Sherwood (109) have recently suggested that the degree and scale of turbulence in the gas stream might influence the rate of evaporation by affecting the thickness of the stagnant or laminar layer. Their experimental results certainly indicate that an increase in the rate of evaporation (or in the value of K_C defined on page 20) of from 20 to 25% may be obtained when turbulence is induced in the gas flow by means of perforated plates.

In the light of this evidence, it appears that an increase in the value of the relative velocity, or in the degree of turbulence in the gas stream, will cause an effective decrease in the thickness of the laminar layer. While the importance of this effect is sometimes minimized (145), other authors (20) emphasize it to a considerable extent. However, application of these concepts to practical installations involves certain complicating problems: counter-current flow, which at first sight appears highly desirable, however, causes the fully dried product to come in contact with air at a higher temperature with possible damage to heat sensitive materials. A possibility also exists that such dried particles might hit droplets or other partially wet material. Use of additional turbulence in the gas stream must be carefully controlled, as eddy currents might easily direct partially or completely dried particles towards the walls of the chamber.

(v) Chamber Design

The spray drying chamber must accommodate the drying paths of the sprayed material in the turbulent drying medium. The size of a chamber for a given capacity will be determined by the condition that the largest particles issuing from spray nozzles will not hit the walls of the chamber, before being thoroughly dried. Thus, uniformity of particle size becomes a critical factor. The height of the chamber will be determined by the trajectory of the spray and the aerodynamics of particle flow in turbulent air streams (57).

Actually, the greatest variation in design of spray drying chambers depends on the initial relative directions of spray trajectory and drying gases, although a number of other factors contribute to minor differences in design. D. A. Smith has accordingly divided spray drying chambers into five distinct types (145).

(a) Mixed Flow Type

In this type of spray dryer, both concurrent and countercurrent drying occurs. The drying gases initially enter tangentially to the chamber and travel concurrently with the descending spray. They then reverse their direction of flow and ascend the chamber in the center, meeting the spray countercurrently, and are finally exhausted through a duct at the top, while the product is collected at the bottom.

There are certain advantages to this type of dryer, most important of which is the lower outlet temperature and consequent increase in thermal efficiency. This dryer is used extensively in the production of whole and skim milk powder. Early designs are associated with the names of Gray, Jensen, and Douthitt (43, 67, 68), while later designs have been produced by Swenson. Moreover, the chamber acts as a cyclone

separator, and certain authors (69) have used this distinction as a method of classification.

(b) Horizontal Concurrent Type

In this type of dryer the spray and air enter horizontally at one end of a rectangular chamber. This represents an early design and is associated with the names of Merrell-Soule (112, 113, 147) and Fleischer (54).

(c) Vertical Up-Flow Countercurrent Type

The air is admitted at the base of this drying chamber, while the spray enters at the top. Usually the product is collected at the bottom, while the exhaust air leaving the top will contain the fines which may be recovered by some suitable device. This type of chamber is used for spray drying soap and detergents. On the continent it is represented by the Ravo-Rapid design (130).

(d) Vertical Down-Flow Concurrent Type

In this dryer the inlet air enters approximately at right angle to the spray, and both streams flow concurrently down the chamber generally with a swirling motion, imparted by the tangential entrance of the drying medium. The Dickerson tower type of spray dryer, based on the Holliday and Lamont patents (78, 94), and used in the soap powder industry, is of this type. Both air and powder leave at the bottom. The Mojonnier dryer is also representative of this design (69).

(e) Vertical Up-Flow Concurrent Type

Both air and spray enter at the bottom while the powder tends to be classified, the coarser particles falling to the bottom and the fines being carried out with the exhaust gases at the top.

Special Types

The patent literature abounds in various other types of spray dryers, many of which may be distinguished by special methods of powder collection and will be discussed in a later section. However, there are a few dryers whose special designs merit attention. Among these is the Bowen spray dryer (20, 21), in which the air is introduced through long vertical slots into the drying chamber, in such a manner that a "controlled turbulence" results, preventing the accumulation of dried product on the walls of the chamber. Another design is the Peebles (127, 130) used by the Western Precipitation Co. This dryer utilizes two concentric currents of air, both entering the chamber tangentially but revolving in opposite directions. One of the most efficient dryers, used extensively in England, is the Kestner (130). This dryer is itself a cyclone separator and has a very efficient patented system of air distribution and withdrawal. The air stream passes downward into the atomized feed sprayed from a centrifugal nozzle. The Kestner also employs a wet collector, utilizing the heat in the waste flue gases to preheat the liquid feed. It should be noted that the increased efficiency of these newer types allows equal capacity with smaller chambers than older types of dryers.

In general, it is customary to provide the feed lines with steam and water for cleaning prior to shut-down, as well as for fire control. Also, it is common practice to commence and end the operation with water. Nozzles, of course, should be mounted so as to facilitate maintenance and handling, and inspection ports should be provided. Spray chambers are often run under suction in order to avoid loss of powder when inspection ports are opened (57).

III COLLECTION OF THE PRODUCT

The necessity for separating the dried material from the spent gases as quickly as possible should be obvious from previous considerations. Certain drying chambers act themselves as cyclone separators and classifiers (68, 69, 130). But it should be noted that all atomizers produce air-float material which will be invariably carried out with the exhaust gases. Thus, it is always necessary to provide auxiliary collection equipment in all spray drying plants.

In most spray dryers, the bottom of the chamber tapers into exhaust ducts of sufficiently small diameter to impart high conveying velocities to the gas stream. This discharge duct normally leads to cyclone separators, very often followed by auxiliary collection devices like shaking fabric filters, bag collectors, scrubbing towers, electrostatic separators and pre-concentration chambers.

Where the product is relatively cheap and the nuisance situation low, single cyclone separators may be used (57). Their efficiency is limited and newer types of separators have been evolved. The parallel multi-tube design is the most efficient of these. The Sirocco type 'D', the Western Precipitation Company's 'Multicone' and the Aerotec Industrial Collector are all in popular use. Collection efficiencies over 95% for particle sizes over $8\frac{3}{4}$ microns are possible with these units.

The use of fabric filters, especially of the continuous type, is limited, due to the deleterious effect of the hot exhaust gases on the fabric as well as on the collected product. Moreover, the collected powder may be wetted by the moist exhaust gases, impairing the filter permeability and causing increased resistance.

A very popular method of collecting fines which escape in

exhaust gases is to pass them directly to a wet collector either of the scrubber or preconcentration design (57). They are then returned to the dryer with the feed. In this way, there is both heat and product recovery. However, the problem in each case will be an economic balance between the value of heat and product recovery and the increased operating and capital costs of additional recovery equipment.

Certain spray dryers employ special collection methods. In the Rogers dryer (69) the chamber bottom terminates in a hopper with shaking bag filters feeding one or more conveyors which continually remove the powder. The Ravo-Rapid design (130) utilizes a scraping device for removing powder from the walls of the drying chamber. In connection with this, scale problems in spray dryers are discussed by T. K. de Haas (38).

PRACTICAL ASPECTS OF SPRAY DRYING

HEATING OF THE DRYING GAS

The drying gases must be heated by some suitable device to the required entrance temperature which, in practice, ranges from 300° - 1200°F. In general, there are two main classes of heaters used: direct heaters where the products of combustion pass directly into the stream and indirect heaters which will involve the use of some form of heat exchanger.

In direct heaters, either waste flue gases which have been cleaned by one of the available methods (51), or the products of combustion of gas or of clean grades of oil and coal, are mixed directly with air. According to Bowen (20), the best method is a 'carbofax' lined oil furnace while other plants use natural gas (1) and coal-fired furnaces (9).

Exhaust gases from combustion reactions often contain soot, ash and other undesirable by-products of incomplete combustion processes, which may contaminate the spray-dried material. This difficulty may be overcome by filtering or scrubbing the gases or by improved combustion methods. In some cases it is necessary to limit the diluent air in order to reduce the amount of free oxygen, and thus prevent the oxidation or explosion of susceptible material.

The indirect type of heater is available in several types. Steam is sometimes used but is often too expensive for high temperature work. A steam pressure of 160 psia. gives a temperature of only 160°C.

Above this pressure, considerable increase in pressure is required for useful increases in temperature (130). In general, about 2½ to 3 pounds of steam are necessary to evaporate one pound of water (130). It would, however, be possible to use small oil or gas-fired heaters as boosters (57). Superheated steam possesses the disadvantage of having low heat transfer coefficients and thermal capacities. The use of oil, diphenyl or other high temperature heat transfer media which would permit higher operating temperatures may well come into use. Electrical heating is usually limited by its expensiveness, to small laboratory and experimental dryers (154).

NATURE AND PROPERTIES OF SPRAY-DRIED MATERIALS

Spray drying owes its unique applications mostly to the nature of the spray-dried product. Due to the short period of contact and the low temperatures encountered, the physical and chemical properties of spray-dried materials tend to be unaffected by the drying process.

Fogler and Kleinschmidt (57) have done a study of the nature and properties of spray-dried particles formed by various types of nozzles. According to their analysis the pressure nozzles will produce thin-walled hollow spherical particles. Sometimes the hollow spheres have one or two tails and often collapsed spheres are formed due to the expansion of entrapped air or vapor. It is also not uncommon to find one sphere within another. This tendency is prohibitive in the spray drying of such materials as gelatin since the final material encloses too much air. The result is a very low bulk density and the production of a frothy solution when re-dissolved.

T. B. Philip (130) has given a qualitative picture of the physical properties of materials formed by a rotating disk spray mechanism. As an example he chose the spray drying of saponin which is a material with a low surface tension. At low speeds of disk rotation solid and spherical particles are formed upon drying. As the speed is increased the particles decrease in size but remain solid. During this period the bulk density remains relatively constant. At a certain disk speed, a larger but hollow spherical particle is formed. Now as the disk speed continues to increase hollow spherical particles of increased diameter are formed until the particle eventually bursts. In this second period the bulk density is not constant.

It is also pointed out that most solutions sprayed with rotating disks will go through the above variation, depending, of course, on their surface tension and viscosity. With certain solutions only a limited range is available. For example they may only give the hollow range, while with others the hollow range cannot be reached with the available disk speeds (130).

The control of bulk density, which is one of the most important properties of the dried material, does not usually follow so simple a rule as for saponin. D. A. Smith (145) provides the following general variation in bulk density of most spray-dried products. The bulk density tends to decrease with increasing inlet temperatures and decreasing drying rates, while it tends to increase with increasing feed concentrations, non-uniform atomization and increasing liquid feed temperature. Actually, the best method of controlling this variable is by control of the atomization.

It is pointed out (57) that suspensions tend to produce dense free running powders. An interesting application of this principle was utilized by a certain food stuff industry where an intimate mixture of a number of materials was required. Ordinary drying did not produce the desired intimate mixture, whereas this was accomplished by spray drying a previously mixed suspension (57).

Due to the very large surface area per unit weight of spray-dried products, properties like solubility are increased above products of other drying methods. The grading standards of the American Dry Milk Institute (2) specify that the solubility index of Extra Grade non-fat spray-dried milk solids shall not exceed 1.25 ml., while the same grade of drum-dried milk solids has a similar index of 15 ml. The uniformity and degree of atomization tend to affect the solubility.

The beneficial effect on stability and preservative powers of spray-dried products has been discussed in a number of articles. The conservation properties of digitalis were improved over the material produced by vacuum drying (12). Addition agents which tend to promote stability have been successfully utilized (69, 92). Greene et al (69) discuss various techniques for the improved quality and stability of spray-dried egg powders. R. Ladisch (92) discusses and cites examples of strengthening the walls of hollow particles by the addition of alcohols or benzene. He also discusses the improvement on product properties of maltose by the addition of alcohol and hydrochloric acid. The bulk density was radically affected.

In an article on the spray drying of potato mash, Burton (26) discovered an inverse correlation between the pH of the reconstituted powder and its color marking. A group of I. G. Farben chemists (91)

discovered that a small amount of a volatile ammonium salt added to suspensions prior to spray drying produced remarkable constant volume-weight values.

There seems to be no doubt that the scope of control over the properties of spray-dried material can be radically extended.

EFFICIENCY OF SPRAY DRYERS

(i) General Principles

The theoretical efficiency of a spray dryer will depend on the extent to which the spent drying gases approach a condition of equilibrium with respect to the water vapor pressure of the material being dried. As long as the latter is greater than the existing pressure in the surrounding medium, water vapor will continue to diffuse from the material. Thus a greater theoretical efficiency is possible in spray drying colloidal solutions or suspensions than true solutions. As mentioned in a previous section, the evaporation of water from a true solution results in a decrease of vapor pressure as the concentration of the dissolved material increases. As a result, this raises the equilibrium temperature of the exit gases. This effect would, of course, be reduced if true countercurrent conditions prevailed, since the exit gases would then be in contact with the initial feed concentrations.

Actually, exit air saturation is not often obtained in practice, and in most cases would not be desirable. This follows because, in the area of collection, the temperature of the powder falls, resulting in a reduced vapor pressure, and thus the material would absorb water from the moist air stream. Thus, in most commercial installations, the exit temperature of the drying gases is considerably above its equilibrium

value. J. A. Reavell (135) contends that this exit temperature is limited by the point at which useful heat transfer ceases, due to a greatly reduced temperature potential. The above author supports this contention with the additional fact that, due to the low specific heat of air, the cooling due to a relatively small amount of evaporation is substantial. Thus he proposes that it is the greatly reduced heat transfer rates and not air saturation that in practice determines the minimum exit air temperature.

(ii) Factors Affecting Efficiency

A great number of factors tend to decrease spray drying efficiency. For one thing, there is the difficulty of attaining equilibrium between the spray particle and the drying medium, due to poor or insufficiently complete contact within the drying chamber. Moreover, the efficiency will vary considerably with the properties of the material being dried. For example, it is not possible to utilize temperatures that are too high when drying heat sensitive materials. Other materials tend to "case harden" as they dry, creating a high resistance to diffusion. Still another source tending to limit efficiency will be heat losses through the walls of the towers and ducts. Again, since the velocities of the inlet drying air are limited due to the fact that control of the movement of particles must be maintained and the time of contact sufficient, it is not always possible to take advantage of higher relative velocities of particles in the gas stream. Actually, proper design for higher efficiency would include the utilization of high velocities under strict control.

In general, limiting inlet air velocities and temperatures have been determined empirically, each case being decided on its own

merits. S. J. Friedman has pointed out on several occasions that there is a serious lack of fundamental design and performance data for spray drying operations (62).

The theoretical efficiency of the cycle will, of course, be improved by such steps as heat recovery from the exhaust gases and improved insulation to reduce heat losses. The former step has been accomplished in a number of ways.

(iii) Economizers

There is a considerable problem involved in the utilization of the heat in the exhaust air to preheat either incoming drying gases or feed. The air-float material or fines which the exhaust gas contains will foul the surface of the heat exchanger to which it is exposed. The presence of this material also seriously prohibits its use for direct mixing with fresh drying air, since fire hazards and contamination would ensue. The capital and operating cost of air cleaning equipment for the exhaust gases most likely also prohibits its use. The Peebles dryer (127, 130) overcomes this difficulty by partial recycling of the gas stream.

The most efficient method of heat recovery from exhaust gases is to scrub them in a pre-concentration chamber into which the feed liquor is sprayed. This constitutes a recovery of both heat and air-float material. The Gray-Jensen and Kestner designs (130) utilize this procedure.

APPLICATIONS OF SPRAY DRYING

Although the spray drying process is particularly applicable to the drying of heat sensitive materials, it is by no means limited to

this field. It has been used successfully in the production of insecticides, insecticide raw materials as well as metallic stearates and precipitated carbonates (1). It has also been used to dry aluminum hydroxide, amino acids, soluble coffee, resins, vegetable juices, blood plasma, and is said to be the only known method of obtaining dry glucose powders (129). Anhydrous Glauber salt can be formed from a 30% sodium sulphate solution (148). Alkaloids such as valerian, ergot and 'krasavka' extracts (132) and thermolabile concentrates (12) have been successfully spray dried after vacuum drying had proven inadequate.

Ferrous sulphate can be dried to the monohydrate with no increase in ferric ion, even when the inlet temperature is as high as 670°F (130). Spray drying has been used in the drying of sewage sludge (90) as well as in the recovery of distillers solubles (75, 138), and waste sulphite liquors (41, 42). Penicillin and blood plasma can be produced at lower costs than by the conventional sublimation drying techniques (5).

It has long been the leading method in the production of milk powders (4, 46, 151, 154), egg powders (69, 93) and soap powders and detergents (14, 36, 115, 133). In recent years these three products have been produced by spray drying in enormous amounts. Spray drying has been used in the production of potato powders (26), magnesium chloride (9, 143), and rubber latex (6, 22). It has been used in the production of special catalyst particles for hydro-carbon reactions (66).

The patent literature abounds in a great number of references to the application of spray drying for special materials. Perhaps the earliest reference to spray drying is contained in a patent issued to Charles A. La Mont in 1865 (93), in reference to the dried egg industry.

The dried milk industry provides patents which bear names that have come to be associated with the development of Spray Drying - the names of Gray, Jensen and Douthitt (43, 67, 68); similarly for the numerous patents in reference to the soap industry (78, 82, 94, 117).

Spray dryer patents have been issued for the production of dried fruit juices (55), tan liquor (29, 30), maltose (74), basic chromium sulphite (107), sodium silicate (47), and numerous other products.

ECONOMICS OF SPRAY DRYING

There appears to be considerable variation in opinion on the actual efficiencies of spray dryers. Perry (129) states that the efficiencies of commercial spray dryers vary from 20% for low temperatures (300°F or less) to 70% for high gas temperatures. Many other sources indicate maximum efficiencies of not more than 50% (57). These variations will, of course, depend to a great extent on the actual material handled. Performance data on a number of commercial units have been given in the literature. Fogler and Kleinschmidt give performance data for a 10-ft. diameter dryer, indicating that from 1600 to 2100 B.t.u. are required to evaporate one pound of water sprayed at 212°F. They also give data for commercial dryers operating with organic materials, indicating heat requirements of from 2250 to 3800 B.t.u. per pound of water evaporated. In both cases these heat requirements are based on a datum of 65°F. Perry (129) gives capacities of from 0.1 to 3.0 lb. of water evaporated per cubic foot of chamber volume on commercial dryers. The low value is for 20-50 mesh particles using low gas temperatures while the high value is for 300-mesh particles using temperatures in excess of 800°F. Burton (26) gives performance data for spray dryers

operating on potato mash while Greene et al (69) provide data for dryers producing egg powders. Performance data on laboratory size dryers are given by Waite (151) and Diamond (40). Actually, as previously stated, there has been no agreement on methods of determining and estimating efficiencies.

Commercial drying chambers vary from 10 feet to 30 feet in diameter. Capital costs of the 10-ft. diameter dryer, for which Fogler and Kleinschmidt have provided performance data, range from 30 to 40 thousand dollars, installed. 15-20-ft. chambers will cost from 60 to 100 thousand dollars. Another source quotes installed costs of from 10 dollars per cubic foot for large chambers to between 25 and 60 dollars per cubic foot for small chambers (129).

Labor for operating a dryer, exclusive of materials handling, is 12 to 24 man-hours per day. Maintenance costs are from 5 to 10 per cent of the total installed cost (129).

Energy requirements are from 30 to 90 H.P. for a 10-ft. diameter dryer (57). Of this, the bulk is taken by the fan horsepower required, namely from 25 to 75 H.P., the remainder being necessary for pumping and atomizing. Perry (129) quotes 50 H.P. as the energy requirement of a 20-ft. diameter tower. Philip (130) claims that the thermal efficiency of spray drying compares favorably with other forms of drying, whereas Fogler and Kleinschmidt (57) maintain that direct economy of drying is seldom the determining factor in utilizing spray drying operations. It is rather the other advantages of spray drying previously discussed that make it attractive.

NEW THEORETICAL EXPRESSIONS FOR THE EFFICIENCY OF SPRAY DRYING

INTRODUCTION

There has been marked disagreement on the subject of the efficiency of spray drying, making comparisons with other drying methods impossible. Conflicting opinions have been expressed, typical of which is the discussion accompanying a paper by T. B. Philip (130). Few relationships have been proposed, and those existing are unsatisfactory, due to a lack of clarity and a failure to define rigorously the empirical relations developed.

It is recognized that conflicting elements exist in the concept of thermal efficiency as applied to spray drying, mainly because it is the chamber itself that is under consideration, and not the entire cycle. From the viewpoint of drying, the minimum temperature of the spent drying gases that can possibly be obtained in the chamber is the saturation temperature, whereas purely from the viewpoint of heat utilization, the lower temperature limit would be that of the atmospheric datum. The following expression for the efficiency of a spray drying chamber, proposed by Fogler and Kleinschmidt (57), illustrates this problem:

$$E = \frac{1-\frac{R}{100}(T_1-T_2)}{T_1 - T_o} \qquad (14)$$

where R = radiation loss, per cent of total temperature drop in the drying zone

T_1 = temperature of entering air, ^oF

T_2 = temperature of leaving air, ^oF

T_o = temperature of atmospheric datum, ^oF

If we now assume that conditions are adiabatic, i.e. R = 0, and also that T_2 is a minimum, namely equal to T_s, the adiabatic saturation temperature, then the expression simplifies:

$$E = \frac{T_1 - T_s}{T_1 - T_o} \qquad (15)$$

Now, in actual installations, T_s will be higher than T_o, and thus the efficiency cannot be 100%. The limiting value of the numerator is based on drying considerations, while the limit of the denominator is based strictly on heat utilization. In other words, a different temperature datum is used for each.

A disadvantage of this expression is that the useful utilization of heat, namely the evaporative capacity, is not directly indicated. Similar ratios, based on humidities or enthalpies, could be proposed, but would lend themselves to the same objections. It is the purpose of this section to establish two fundamental expressions for the efficiency of spray drying operations, which will overcome these difficulties and establish a firm basis for the study of comparative performance.

Heat and Material Balances

Consider the spray dryer which is illustrated diagrammatically in figure 1. Before proceeding with analysis, certain assumptions must be made. The liquid feed is assumed to be water, the drying gases air, and the existing pressure in the system, one atmosphere.

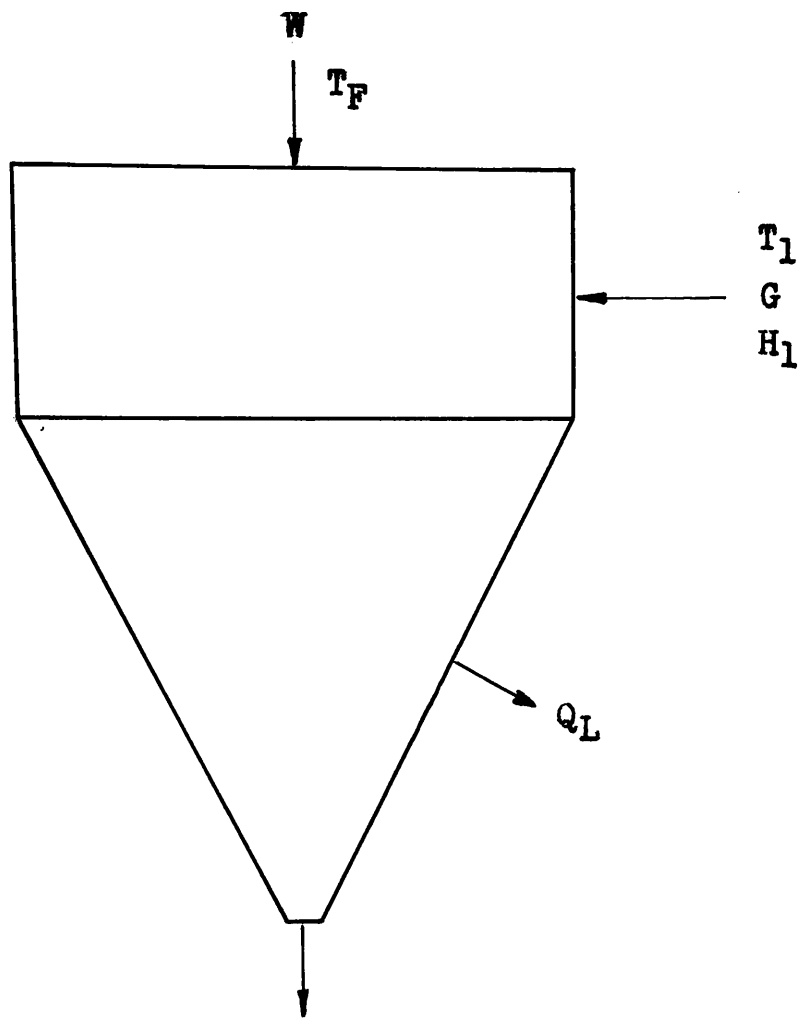

FIG. 1

Material Balance on Water

$$W + GH_1 = GH_2$$

Rearranging, $$\frac{W}{G} = H_2 - H_1$$

$$\therefore \quad W = G(H_2 - H_1) \tag{16}$$

Heat Balance on Chamber

$$G(T_1-T_d)(0.24) + GH_1(T_1-T_d)(0.45) + GH_1\lambda_{T_d} + W(T_F-T_d)(S_F)$$
$$= G(T_2-T_d)(0.24) + GH_2(T_2-T_d)(0.45) + GH_2\lambda_{T_d} + Q_L$$

Rearranging, $$G(T_1-T_d)(0.24+.45H_1) + W(T_F-T_d)(S_F) = G(T_2-T_d)(0.24+.45H_2)$$
$$+ G(H_2-H_1)\lambda_{T_d} + Q_L$$

But, $G(H_2-H_1) = W$; $S_1 = 0.24 + 0.45H_1$; $S_2 = 0.24 + 0.45H_2$

$$\therefore \quad G(T_1-T_d)(S_1) + W(T_F-T_d)(S_F) = G(T_2-T_d)(S_2) + W\lambda_{T_d} + Q_L \quad (17)$$

Now for 100% efficiency of the drying operation, adiabatic saturation of the exit air will be attained. Thus, from the viewpoint of the drying process and the drying chamber itself, maximum efficiency will result when $T_2 = T_s = T_{w.b.}$, the wet-bulb temperature of the air, and $Q_L = 0$. If, in the above equation (17), we select the wet-bulb temperature of the air as the datum, then $T_d = T_{w.b.}$, and all the available heat is used to vaporize water:

$$\text{i.e.} \quad G(T_1-T_{w.b.})(S_1) + W(T_F-T_{w.b.})(S_F) = W\lambda_{T_{w.b.}} \quad (18)$$

$$\text{and,} \quad E_d = \frac{\text{Heat used in Vaporization}}{\text{Heat Available}} = \frac{W\lambda_{T_{w.b.}}(100)}{G(T_1-T_{w.b.})S_1 + W(T_F-T_{w.b.})(S_F)} \quad (19)$$

whence the efficiency would be 100%, based on the equality indicated in equation (18). The above efficiency will be called the "DRYING THERMAL EFFICIENCY".

List of Symbols

W = liquid water evaporated, lb./hr.

G = dry air entering and leaving, lb./hr.

H_1 = absolute humidity of entering air, lb.water vapor/lb. dry air

H_2 = absolute humidity of leaving air, lb. water vapor/lb. dry air

Q_L = heat losses from the surface of the dryer, B.t.u./hr.

S_1 = humid heat of entering air, B.t.u./lb. dry air

S_2 = humid heat of leaving air, B.t.u./lb. dry air

S_F = specific heat of feed (in this case S_F equals 1) B.t.u./lb.

T_1 = temperature of entering air, ^oF

T_2 = temperature of leaving air, ^oF

T_F = temperature of entering feed, ^oF

T_d = datum temperature, ^oF

T_s = adiabatic saturation temperature, ^oF

$T_{w.b.}$ = wet-bulb temperature, ^oF

λ_{T_d} = latent heat of vaporization at datum temperature, B.t.u./lb.

$\lambda_{T_{w.b.}}$ = latent heat of vaporization at wet-bulb temperature, B.t.u./lb.

In an actual spray drying chamber it is unlikely that equilibrium will be attained, and, therefore, the exit temperature of the gases T_2 will be greater than $T_{w.b.}$, representing a loss of available heat in the spent gases. Moreover, perfectly adiabatic conditions will not prevail and there will be a loss, Q_L, from the walls of the chamber. Thus, the drying thermal efficiency will be less than 100%.

The above expression for the efficiency of a spray drying chamber is derived solely from heat and material balances. The heat available for drying is taken as heat in the entering air and feed above a datum of the wet-bulb temperature, whereas in actuality the entering air has a heat availability which is more logically taken above the datum of the temperature of the outside air. On the other hand, it is true that under normal conditions the actual vaporization takes place at the wet-bulb temperature. Thus, as a practical expression of the efficiency of a spray drying chamber, the following equation is proposed:

$$E = \frac{W\lambda_{T_{w.b.}}(100)}{G(T_1-T_d)S_1 + W(T_F-T_d)S_F} \qquad (20)$$

The above ratio will be called the 'Heat Economy of the Drying Chamber'.

This heat economy will normally be based on a datum of from 60° to 70°F, depending, of course, on prevailing atmospheric conditions.

The expression for the heat economy of the spray drying chamber affords a practical thermal ratio, enabling the comparison of different types of chambers operating under different conditions. The theoretical efficiency based on this equation will be less than 100%, since, even if the exit temperature is a minimum, i.e. $T_2 = T_{w.b.}$, there will still be heat lost in the exit air, over the datum.

At this point, it would be well to consider the assumptions made in the above derivations. Basing the heat in the entering feed solely on its water content, and neglecting the heat content of any solid material present, will introduce negligible error, as the heat in the feed is small relative to the other heat quantities involved, and the heat capacity of the solid is low. Considering the entire drying gases as equivalent to air will similarly introduce only slight errors, because of the large volume ratio of air to combustion gases, and because of the fact that the average molecular weight of the products of combustion and their heat capacities approximate those of air. The assumption that the existing pressure in the chamber is atmospheric is also reasonable, since actual pressures will only be measurable in inches of water. The above assumptions enable the use of psychrometric charts for air-water vapor mixtures.

Still another expression for efficiency is the "Overall Thermal Efficiency", which depends upon the actual thermal cycle employed. This, of course, would be based upon the atmospheric datum temperature. Losses incident to the heating of the drying gases in some kind of furnace will

tend to lower this efficiency, while the degree of the recovery of heat from the exhaust gases through the use of economizers, heat exchangers, preconcentration chambers, etc., will add to the credit side of the overall thermal efficiency. Further to this discussion, one could consider a final expression which, from an engineering viewpoint, is possibly the most important. This expression is the "Overall Efficiency of the Process", and would include the energy input to all subsidiary equipment used, such as pumps, motors, fans, etc.

These latter two expressions of efficiency were not calculated in this investigation, because the intention of the research project and the design details were focused on the drying chamber itself.

EXPERIMENTAL SECTION

INTRODUCTION

The experimental work in this project falls into three general sections. The first of these is concerned with experimental runs on the spray drying process with a view to determining the effect of a number of variables on the capacity and efficiency of the drying chamber. Also of concern in this first part is the comparison between operation on water alone as the liquid feed, and operation on an actual solution, under similar conditions.

Based on the previous discussion as to the prime importance of atomization, a short section has been devoted to this variable alone. Moreover, it is this variable which lends itself most readily to a mathematical interpretation of results. Thus, the second section represents experimental runs concerned with the effect of atomization on the spray drying process.

The third section deals with the analysis of the physical properties of the feed and of the dried product. Particle size distributions of the product have been determined as a basis of comparison with liquid feed droplet size.

I SPRAY DRYING

1. EQUIPMENT

The general layout may be seen in figure 2. It consists briefly of a direct gas-fired furnace for heating the drying air, connected to a belt-driven motor-blower assembly, which provides the

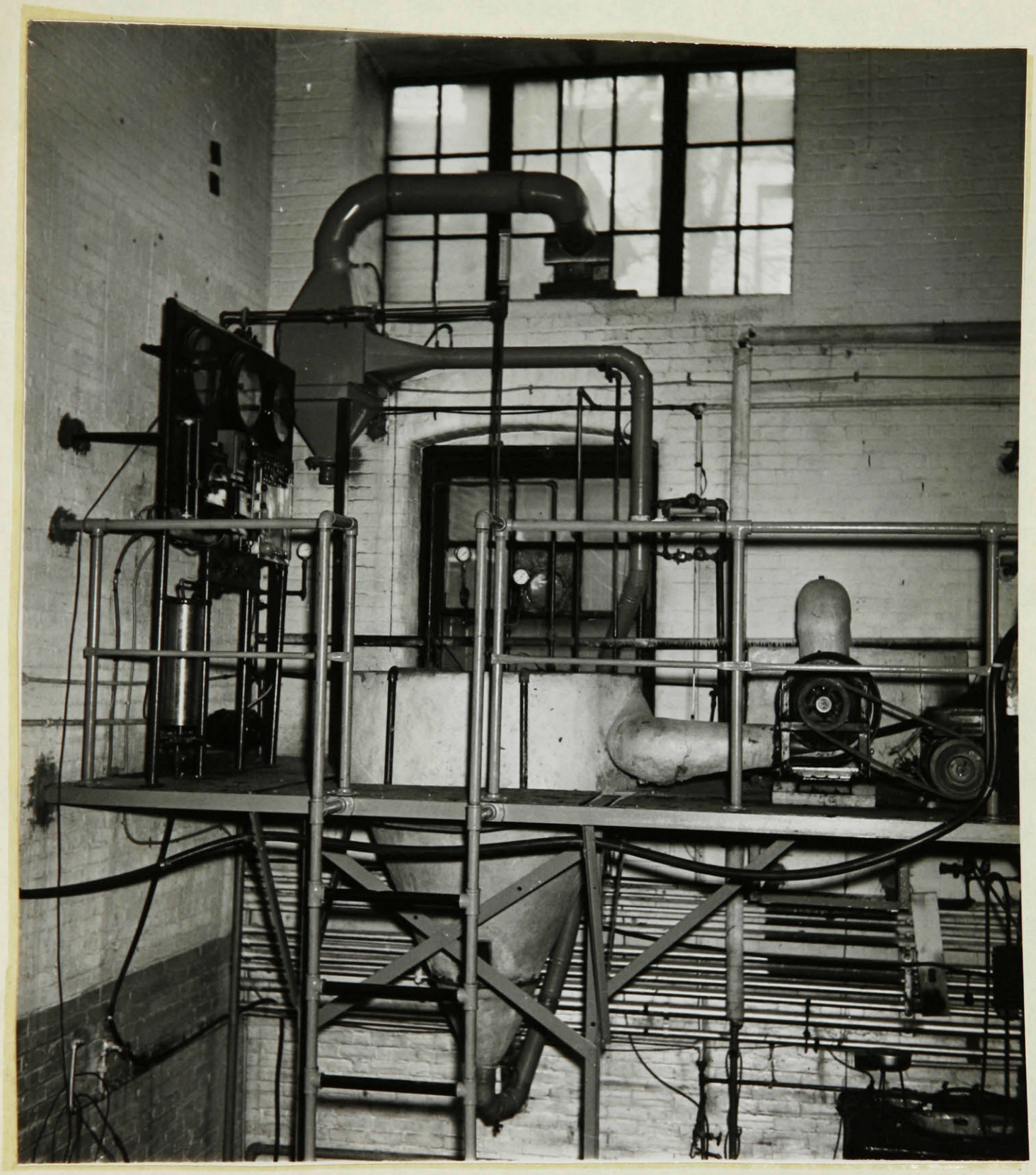

FIG. 2

required drying air; the drying chamber, a concurrent down-flow type with tangential air entry; the spraying system, consisting of a two-fluid nozzle assembly, feed tank and feed pump; and the collection unit, a multi-cone type collector. The spray chamber is the only part of the equipment which was not specifically built for this project, and had been used in a previous investigation (40). However, it was completely modified and rebuilt from a countercurrent flow type to its present design.

Heating of the Drying Gas

The air was heated directly in a gas-fired furnace operated by two gas burners shown in figure 3. The gas burners were supplied from two parallel gas lines, a large one for the main heat source, and a small line for fine control.

The furnace volume was about eight cubic feet, the combustion chamber itself being about six cubic feet, and the mixing chamber above it, two cubic feet. The framework of the chamber was made of angle iron, the walls of 20-gage galvanized steel, and the floor and ceiling of the combustion chamber were made of $\frac{1}{4}$-inch steel plate. A 6-in. x 4-in. hole in the ceiling at the back permitted the combustion gases to enter the mixing chamber. The combustion chamber was lined with fire-bricks and cemented with fire-clay. The furnace, and connected duct work, were insulated with several inches of 'Tartan' cement. Secondary air entered the mixing chamber through a manually controlled damper at the back of the furnace.

The motor-blower assembly consisted of a 3-H.P., 220-volt D.C., compound Bogue Electric Motor, connected with a belt-driven

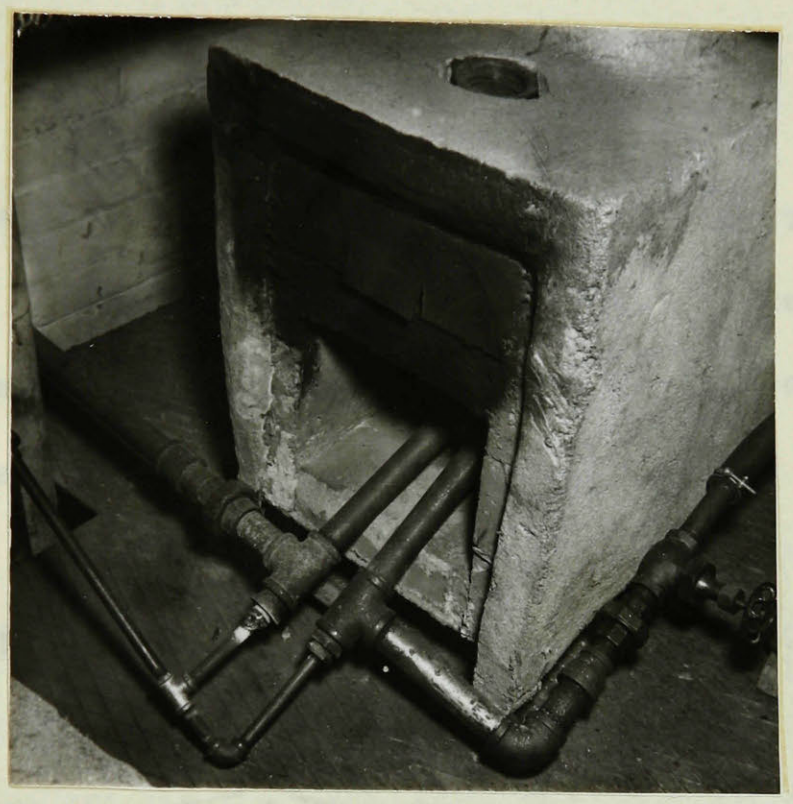

FIG. 3

blower , model RV-2, made by the American Blower Corporation. The inlet and outlet of the blower had outer diameters of six inches, and were connected to appropriate enlarging sections to accommodate the 8-inch galvanized ducts, one coming from the furnace and the other entering the drying chamber. The motor-blower assembly may be seen in figure 2.

Drying Chamber

The chamber design is diagrammatically illustrated in figure 4. It consisted of two main sections, an upper jacketed cylindrical section and a lower conical section with a removable bottom to facilitate entry to the chamber. The chamber had an overall internal height of six feet, the upper cylindrical section being two feet in height and four and one-half feet in diameter. All the segments of the conical sections were double-seamed, the two parts being bolted to $\frac{1}{4}$-inch flanges. A gasket was fitted to the flanges, thus obtaining an air-tight joint. All material was 20-gage galvanized steel.

The hot air from the blower entered the jacketed cylindrical section tangentially, distribution to the chamber proper being provided by six $1\frac{1}{2}$-in. x 6-in. slots cut in the inside wall at an angle of 45 degrees to the perpendicular. The metal was not cut out, but merely bent back along a vertical edge in order to provide a means of changing the air-flow pattern. All protruding joints and screws were in the air jacket, leaving the drying chamber quite smooth.

The entire chamber and entering ducts were insulated with Tartan cement. Two observation windows were installed, one on the top and one on the side of the cone, and a light was provided inside the chamber.

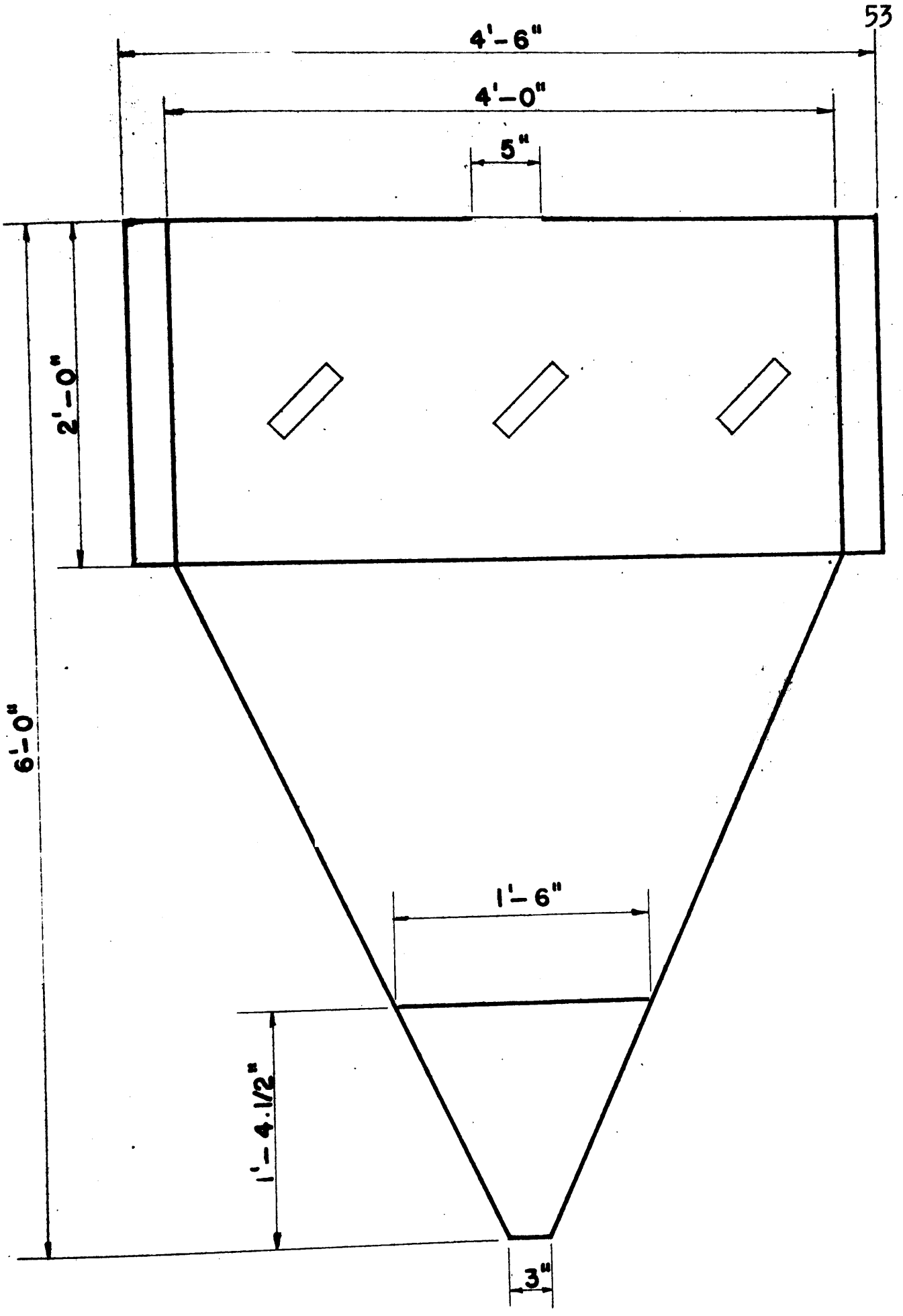

FIG. 4

The general layout of the spraying system may be seen in figures 2 and 5. As shown, the liquid feed was pumped from the feed tank to the nozzle through a $\frac{1}{4}$-in. brass line by means of a $\frac{1}{4}$-in. gear-pump. The feed rate and pressure were controlled by valves at the by-pass of the pump and in the line, and measured by a calibrated rotameter suitably protected by a strainer. The air pressure to the two-fluid nozzle was controlled by a valve in the compressed air line and its rate was measured by an orifice. The pressures at the nozzle were measured by suitably located gages. Water lines were also provided to flush out the system.

Two-fluid, or gas-atomizing, nozzles supplied by the Spraying Systems Company were used exclusively. The nozzle assembly, shown in figure 6, was designed to facilitate changes and maintenance. Sections of the $\frac{1}{4}$-in. liquid feed and compressed air lines were fitted through a circular $\frac{1}{4}$-in. steel plate, 7 inches in diameter. The two $\frac{1}{4}$-in. pipe sections were welded permanently into position and terminated at both ends with unions for quick removal.

Collection of the Product

The powder was collected in a commercial 'Aerotec' powder collector consisting of five parallel banks of five 'Aerotec' cyclone tubes each. The bottom of the drying chamber terminated in a 4-in. galvanized duct which led directly to this powder collector. The collector arrangement may be seen in figure 2, above the control panel in the upper left-hand corner. The spent gases left the collector through an 8-in. galvanized duct and were exhausted to the outside. This Aerotec unit can be used as an efficient metering device as the manufacturers have supplied charts giving rates of flow as a function of the temperature and pressure drop across the unit.

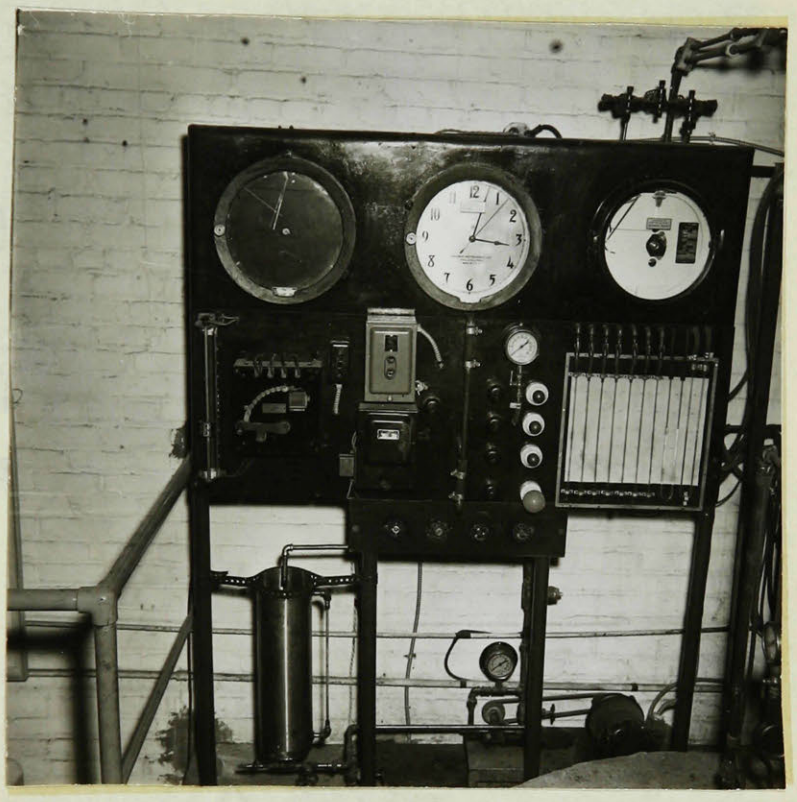

FIG. 5

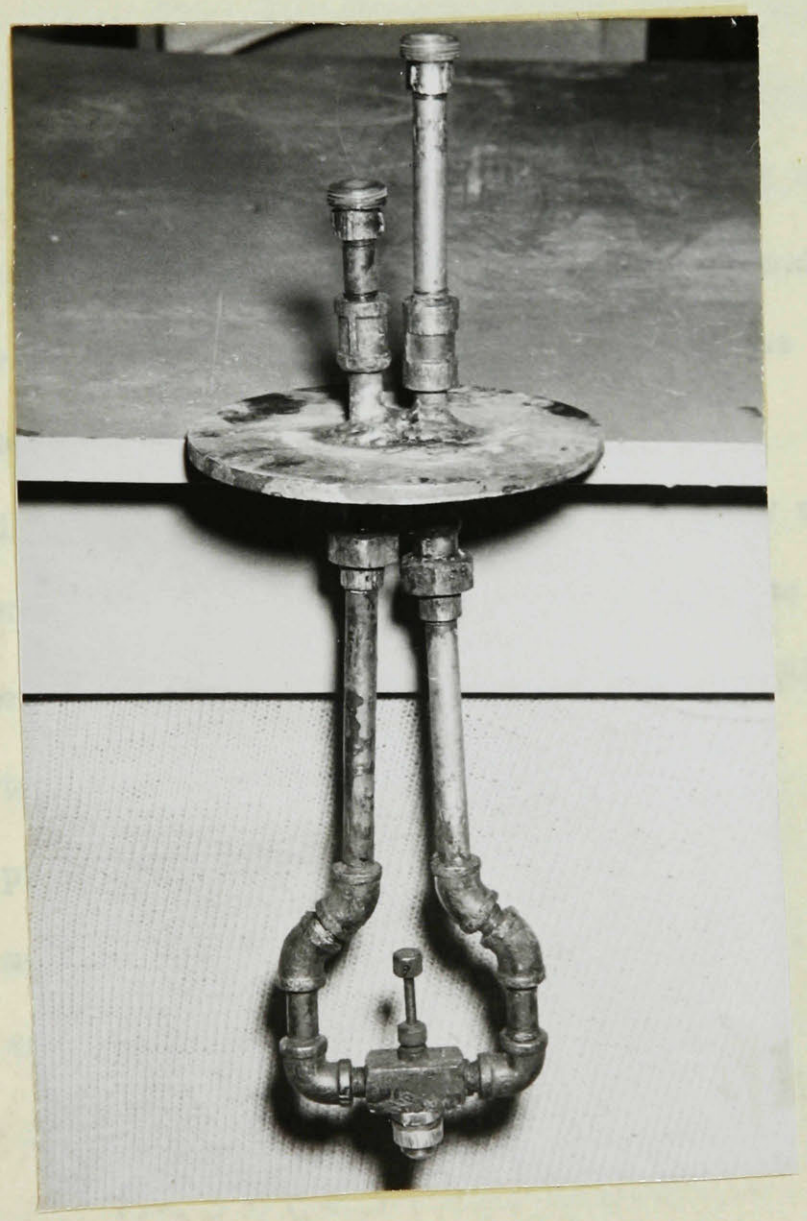

FIG. 6

Control and Recording of Variables

The temperature of the drying air could be maintained within ±1°C, either manually or by means of a bimetallic thermo-regulator located in the chamber air jacket. This thermo-regulator was connected through a delayed action relay to a solenoid valve located in a by-pass of the small gas line. The temperature of the inlet drying air to the chamber, the exit air from the chamber and the air entering the Aerotec were read by suitably located mercury thermometers. A wet-bulb thermometer was provided at the exit of the drying chamber and several other thermometers were attached to the top and side surfaces of the drying chamber insulation.

The volume of drying gases was controlled by means of a variable resistance which changed the voltage and hence the speed of the motor driving the blower. This volume was measured with a water U-tube manometer connected across the Aerotec collector.

The depth of the nozzle in the chamber could be varied merely by removing the nozzle plate assembly and replacing the nipples by others of the desired length.

Static pressures could be taken at various points in the system. The manometers may be seen on the control panel in figure 5. All controlling valves, motor switches and starters, rotameter and recording instruments are located on the control panel. An orifice in the compressed air line to the nozzle permitted the reading of the volume of air.

2. PROCEDURE

The equipment was brought to a steady state at the beginning of each trial in the following manner. The two gas burners were lit,

the blower motor slowly brought to speed and the amount of gas fed to the burners was slowly increased, about three-quarters of an hour being required to reach the desired temperature. When a constant temperature prevailed, the following readings were taken: all static pressures, inlet drying air temperature, surface temperatures of the cylindrical portion of the chamber and also of the conical sections, chamber outlet wet- and dry-bulb temperatures, the temperature before the Aerotec unit, and the pressure drop across the latter. Since no feed was used up to this point, the wet- and dry-bulb temperatures of the hot air determined its humidity.

When water was used as the liquid medium, the actual spraying operation was begun by first slowly adjusting the compressed air pressure at the nozzle to the desired operating value. The feed pump was then started, all readings were once more checked for constancy and then careful observation was made of the spray-drying process through the chamber windows.

To determine the maximum capacity of the chamber when evaporating water, the stringent criterion that no droplet from the spray should hit the walls was adopted. Under a given set of operating conditions, the feed rate was slowly increased until the capacity was just exceeded. The feed was then slowly reduced until the wet spray no longer hit the walls. Owing to the special observation facilities, any droplet hitting the walls could be detected easily as a pinpoint of light and the maximum capacity could thus be sharply determined. At this maximum rate all previous readings were checked and the following additional ones taken: the liquid feed rate and temperature, the air

and liquid pressures at the nozzle, and the orifice reading in the nozzle air line.

Great care was taken in the determination of the wet-bulb temperatures which were estimated as follows. The wick of the thermometer was immersed in water, the temperature of which was approximately that of the estimated wet-bulb temperature. A more accurate determination made possible an even closer adjustment of the two temperatures. At this stage, by wetting the wick with water, no observable rate of change could finally be detected, and it was this final temperature which was taken as the wet-bulb reading.

The method of varying the nozzle depth as well as the volume of drying gases has been clearly indicated in the previous section. The feed temperature was controlled manually by an insertion heater. Once steady state was reached, only occasional adjustments were needed to keep all operating conditions rigidly constant. After completion of an entire trial and before shut-down, a rigorous procedure was followed. The feed pump was first shut off. After about five minutes the gas burners were closed, following which the compressed air valve to the nozzle was also closed. Cool air was blown through the system for about ten minutes, followed by the closing of the motor-blower starter switch.

When an actual solution was used as the feed, the procedure was in every way identical. Water was again used to start the spray drying process, changing over to the feed material when operating conditions were steady. This new feed consisted of a ten per cent by weight solution of a by-product of the sulfite pulp industry. This material, which is called Lignosol, consists of about 50% calcium lignosulfonate, the rest being tannins, carbohydrates and resins. In all runs with

Lignosol the concentration was kept constant at ten per cent by weight. It should be noted that this material forms colloidal solutions in water.

3. CALCULATIONS AND TABLE NOMENCLATURE

From the readings collected during the experimental runs, it was necessary to calculate certain quantities before heat balances could be established and efficiencies determined.

The volumetric rate of flow of the drying gases was calculated by means of measurements of pressure drop across the Aerotec unit, as previously explained. This flow rate was checked by means of a Pitot Tube traverse and cross-checked by a humidity balance on the combustion of a known volume of fuel gas, of known composition. The actual mass rate of air was determined by applying the ideal-gas equation of state to the determined volumetric rate. These mass rates were checked by means of equation (16), page 42, the humidities having been obtained by psychrometric methods from the known dry- and wet-bulb temperatures.

The humid heats of the inlet and spent air were determined from the known temperatures and humidities, the latter having been previously assessed by the method already described. The heat losses were determined from data supplied by the manufacturers of the insulating 'Tartan' cement. A plot of these losses as a function of the outside insulation temperatures is shown in figure 7. Values thus obtained checked very well against heat losses calculated from the heat balance given in equation (17) on page 43.

Finally, the efficiency was calculated from equation (19), derived on page 43, each of the terms being calculated as indicated.

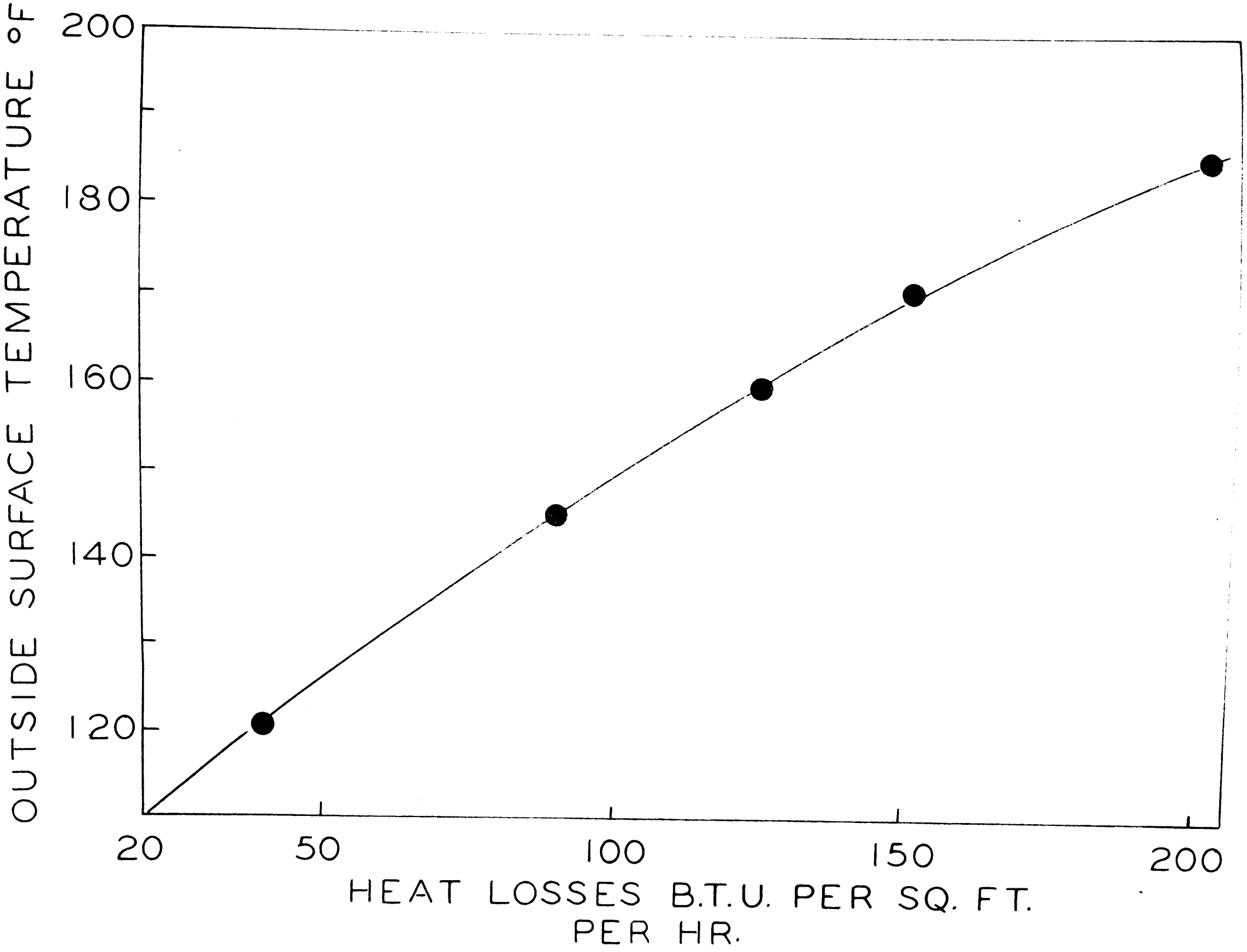
OUTSIDE SURFACE TEMPERATURE °F
200
180
160
140
120
20
50
100
150
200
HEAT LOSSES B.T.U. PER SQ. F T.
PER HR.

FIG. 7

For the purpose of presentation, observed data and calculated results were divided into three tables for the water runs, the first reporting observed readings only; the second represents a material balance and gives the capacity; while in the third all the terms of the heat balance required for the calculation of efficiency are indicated. In the case of the Lignosol runs, in addition to the above three tables, a fourth showing heat balances has been given. Owing to lack of space, table headings had to be restricted to symbols only, full nomenclature for which is as follows:

l = nozzle depth below roof of chamber, in.

V = volumetric rate of entering hot gases, expressed on a free basis at 70°F and 1 atm., cu.ft./min.

T_1 = temperature of entering hot gases, °F

T_F = temperature of liquid feed, °F

T_2 = temperature of spent drying gases, °F

$T_{w.b.}$ = wet-bulb temperature of spent gases, °F

P_a = pressure of compressed air at the nozzle, psig.

P_L = pressure of liquid feed at the nozzle, psig.

F = rate of liquid feed, U.S. G./min.

w = water evaporated, lb./min.

H_2 = absolute humidity of spent drying air, lb. water vapor/lb. dry air

H = gain in humidity of drying air, lb. water vapor/lb. dry air

a_C = rate of drying air, calculated, lb./min.

a = rate of drying air, actual, lb./min.

G = rate of drying air, actual, lb./hr.

W = chamber capacity expressed as water evaporated, lb./hr.

S_1 = humid heat of entering air, B.t.u./lb.dry air

S_2 = humid heat of leaving air, B.t.u./lb.dry air

w.b. = latent heat of vaporization at the wet-bulb temperature, B.t.u./lb.

Q_1 = sensible heat in entering air, B.t.u./hr.

Q_2 = sensible heat in leaving air, B.t.u./hr.

Q_v = heat of evaporation (i.e. $W\lambda_{w.b.}$), B.t.u./hr.

Q_F = heat in entering liquid feed, B.t.u./hr.

Q_L = heat losses, by convection and radiation, from spray chamber, actual, B.t.u./hr.

E_d = Drying Thermal Efficiency, per cent

T_T = temperature of top outside insulating surface, ^oF

T_C = temperature of outside insulating surface of conical section, ^oF

Q_T = heat losses from top cylindrical section of chamber, calculated, B.t.u./hr.

Q_C = heat losses from conical section, calculated, B.t.u./hr.

Q_{Ic} = total heat losses, calculated, B.t.u./hr.

4. EXPERIMENTAL RESULTS

WATER RUNS

(a) Variation of Inlet Air Temperature

Six runs were made at a constant volumetric rate of entering gases of 308 C.F.M. (free air, measured at 70°F and 14.7 psia.), a fixed feed temperature of 53°F and a fixed nozzle depth of 12.875 inches. The complete results are given in Tables I-a, I-b, and I-c, and the effects on capacity, efficiency and heat losses are shown in figure 8. These terms are entered as W, E_d and Q_1, respectively, in the Tables.

It may be observed from the above figure that both the capacity and efficiency pass through a maximum with increase in inlet air tempera-

WATER-VARIATION OF INLET AIR TEMPERATURE

Table I-a

Trial No.	l in.	V cfm.	T_1 ^oF	T_F ^oF	T_2 ^oF	$T_{w.b.}$ ^oF	P_a psig.	P_L psig.	F U.S.P.M.
1	12.875	308	253.4	53.4	197.2	108	40	17	0.0215
2	12.875	308	283	54.2	219.0	111.8	40	18	0.0275
3	12.875	308	329.2	53.0	259.0	115.2	40	19	0.031
4	12.875	308	364	53.4	293.3	124	40	20	0.0335
5	12.875	308	393	53.6	337.3	125.5	40	20	0.033
6	12.875	308	411	53.4	350.9	128	40	20	0.033

Table I-b

Trial No.	w lb/min	H_2 lb/lb	H lb/lb	a_C lb/min	a lb/min	G lb/hr	W lb/hr
1	0.1791	.032	0.008	22.45	23	1380	10.75
2	0.2293	.0355	0.0095	24.1	23	1380	13.78
3	0.2581	.034	0.0115	22.5	23	1380	15,75
4	0.2793	.049	0.012	23.28	23	1380	16.77
5	0.275	.046	0.0115	23.9	23	1380	16.5
6	0.275	.0485	0.012	22.9	23	1380	16.5

Table I-c

Trial No.	S_1 btu/lb	S_2 btu/lb	w.b. btu/lb	Q_1 btu/hr	Q_2 btu/hr	Q_v btu/hr	Q_F btu/hr	Q_L btu/hr	E_d %
1	0.251	0.2545	1032.6	50398	31550	11100	588	7160	22.25
2	0.252	0.256	1031	58200	37900	14200	793	5307	24.75
3	0.250	0.255	1028.7	73700	50598	16200	976	4926	22.3
4	0.257	0.262	1023.4	85000	61150	17150	1182	5518	20.5
5	0.256	0.261	1022.5	94400	76320	16890	1190	6010	18.15
6	0.257	0.262	1021.4	100500	82710	16870	1220	7270	17.0

Table heading nomenclature given on page 62.

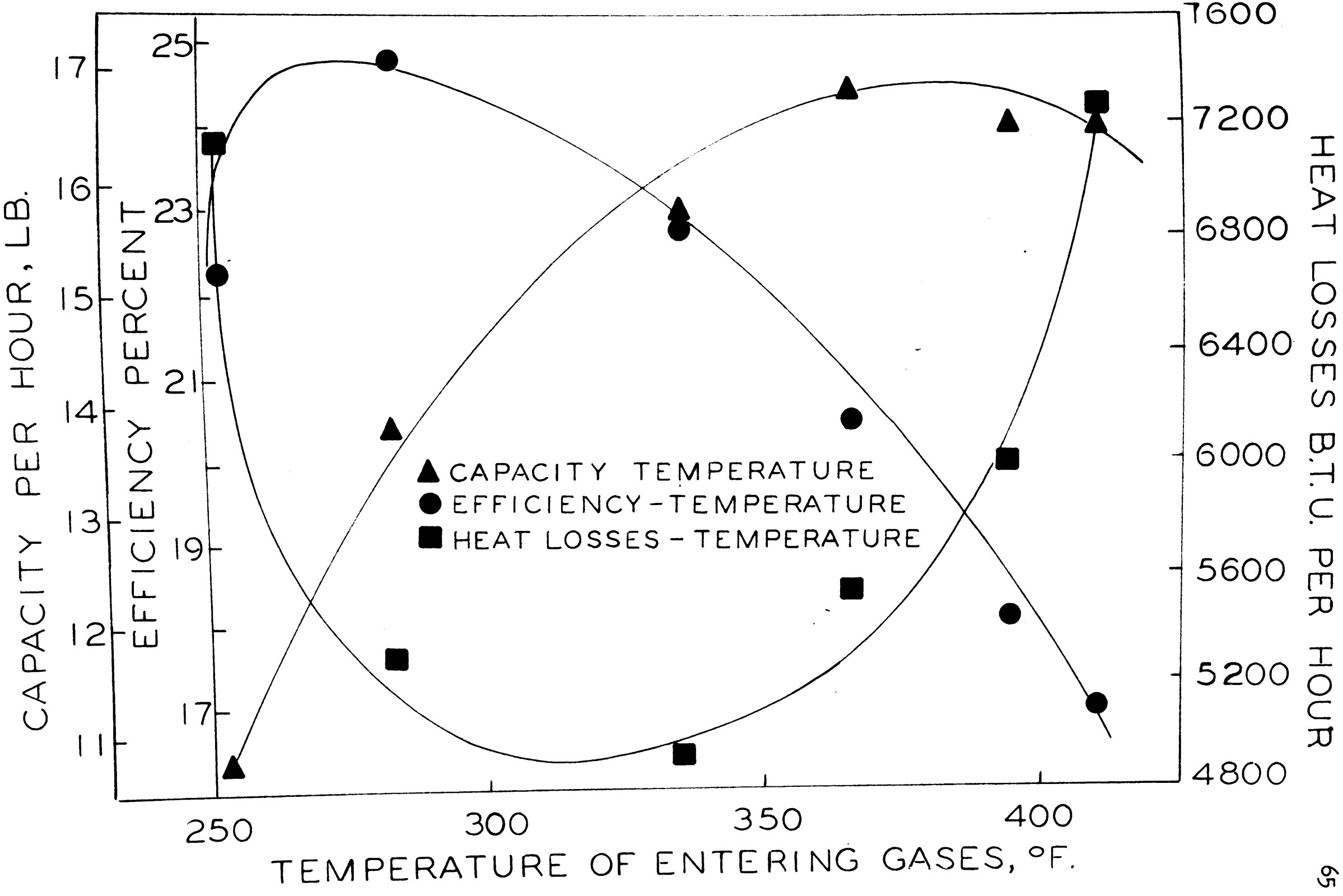

FIG. 8

WATER-VARIATION OF INLET AIR TEMPERATURE

ture, but the two maxima do not occur at the same temperature. The curve for heat losses passes through a minimum at a point in the region of maximum efficiency.

It also may be noted that, although increased capacity occurs as the temperature increases to 364°F, nevertheless, after an inlet air temperature of 282°F, this increased capacity is at the expense of decreasing efficiency and increasing heat losses.

(b) Variation of Nozzle Position and Inlet Air Rate

The effects of varying the rate of inlet gases and the nozzle depth from the top of the chamber, at constant inlet gas and feed temperatures, are shown in Tables II-a, II-b and II-c and figure 9. In order to show clearly the effect of air rates on capacity, runs Nos. 26, 22, 15 and 8 are plotted separately in figure 10. These runs are at a constant nozzle depth of 12.5 inches.

Figure 9 clearly demonstrates the importance of the nozzle location, and the existence of a sharply defined optimum position between depths of 10.75 and 11.75 inches. More striking still is the fact that this optimum position appears to be independent of the drying gas rate, although the latter most certainly exerts a profound influence on the turbulent flow pattern in the chamber. Figure 9, and more particularly figure 10, show that capacity also passes through a maximum at air rates of 262 to 208 C.F.M. Finally, the results indicate that at maximum capacity the efficiency is maximum and the heat losses are minimum. It is obvious, of course, that increased efficiency should result when equal capacities are attained at lower rates of entering air, as shown by the efficiency values of 71% and 92%, for runs 23 and 28, respectively.

WATER-VARIATION OF NOZZLE POSITION AND INLET AIR RATE

Table II-a

Trial No.	l in.	V cfm.	T_1 ^oF	T_F ^oF	T_2 ^oF	$T_{w.b.}$ ^oF	P_a psig.	P_L psig.	F U.S.P.M.
7	12.875	308	365.0	53	295	121	40	20.5	0.0335
8	12.50	308	366.0	53	285	123	40	22.5	0.038
9	11.75	308	366.6	52	228	117	50	31	0.0745
10	10.75	308	365	53	209.5	115	50	34	0.087
11	10.25	308	364.5	52.0	265	118.5	50	29	0.0483
12	9.5	308	365	51.5	282	123	50	26	0.0395
13	8.5	308	365	51	290	117	50	25	0.0315
14	12.875	262	365	53	280	123	50	26	0.035
15	12.5	262	365.8	53	261.7	123.8	40	24	0.044
16	11.75	262	366.8	51	172.4	119	50	35	0.096
17	10.75	262	366	51	162	117	50	36	0.1
18	10.250	262	366.8	53	243.5	119	50	28	0.054
19	9.5	262	365	53	267.5	123.8	50	26.5	0.042
20	8.5	262	365	53	285	123.2	50	25	0.0335
21	12.875	208	366	53	271	123	50	24	0.03
22	12.50	208	365.8	53	261.5	123	50	25.5	0.0350
23	11.75	208	366.8	53	149.1	119	50	35	0.0925
24	10.75	208	366	53	157.4	117.1	50	34	0.088
25	12.875	176	365	52	255.3	121.2	50	24	0.0315
26	12.50	176	364.6	53	251.8	120.8	40	20	0.0330
27	11.75	176	365	53	136	116	50	33	0.084
28	10.75	176	366	53	128	116	50	34	0.089

WATER-VARIATION OF NOZZLE POSITION AND INLET AIR RATE

Table II-b

Trial No.	w lb/min	H_2 lb/lb	H lb/lb	a_c lb/min	a lb/min	G lb/hr	W lb/hr
7	0.2793	.040	0.012	23.3	23	1380	16.77
8	0.3165	.048	0.013	24.35	23	1380	19.0
9	0.621	.0455	0.0265	23.45	23	1380	37.1
10	0.725	.0455	0.0305	23.75	23	1380	43.5
11	0.415	.0405	0.017	22.75	23	1380	25.0
12	0.329	.0485	0.0145	22.7	23	1380	19.71
13	0.263	.031	0.011	23.9	23	1380	15.78
14	0.2920	.0495	0.015	19.45	19.5	1170	17.51
15	0.376	.0565	0.0190	19.75	19.5	1170	22.55
16	0.800	.065	0.041	19.5	19.5	1170	48.0
17	0.833	.062	0.042	19.8	19.5	1170	50.0
18	0.450	.0465	0.023	19.6	19.5	1170	27.0
19	0.350	.0555	0.018	19.45	19.5	1170	21.0
20	0.2795	.0485	0.014	19.95	19.5	1170	16.77
21	0.250	0.0515	0.0155	16.15	16.33	980	15.0
22	0.2930	0.054	0.018	16.3	16.33	980	17.57
23	0.771	0.0705	0.046	16.75	16.33	980	46.7
24	0.733	0.0635	0.0435	16.85	16.33	980	44.0
25	0.2625	0.050	0.0185	14.2	14.0	840	15.76
26	0.2745	0.050	0.02	13.73	14.0	840	16.48
27	0.700	0.0668	0.0480	14.6	14.0	840	42.0
28	0.737	0.0685	0.0497	14.85	14.0	840	44.2

WATER-VARIATION OF NOZZLE POSITION AND INLET AIR RATE

Table II-c

Trial No.	S_1 btu/lb	S_2 btu/lb	w.b. btu/lb	Q_1 btu/hr	Q_2 btu/hr	Q_V btu/hr	Q_F btu/hr	Q_L btu/hr	E_d %
7	0.253	0.258	1025.6	85500	62000	17190	1124	5186	20.4
8	0.256	0.262	1024	85500	60000	19450	1330	4720	23.1
9	0.248	0.261	1027.5	84800	40100	38150	2410	4140	46.3
10	0.247	0.261	1028.5	85100	33900	44600	2697	3903	54.1
11	0.250	0.258	1026.2	84800	52030	25650	1660	5258	30.8
12	0.255	0.262	1024	85000	57500	20200	1409	5891	24.15
13	0.249	0.254	1027.5	85200	60500	16200	1033	7467	19.25
14	0.256	0.263	1024	72500	48250	17930	1227	5093	25.15
15	0.257	0.266	1023.5	72900	42800	23100	1577	5423	32.4
16	0.251	0.269	1026.2	72600	16800	49200	3620	3340	71.0
17	0.249	0.268	1027.5	72100	14000	51380	3350	3370	74.7
18	0.251	0.261	1026.2	72600	38000	27700	1780	5120	39.1
19	0.257	0.265	1023.5	72500	44500	21500	1489	5011	30.3
20	0.256	0.261	1023.8	72450	49400	17170	1175	4705	24.1
21	0.2565	0.263	1024	61100	38100	15370	1050	6580	25.4
22	0.2565	0.264	1024	61100	35850	18000	1230	6020	30.1
23	0.251	0.272	1026.5	60800	8030	48000	3080	1690	71.0
24	0.249	0.2685	1028	60400	10570	45200	2820	1910	66.9
25	0.254	0.263	1025	51800	28600	46160	1073	5967	31.9
26	0.253	0.262	1025.4	51700	27850	16800	1115	5935	33.2
27	0.2485	0.270	1027.3	52150	4530	43300	2645	1675	87.5
28	0.2485	0.271	1028	52150	2720	45400	2785	1245	92.0

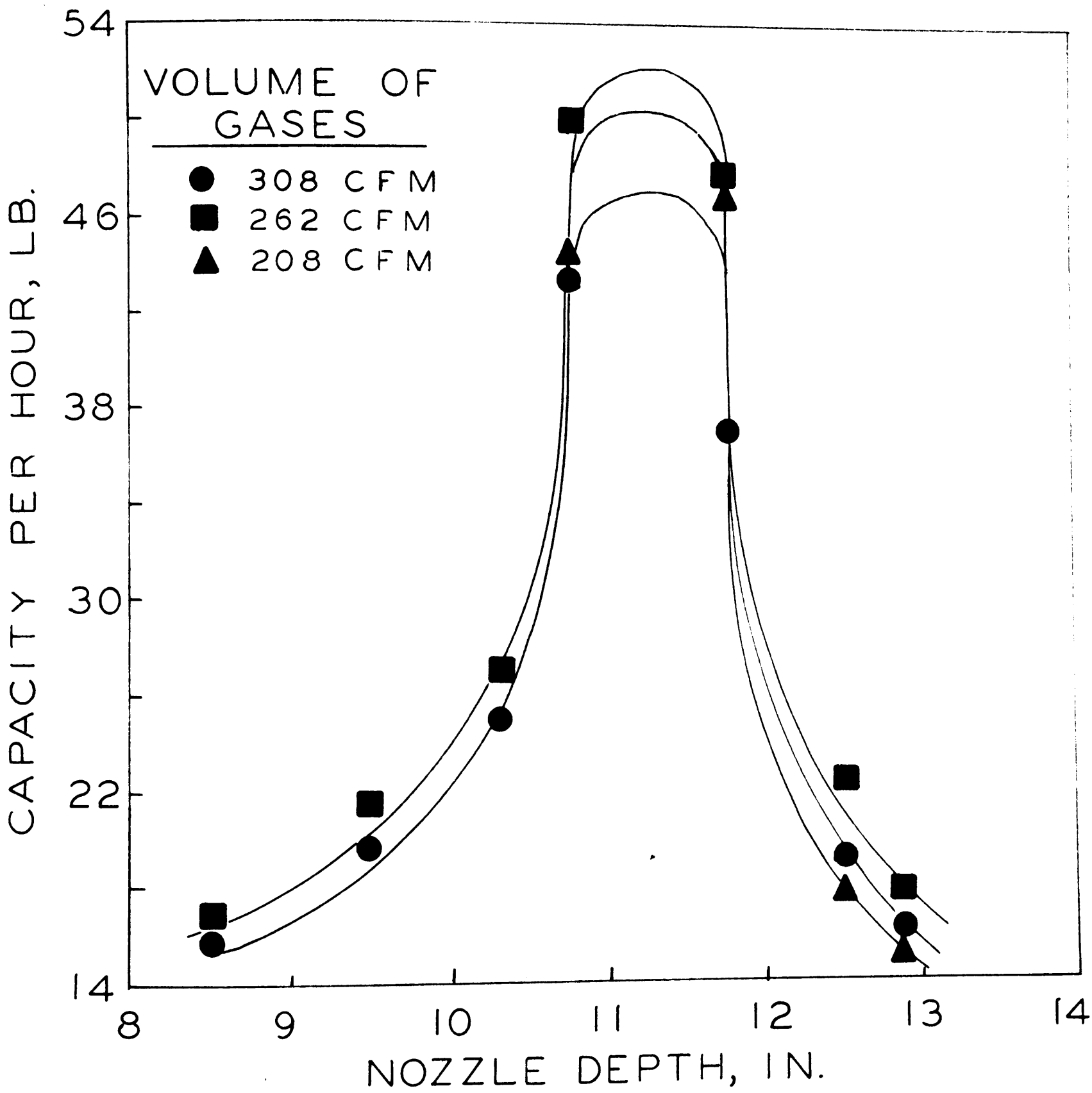

FIG. 9

WATER-VARIATION OF NOZZLE DEPTH

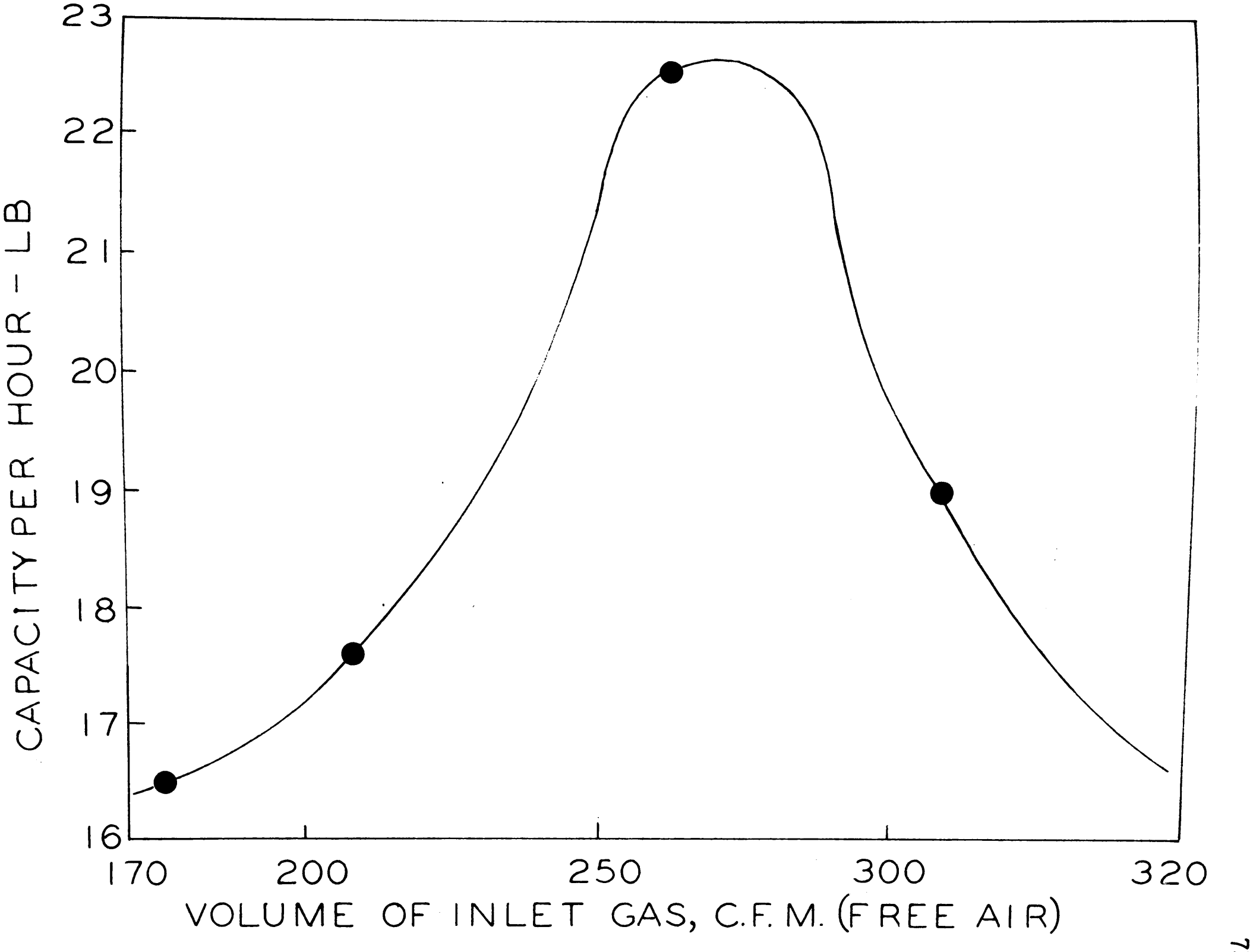

FIG. 10

WATER-VARIATION OF INLET AIR RATE

(c) Variation of Temperature at Optimum Air Rate and Nozzle Depth

From previous investigations, an optimum air rate of 262 C.F.M. free air and an optimum nozzle depth of 10.75 inches were selected, and at these fixed values the inlet air temperature was again varied. The results are tabulated in Tables III-a, III-b and III-c, and the effects on capacity and efficiency are shown in figure 11.

The results indicate that a maximum was again found for the capacity of the chamber, but that this maximum did not correspond to a maximum efficiency nor to minimum heat losses. As a matter of fact, this efficiency is far below values found for trials 29, and more particularly 27 and 28.

(d) Variation of Inlet Feed Temperature

The inlet feed temperature was varied at conditions representing the optimum of all other variables, namely an air rate of 262 C.F.M., a nozzle depth of 10.75 inches and an inlet air temperature of 420°F. The results are entered in Tables IV-a, IV-b and IV-c, and the relation to capacity and efficiency may be seen in figure 12.

These results are particularly interesting because they show large effects on the capacity and efficiency which were totally unexpected. The capacity passes through a maximum at a temperature of the inlet feed corresponding to the wet-bulb temperature of the drying gases.

LIGNOSOL RUNS

(a) Variation of Inlet Air Temperature

Four runs were made at a constant air rate of 308 C.F.M. (free air), a fixed feed temperature of 53°F and a fixed nozzle depth of 12.5

WATER-VARIATION OF TEMPERATURE AT OPTIMUM AIR RATE AND NOZZLE DEPTH

Table III-a

Trial No.	l in.	V cfm.	T_1 ^oF	T_F ^oF	T_2 ^oF	$T_{w.b.}$ ^lF	P_a psig.	P_L psig.	F U.S.P.M.
29	10.75	262	329	54	151.6	115	50	34	0.088
30			366	51	162	117	50	36	0.1
31			420.5	54	209.5	127	50	37	0.104
32			482	54	271	135.5	50	36	0.1

Table III-b

Trial No.	w lb/min	H_2 lb/lb	H lb/lb	a_c lb/min	a lb/min	G lb/hr	W lb/hr
29	0.733	0.0602	0.0382	19.2	19.5	1170	44.0
30	0.833	0.062	0.042	19.8			50.0
31	0.867	0.0490	0.0450	19.25			52.0
32	0.833	0.0935	0.0422	19.75			50.0

Table III-c

Trial No.	S_1 btu/lb	S_2 btu/lb	w.b. btu/lb	Q_1 btu/hr	Q_2 btu/hr	Q_v btu/hr	Q_F btu/hr	Q_L btu/hr	E_d %
29	0.250	0.2675	1028.5	62550	11480	45300	2684	3086	75.8
30	0.249	0.268	1027.5	72100	14000	51380	3350	3370	74.7
31	0.255	0.277	1021.5	87600	26610	53100	3795	4095	63.5
32	0.263	0.282	1016.5	106800	45050	50825	4075	6850	49.4

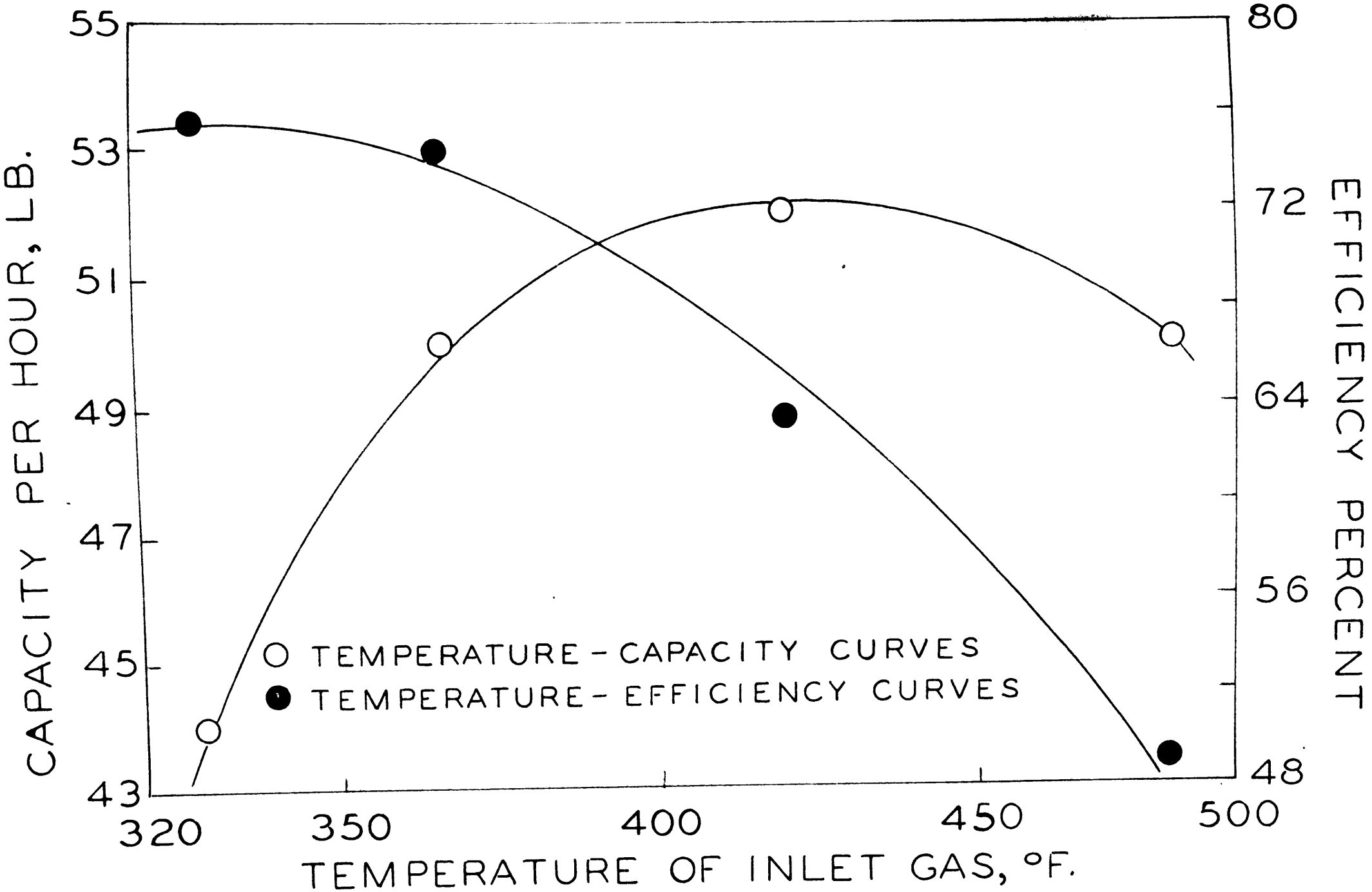

FIG. 11

WATER-VARIATION OF AIR TEMPERATURE AT OPTIMUM NOZZLE DEPTH AND AIR-RATE

WATER-VARIATION OF INLET FEED TEMPERATURE

Table IV-a

Trial No.	l in.	V cfm.	T_1 °F	T_F °F	T_2 °F	$T_{w.b.}$ °F	P_a psig.	P_L psig.	F U.S.P.M.
33	10.75	262	420.5	54	209.5	127	50	37	0.104
34				70	197	127	50	39	.115
35				128	190	127	50	41	.125
36				158	200	127.7	50	40	.120

Table IV-b

Trial No.	w lb/min	H_2 lb/lb	H lb/lb	a_C lb/min	a lb/min	G lb/hr	W lb/hr
33	0.867	0.0490	0.0450	19.25			52.0
34	0.96	0.0485	0.0485	19.8			57.6
35	1.04	0.087	0.053	19.65			62.4
36	1.0	0.0845	0.050	20.0			60.0

Table IV-c

Trial No.	S_1 btu/lb	S_2 btu/lb	w.b. btu/lb	Q_1 btu/hr	Q_2 btu/hr	Q_v btu/hr	Q_F btu/hr	Q_L btu/hr	E_d %
33	0.255	0.277	1021.5	87600	26610	53100	3795	4095	63.5
34	0.255	0.2785	1021.5	87600	21770	58800	3280	3750	69.8
35	0.255	0.2795	1021.5	87600	20600	63700	0	3300	71.9
36	0.255	0.279	1021.5	87600	23600	61290	-1860	4570	68.6

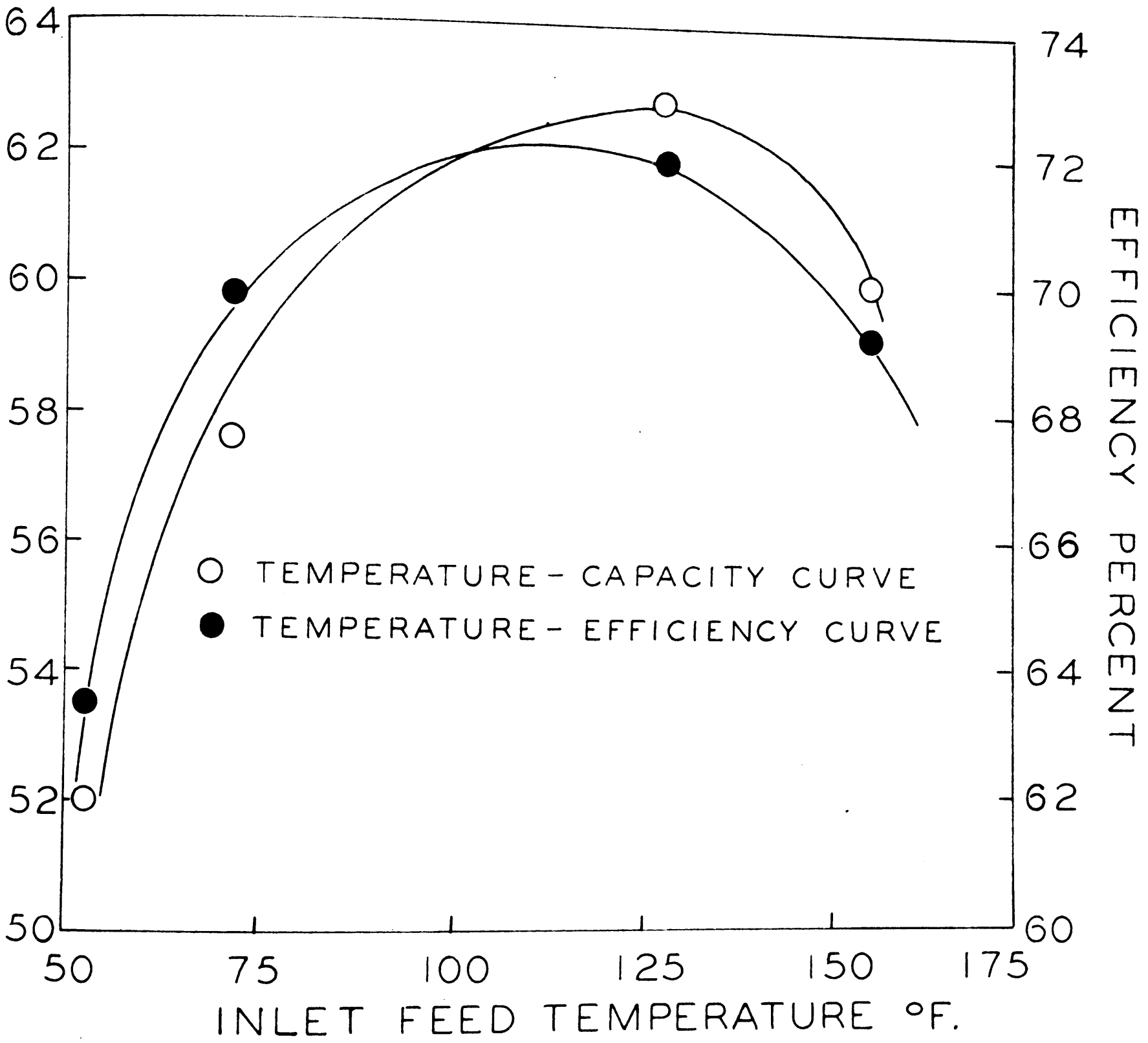

FIG. 12

WATER-VARIATION OF INLET FEED TEMPERATURE

inches. The tabulated results are given in Tables V-a, V-b, V-c and V-d, and a plot of capacity against inlet air temperatures is shown in figure 13.

These results exhibit the same general behaviour as the equivalent trials on water alone. The curve passes through a maximum with increasing air inlet temperature, but lower capacities are attained than in the case of the water runs. Although both greater capacity and greater efficiency result from increasing the air temperatures to the optimum, nevertheless, there is a steady increase in heat losses, which rise rapidly beyond the point of maximum capacity.

(b) Variation of Nozzle Depth and Inlet Air Rate

At a constant inlet air temperature of 365°F and a constant air rate of 308 C.F.M. (free air) the effect of varying the nozzle depth was studied. This variation was also studied at gas volumes of 262 C.F.M. and 208 C.F.M. The results are tabulated in Tables VI-a, VI-b, VI-c, VI-d, and the effects on capacity are shown in figure 14.

Two additional plots, based on trials 18, 15, 11 and 7, and trials 19, 16, 12 and 8, are shown in figure 15. These runs show the effect of volume of entering gases on the capacity at two fixed nozzle positions. The form of the curve indicates that a maximum is logically to be expected at higher air rates, as it appears quite similar to the comparable plot for the water runs, figure 10.

Figures 14 and 15 show curves of the same general shape as in the equivalent water runs, figures 9 and 10, but the increase in capacity is not as sharp. Totally unexpected is the fact that the optimum nozzle depth is not the same, but is now much lower in the spray-chamber, at 12.375 inches below the roof.

LIGNOSOL-VARIATION OF INLET AIR TEMPERATURE

Table V-a

Trial No.	l in.	V cfm.	T_1 °F	T_F °F	T_2 °F	$T_{w.b.}$ °F	P_a psig.	P_L psig.	F U.S.P.M.
1	12.5	308	305	53	268	112	40	17	0.0211
2			350	52	270	118	40	23	0.0444
3			420	50	300	125.5	40	25	0.065
4			482	53	383	135.2	40	23	0.0467

Table V-b

Trial No.	w lb/min	H_2 lb/lb	H lb/lb	a_c lb/min	a lb/min	G lb/hr	W lb/hr
1	0.1585	0.0260	0.007	22.7	23.0	1380	9.51
2	0.333	0.0385	0.014	23.5			20.0
3	0.485	0.0515	0.021	23.1			29.0
4	0.350	0.066	0.0145	22.6			21.02

Table V-c

Trial No.	S_1 btu/lb	S_2 btu/lb	w.b. btu/lb	Q_1 btu/hr	Q_2 btu/hr	Q_v btu/hr	Q_F btu/hr	E_d %
1	0.249	0.252	1031.5	67800	52500	9800	561	14.55
2	0.251	0.258	1026.8	80400	54200	20540	1340	26.0
3	0.254	0.264	1023	103200	63580	29700	2175	29.4
4	0.263	0.270	1017	126000	92300	21600	1725	17.38

Table V-d

Trial No.	T_T °F	T_C °F	Q_T btu/hr	Q_C btu/hr	Q_{Lc} btu/hr	Q_L btu/hr
1	114.3	149.1	1570	3390	4960	4939
2	116	142	1770	2700	4470	4320
3	125.2	174.5	2805	4960	7765	7755
4	130.1	200	3360	7050	10410	10375

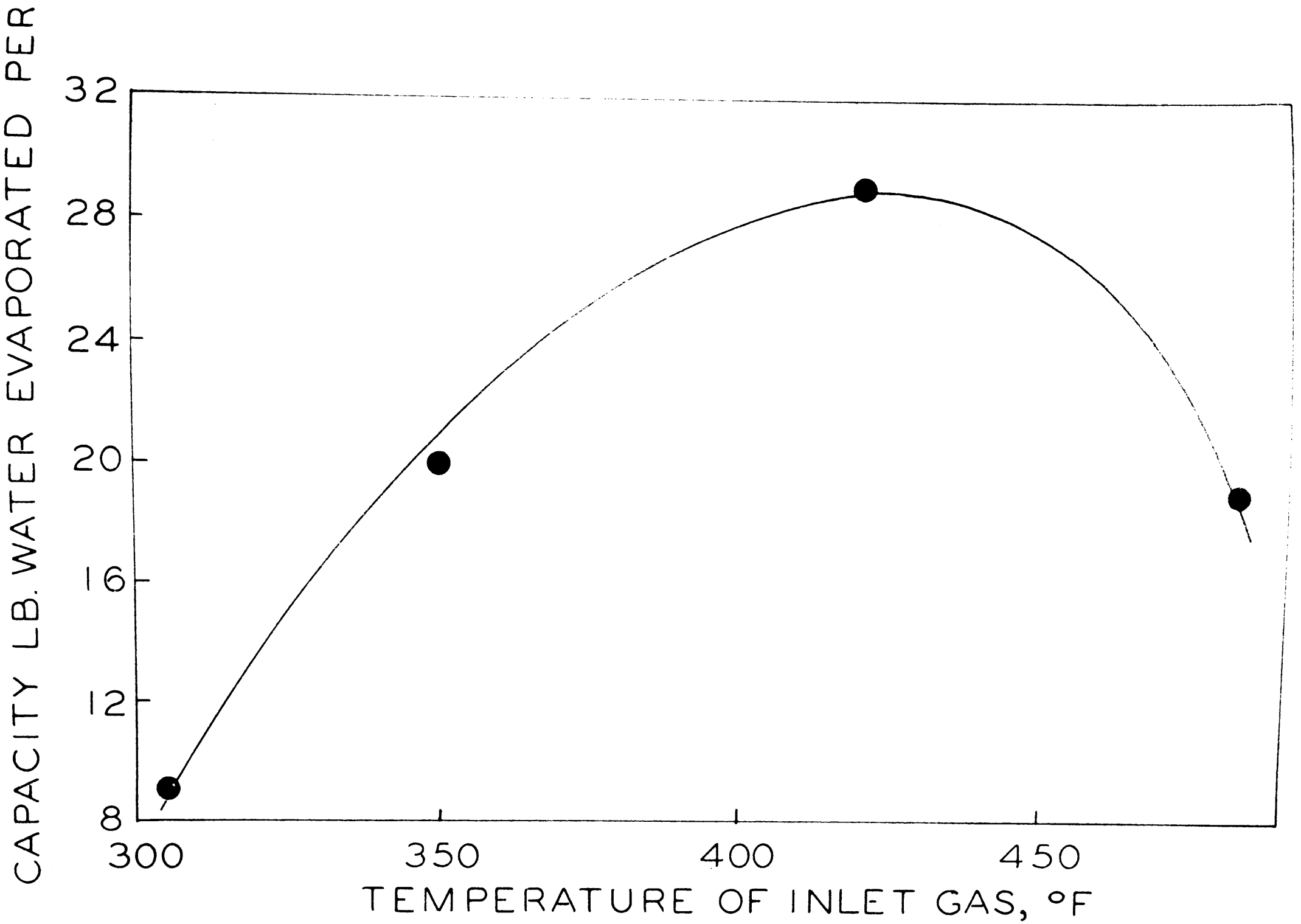

FIG. 13

LIGNOSOL-VARIATION OF INLET FEED TEMPERATURE

LIGNOSOL-VARIATION OF NOZZLE DEPTH AND INLET AIR RATE

Table VI-a

Trial No.	l in.	V cfm.	T_1 °F	T_F °F	T_2 °F	$T_{w.b.}$ °F	P_a psig.	P_L psig.	F U.S.P.M.
5	9.625	308	365	52	301.5	121.5	40	17.5	0.03055
6	11.125	308	365	53	295.2	121.2	50	22.5	0.03495
7	12.375	308	365	51	288.2	121	40	23	0.0425
8	12.875	308	365	52	279	121	40	24	0.0488
9	13.375	308	365	52	293	122.5	40	21.5	0.0372
10	11.125	262	365	53	296.5	121	50	21	0.0267
11	12.375	262	365	51	288.2	121.3	40	20	0.0335
12	12.875	262	365	52	285	121.5	40	21	0.0370
13	13.375	262	365	52	290	121	40	17.5	0.03055
14	11.125	208	365	52	295.8	121.3	50	20	0.0211
15	12.375	208	365	51	282.5	121	40	17	0.0257
16	12.875	208	365	52	275	119	40	20	0.03275
17	13.375	208	365	52	290	122	40	16	0.0239
18	12.375	176	365	51	285.9	123	40	17	0.0211
19	12.875	176	365	52	271	119	40	17.5	0.03055

LIGNOSOL-VARIATION OF NOZZLE DEPTH AND INLET AIR RATE

Table VI-b

Trial No.	w lb/min	H_2 lb/lb	H lb/lb	a_C lb/min	a lb/min	G lb/hr	W lb/hr
5	0.2295	0.0395	0.01	22.95	23	1380	13.73
6	0.2625	0.0405	0.012	23.8			15.76
7	0.3170	0.0415	0.0135	23.5			19.0
8	0.367	0.0435	0.0155	23.65			21.45
9	0.2795	0.0465	0.012	23.2			16.77
10	0.200	0.040	0.01	20.0	19.5	1170	12.0
11	0.250	0.0425	0.013	19.2			15.0
12	0.2795	0.04375	0.01425	19.6			16.77
13	0.2295	0.0410	0.0115	19.9			13.73
14	0.1585	0.041	0.01	15.85	16.33	980	9.51
15	0.192	0.0445	0.0115	16.7			11.5
16	0.249	0.0395	0.015	16.6			14.95
17	0.1795	0.044	0.011	16.3			10.75
18	0.1585	0.0468	0.0112	14.15	14.0	840	9.51
19	0.20	0.0405	0.0135	14.5	14.0	840	12.0

LIGNOSOL-VARIATION OF NOZZLE DEPTH AND AIR RATE

Table VI-c

Trial No.	S_1 btu/lb	S_2 btu/lb	w.b. btu/lb	Q_1 btu/hr	Q_2 btu/hr	Q_v btu/hr	Q_F btu/hr	E_d %
5	0.253	0.258	1024.5	84950	64000	14080	955	16.77
6	0.253	0.259	1024.3	85000	62240	16120	1074	19.22
7	0.2525	0.2595	1025	85000	59600	19200	1330	22.95
8	0.253	0.2605	1025	85100	56800	22020	1480	26.3
9	0.256	0.261	1024	85600	61500	17180	1181	20.35
10	0.254	0.258	1025	72500	53000	12300	816	17.18
11	0.253	0.259	1024.5	71850	50600	15390	1054.5	21.7
12	0.253	0.260	1025	72500	49700	17200	1155	24.1
13	0.253	0.259	1025	72500	51200	14080	947	19.7
14	0.254	0.259	1024.5	60450	44150	9740	658	16.3
15	0.255	0.260	1025	60700	41850	11800	805.7	19.75
16	0.252	0.260	1026.2	61500	39700	15350	1001	25.43
17	0.255	0.258	1024.8	60700	42500	11010	751	18.4
18	0.257	0.262	1024	52250	35800	9745	684	22.9
19	0.252	0.260	1026.2	52000	33150	12320	804	24.15

LIGNOSOL-VARIATION OF NOZZLE DEPTH AND INLET AIR RATE

Table VI-d

Trial No.	T_T °F	T_C °F	Q_T btu/hr	Q_C btu/hr	Q_{L_c} btu/hr	Q_L btu/hr
5	116.0	165	1560	4500	6060	5915
6	117.0	159.5	1670	4010	5680	5570
7	119.0	149.0	1895	3080	4975	4870
8	119.5	148.0	1930	2980	4910	4800
9	121.5	158.0	2135	3700	5835	5739
10	115.15	171.0	1690	4680	6370	6384
11	117.8	149.1	1960	3090	5050	4806
12	115.2	145.0	1675	2970	4645	4445
13	119.8	169	2010	4470	6480	6373
14	115.1	168.5	1670	4400	6070	5902
15	118	164.8	1990	4210	6200	6245
16	118.8	155.5	2060	3520	5580	5449
17	120	169	2030	4500	6530	6439
18	117.2	165.0	1900	4240	6140	6021
19	120.1	157.5	2230	3670	4900	5826

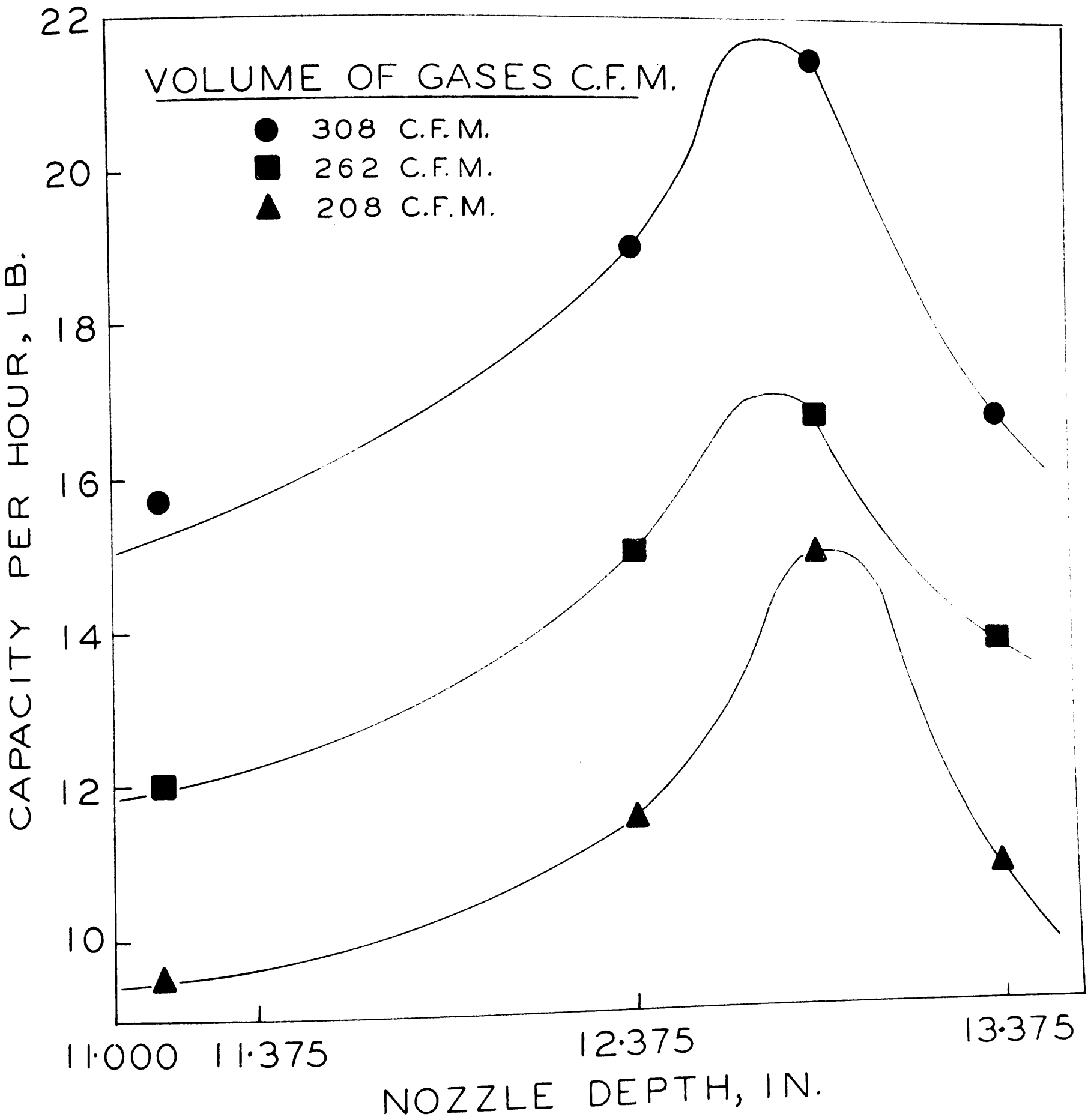

FIG. 14

LIGNOSOL-VARIATION IN NOZZLE DEPTH

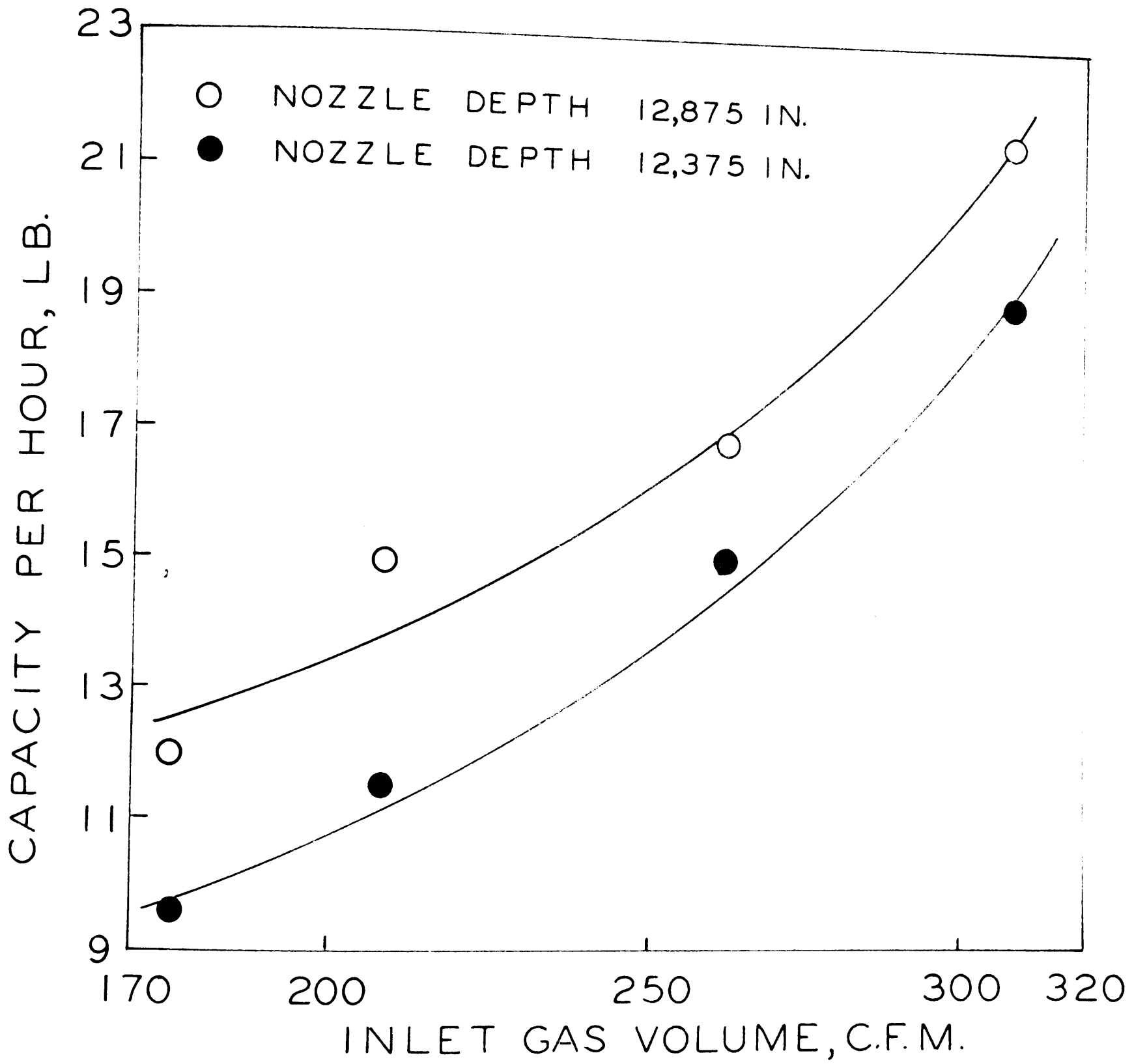

FIG. 15

LIGNOSOL-VARIATION IN INLET AIR RATE

In general, maximum capacity and efficiency, and minimum heat losses occur for the same conditions. The heat balances indicate that, for the same capacity, as the nozzle depth increases the heat losses for the upper section increase while those for the conical section decrease. This interesting behaviour indicates that, as the nozzle location gets further away from the chamber roof, the strong cooling effect of the drying process on the air takes place at lower regions of the chamber. Due to much thicker insulation, the losses from the top of the chamber are less than that of the conical section. It should also be noted that, in general, losses increase with decreasing air rates, all other things being equal.

(c) Variation of Inlet Feed Temperature

The effects of varying the inlet feed temperature at a fixed nozzle position of 12.375 inches, a fixed air rate of 308 C.F.M. (free air) and at a constant inlet gas temperature of 365°F, are shown in figure 16, and the results are tabulated in Tables VII-a, VII-b, VII-c and VII-d.

The above curve is again similar to figure 12, obtained with the evaporation of water alone. A maximum is once more reached in the region of the wet-bulb temperature, but the capacities are, however, much lower than those attained with water. The maximum efficiency occurs at the point of maximum capacity, in spite of the fact that heat losses increase as the inlet feed temperature increases.

(d) Variation of Inlet Feed Temperature at Optimum Conditions

Two additional runs were made, varying the inlet feed temperature at the optimum conditions of all other variables. These runs were made in order to determine the maximum capacity of the chamber in the

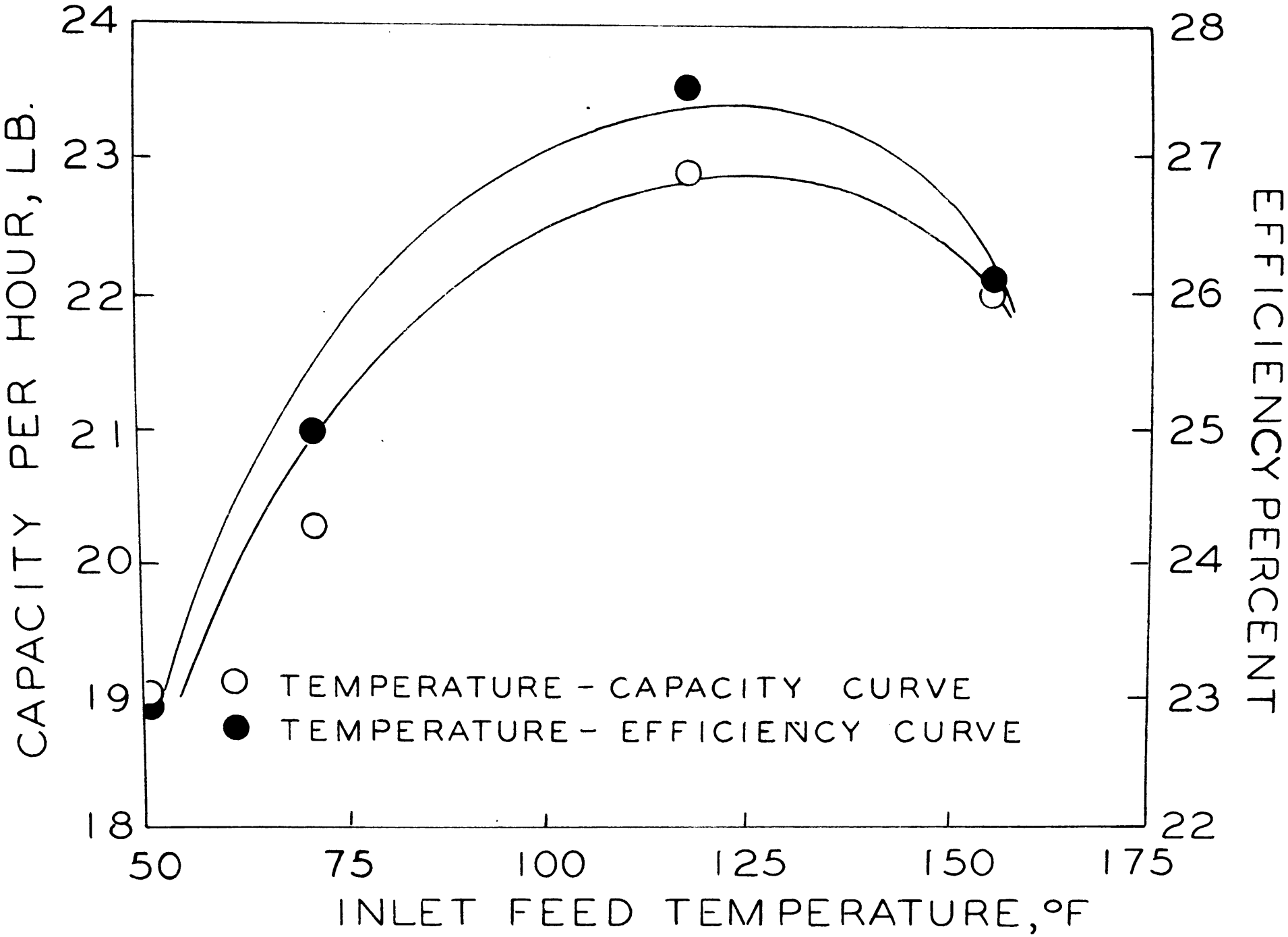

FIG. 16

LIGNOSOL-VARIATION IN INLET FEED TEMPERATURE

LIGNOSOL-VARIATION OF INLET FEED TEMPERATURE

Table VII-a

Trial No.	l in.	V cfm.	T_1 °F	T_F °F	T_2 °F	$T_{w.b.}$ °F	P_a psig.	P_L psig.	F U.S.P.M.
20	12375	308	365	51	288.2	121	40	23	0.0425
21			365	70	282	123	40	23	0.0453
22			365	123	277.8	122.8	40	24.2	0.05115
23			367	158	284	123	40	24	0.0489

Table VII-b

Trial No.	w lb/min	H_2 lb/lb	H lb/lb	a_C lb/min	a lb/min	G lb/hr	W lb/hr
20	0.3170	0.0415	0.0135	23.5	23.0	1380	19.0
21	0.3385	0.0485	0.0145	23.3			20.28
22	0.382	0.049	0.017	22.5			22.88
23	0.367	0.048	0.016	22.95			22.0

Table VII-c

Trial No.	S_1 btu/lb	S_2 btu/lb	w.b. btu/lb	Q_1 btu/hr	Q_2 btu/hr	Q_v btu/hr	Q_F btu/hr	E_d %
20	0.2525	0.2595	1025	85000	59600	19200	1330	22.95
21	0.255	0.2615	1024	85200	57400	21000	1085	25
22	0.255	0.263	1024.1	85300	56200	23450	0	27.5
23	0.254	0.262	1024	85500	58200	22550	-770	26.1

Table VII-d

Trial No.	T_T °F	T_C °F	Q_T btu/hr	Q_C btu/hr	Q_{Lc} btu/hr	Q_L btu/hr
20	119.0	149.0	1895	3080	4975	4870
21	118	161.5	1930	3950	5880	5715
22	117.8	160.5	1920	3910	5830	5650
23	117.0	159.5	1870	3830	5700	5520

spray drying of Lignosol. The results may be seen in Tables VIII-a, VIII-b, VIII-c, and VIII-d.

Only two runs were made, one at the wet-bulb temperature and one above this temperature. The greatest capacity, 42 pounds of water evaporated per hour, and the maximum efficiency of 41.6% occurred when the feed entered at the wet-bulb temperature of the air. They are both much lower than the corresponding values of 62.4 pounds per hour and 71.9% respectively, obtained with water alone.

LIGNOSOL-VARIATION OF INLET FEED TEMPERATURE

Table VIII-a

Trial No.	l in.	V cfm.	T_1 °F	T_F °F	T_2 °F	$T_{w.b.}$ °F	P_a psig.	P_L psig.	F U.S.P.M.
24	12.875	461	420	126	269.5	126	40	28	0.0935
25			420	158	278.5	126	40	26	0.087

Table VIII-b

Trial No.	w lb/min	H_2 lb/lb	H lb/lb	a_c lb/min	a lb/min	G lb/hr	W lb/hr
24	0.700	0.0605	0.030	23.3	23.0	1380	42.0
25	0.653	0.0585	0.0285	22.8			39.2

Table VIII-c

Trial No.	S_1 btu/lb	S_2 btu/lb	w.b. btu/lb	Q_1 btu/hr	Q_2 btu/hr	Q_v btu/hr	Q_F btu/hr	E_d %
24	0.253	0.2655	1023	103000	52700	42970	0	41.6
25	0.254	0.265	1022	103100	55820	40065	-1225	37.5

Table VIII-d

Trial No.	T_T °F	T_C °F	Q_T btu/hr	Q_C btu/hr	Q_{Lc} btu/hr	Q_L btu/hr
24	127.0	168.0	3020	4470	7490	7430
25	128.5	177.0	3160	5190	8350	8470

II ATOMIZATION

1. EQUIPMENT AND PROCEDURE

The procedure and equipment used in this section were identical in every respect with those used in the spray drying section. Trials were again performed on both water and Lignosol as the feed. Where actual capacities were being determined, the criteria already established were applied. However, in certain trials, where the immediate purpose was not the determination of capacity, but a study of atomization under various conditions, the criteria, of course, were no longer applied, since the capacity was often exceeded. In the case of Lignosol runs, the average diameter of the dried particle, D_p, was included in order to examine the subsequent effects of drying conditions on droplet sizes.

2. CALCULATIONS AND TABLE NOMENCLATURE

In this section, since attention was primarily focused on atomization and its relation to certain operating conditions, only the immediately relevant variables and quantities were calculated. This permitted the use of a single table for each set of runs.

The average droplet diameter, D_o, was calculated from equation (2) on page 9. The value of the liquid rate, Q_l, was obtained directly from measured feed rates. The value of Q_a was calculated by measuring the flow across the orifice in the compressed air line to the nozzle, and correcting for conditions existing at the vena contracta. These conditions were determined by means of equation (1) given on page 8. The above flow rates were checked by data supplied by the nozzle manufacturers, and also by other available tables (34). The velocity of the

air, v_a, was calculated by equation (3) shown on page 9. In all cases where the pressure of the air to the nozzle was greater than 15 psig., the ratio P_2/P_1 was replaced by its critical value, 0.53.

When operating on water alone, the physical properties required to solve equation (2) were obtained from available data (129). The physical properties of the Lignosol solution and the average particle diameter, D_p, were determined experimentally, the methods being described and the values tabulated in a later section. As in the first experimental section, a system of table nomenclature has been used:

T_F = temperature of inlet feed, ^oF

P_a = pressure of compressed air at the nozzle, psig.

P_L = pressure of liquid feed at the nozzle, psig.

W' = feed rate, lb./hr.

W = actual capacity, lb. water evaporated/hr..

Q_l/Q_a = ratio of volumetric liquid to air rate at the vena contracta

v_a = velocity of air at vena contracta, metres/sec.

v_l = velocity of liquid at throat, metres/sec.

v = relative velocity of air and liquid in nozzle = $v_a - v_l$

D_o = average droplet diameter, microns

D_p = average particle diameter, microns

3. EXPERIMENTAL RESULTS

WATER RUNS

a) Variation of Air Rates to the Nozzle

Eight runs were made at a constant nozzle depth, 12.375 in., temperature of inlet drying gases, 365°F, volumetric rate of drying gases, 308 C.F.M., feed rate, 19.6 lb./hr., and feed temperature, 65°F. The

air pressures at the nozzle were increased from 3 psig. to 50 psig. Since it was observed that droplets hit the walls of the chamber at all but the two highest air pressures, additional spray drying runs were made to determine the maximum capacity, W, at each pressure, under otherwise identical operating conditions. The complete results are shown in Table IX, and the variation of droplet size with the absolute air pressure at the nozzle is shown in figure 17.

The above results indicate that, as the air pressure at the nozzle increases, with a subsequent increase in the air rates, the average droplet diameter, D_o, decreases, levelling off at the point at which the critical pressure rate, $P_2/P_1 = 0.53$, is reached. It may also be observed from the tabulated results that actual maximum capacities increase with decreasing values of D_o, and reach a maximum at a nozzle air pressure of about 40 psig. Further increase in pressure shows no indication of producing increased capacities. It should be noted that the range of values of D_o is considerably higher than predicted in the theory, owing to the fact that Q_l/Q_a in the second term of the Nukiyama and Tanasawa equation is not a negligible quantity.

b) Variation of Feed Temperature

The effects on average droplet diameter of varying the feed rates, all other conditions being fixed, are presented in Table X, page 94, and a curve of this variation may be seen in figure 18. The fixed operating conditions were nozzle depth, 12.875 in., inlet air temperature, 365°F, and volumetric rate, 308 C.F.M.

It may be noted that the average drop size decreases with increasing feed temperatures, in spite of larger values of Q_l/Q_a at

TABLE IX

WATER-VARIATION OF NOZZLE AIR PRESSURE

Trial No.	T_F °F	P_a psig.	P_L psig.	W' lb/hr	W lb/hr	Q_l/Q_a ratio	v_a m/sec	v_l m/sec	v m/sec	D_o microns
1	65	3	22	19.6	-	.00341	197.5	2.9	194.6	223.2
2		6	22	19.6	-	.002425	223	2.9	220.1	134.4
3		12	22	19.6	8.33	.001745	300	2.9	297.1	85.05
4		16	22	19.6	9.51	.001675	309.5	2.9	295.6	78
5		20	22	19.6	10.75	.00166	309.5	2.9	295.6	79
6		30	22	19.6	12.5	.001535	309.5	2.9	295.6	72.7
7		40	22	19.6	19.6	.001675	309.5	2.9	295.6	78.0
8		50	22	19.6	19.5	.001670	309.5	2.9	295	79.2

TABLE X

WATER-VARIATION OF INLET FEED TEMPERATURE

Trial No.	T_F °F	P_a psig.	P_L psig.	W lb/hr	Q_l/Q_a ratio	v_a m/sec	v_l m/sec	v m/sec	D_o microns
9	53	40	20	16.77	.00143	309.5	2.48	307.02	68.05
10	70	40	21	17.5	.00149	309.5	2.56	306.96	66.1
11	123	40	24	20.0	.00171	309.5	2.96	306.54	64.55
12	158	40	23	19.6	.001675	309.5	2.9	306.6	55.65

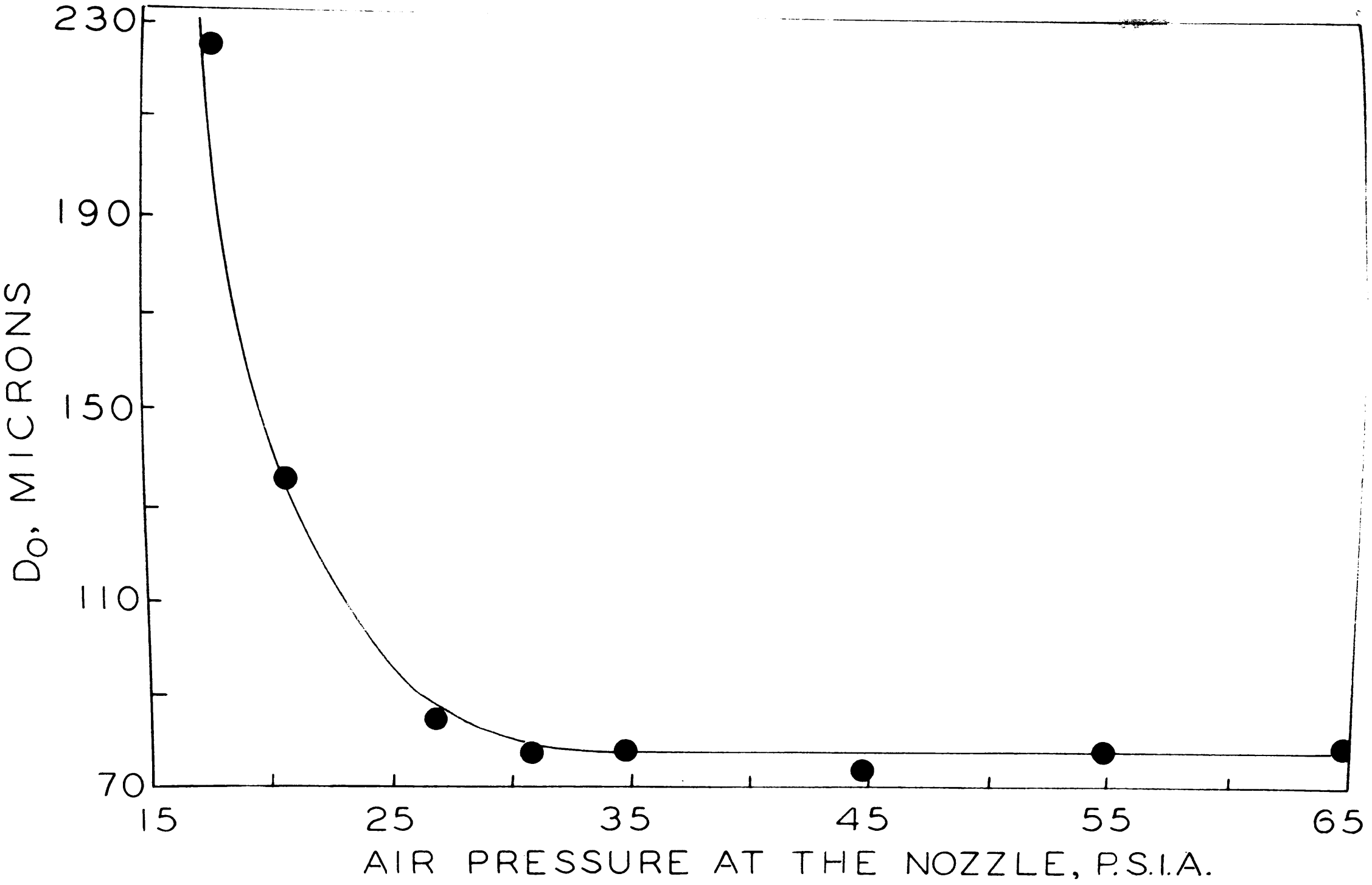

FIG. 17

WATER-VARIATION OF NOZZLE AIR-RATE

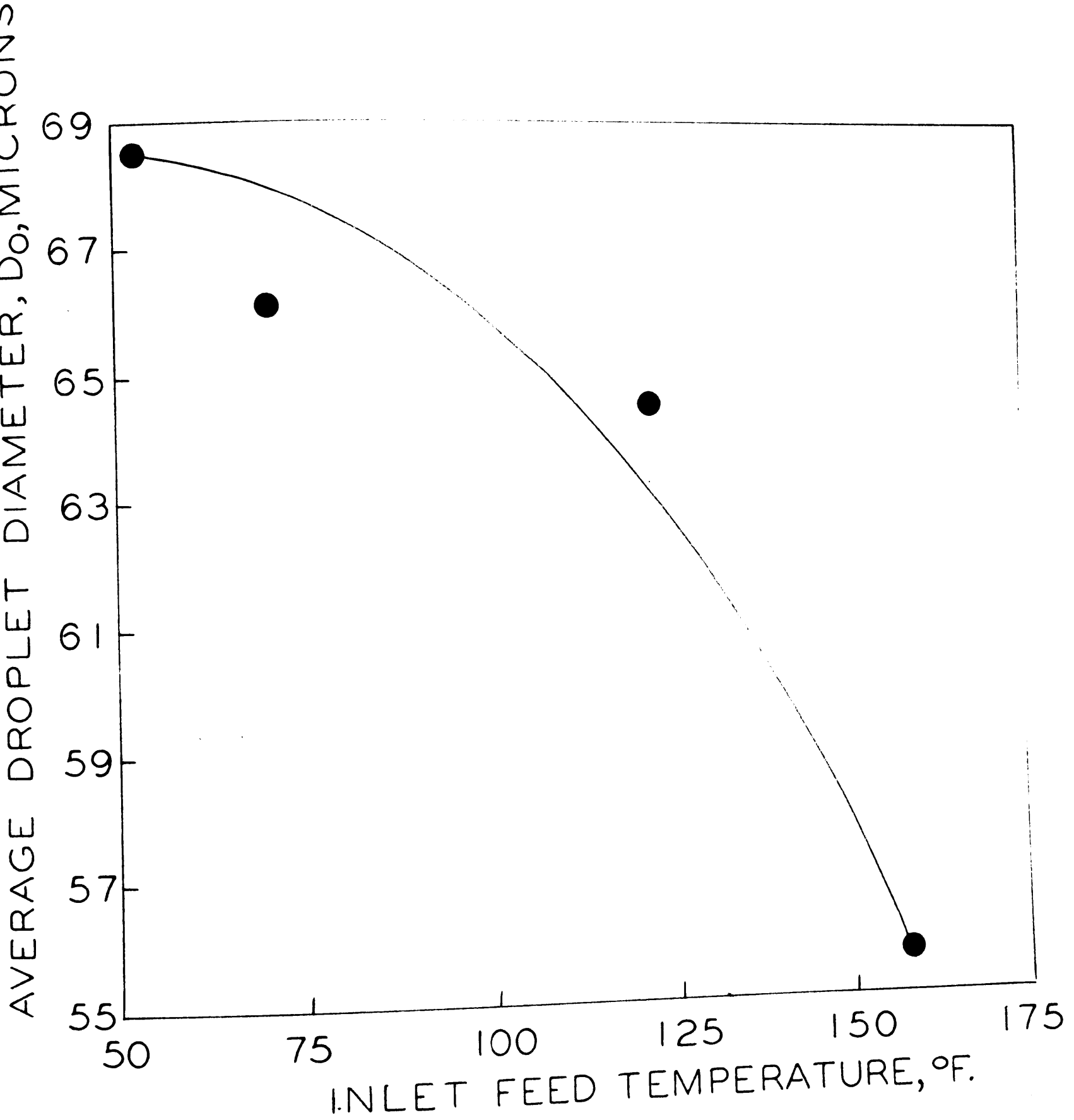

FIG. 18

WATER-VARIATION OF INLET FEED TEMPERATURE

higher temperatures, because the physical properties of the feed are affected to an even larger extent.

LIGNOSOL RUNS

a) Variation of Air Rates to the Nozzle

At a fixed nozzle position of 12.875 in., inlet drying air temperature, 365°F, volumetric rate, 308 C.F.M., fixed feed temperature, 65°F, and feed rate, 15.76 lb./hr., the effect of varying the air rate to the nozzle was studied. The results may be seen in Table XI and figure 19.

As in the case of the equivalent water run (see figure 17), the average droplet size, D_o, decreases with increasing air pressure at the nozzle. Figure 19 also indicates the variation of average particle diameters obtained from products collected in this trial. As can be seen, both curves indicate a similar variation, a levelling-off, occurring after air pressures exceeding 12 psig. Also notable is the considerable difference in magnitude between D_o and D_p.

b) Variation of Temperature of Drying Air

A series of four runs were performed at a fixed nozzle position, 12.5 in., volumetric flow rate, 308 C.F.M., and inlet feed temperature, 65° F, to study the effect of the temperature of the inlet drying gases on the average droplet diameter, D_o, and the average particle diameter, D_p. The results are shown in Table XII, page 98, and figure 20. D_o, and the corresponding particle diameter, D_p, were plotted against the inlet drying temperature, as shown in the above figure.

TABLE XI

LIGNOSOL-VARIATION OF NOZZLE AIR PRESSURE

Trial No.	T_F °F	P_a psig.	P_L psig.	W' lb/hr	W lb/hr	Q_l/Q_a ratio	v_a m/sec	v_l m/sec	v m/sec	D_o microns	D_p microns
1	65	3	17	15.76	-	.00275	197.5	2.33	195.17	207.7	24.2
2	65	6	17	15.76	-	.00195	223	2.33	220.67	131.1	17.8
3	65	12	17	15.76	9.51	.001405	300	2.33	297.67	82.6	16.25
4	65	30	17	15.76	15.76	.00125	309.5	2.33	306.17	71.2	14.6
5	65	40	17	15.76	20.28	.00134	309.5	2.33	306.17	77.4	15.3
6	65	50	17	15.76	20.28	.00134	309.5	2.33	306.17	77.4	14.5

TABLE XII

LIGNOSOL-VARIATION OF TEMPERATURE OF DRYING AIR

Trial No.	T_1 °F	T_F °F.	P_a psig.	P_L psig.	W lb/hr	Q_l/Q_a ratio	v_a m/sec	v_l m/sec	v m/sec	D_o microns	D_p microns
7	282	65	40	17	9.51	.000814	309.5	1.41	307.09	43.05	13.1
8	365	65	40	23	20.28	.001735	309.5	3.0	306.5	111.46	14.5
9	420	65	40	25.5	29.0	.00245	309.5	4.43	304.07	168.07	15.4
10	482	65	40	23.5	23.0	.00196	309.5	2.81	306.1	155.99	19.0

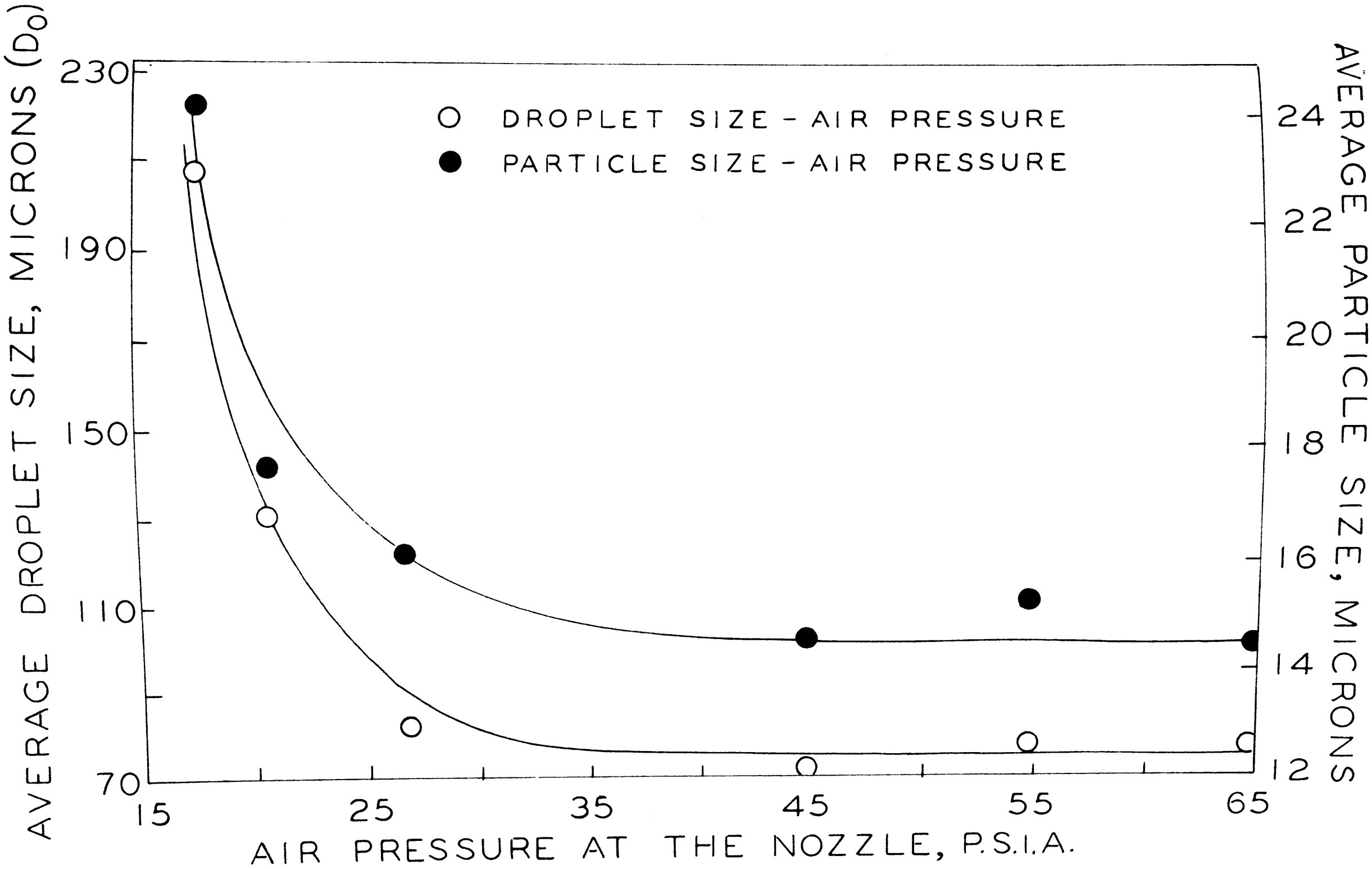

FIG. 19

LIGNOSOL-VARIATION OF NOZZLE AIR RATE

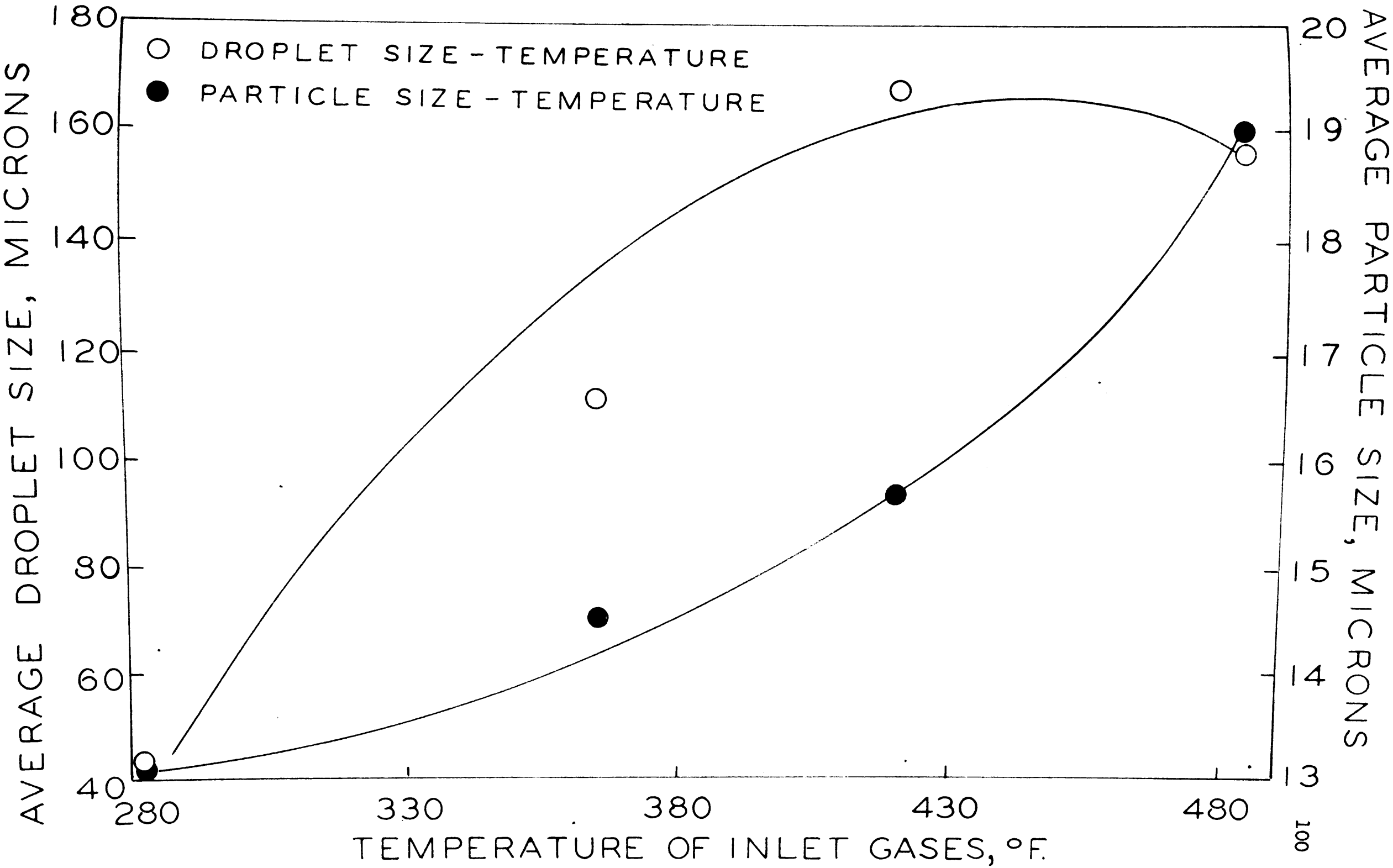

FIG. 20

LIGNOSOL-VARIATION OF INLET AIR TEMPERATURE

Both droplet and particle diameters increase with increasing temperature. However, the effect is considerably more pronounced in the case of the droplet size.

c) Variation of Inlet Feed Temperature

All other conditions being kept constant, the effect of varying the inlet feed temperatures on the droplet and particle diameters is presented in Table XIII and figure 21. The fixed conditions were nozzle depth 12.375 in., temperature of inlet air, 365°F, and volumetric rate, 308 C.F.M.

It is extremely interesting to note that the droplet diameters decrease, while under the existing drying conditions, the equivalent particle diameters increase. Again, the order of magnitudes is considerably higher in the case of average droplet diameters. Of considerable interest also is the fact that, in run 13, the feed enters at the wet-bulb temperature of the air.

d) Variation of Volumetric Rate of Drying Gases

The effect of varying the volumetric rate of drying gases, on average droplet and particle diameters, other conditions being identical to the previous set of runs, may be seen in Table XIV, page 102, and figure 22.

It may be noted that, as in the previous set of runs, the increase in diameter is in opposite directions, droplet diameters decrease with a decrease in volumetric rate, while particle diameters increase. Once more, a considerable disparity in magnitude of these two dimensions is evident.

TABLE XIII

LIGNOSOL-VARIATION OF INLET FEED TEMPERATURE

Trial No.	T_F °F	P_a psig.	P_L psig.	W lb/hr	Q_l/Q_a ratio	v_a m/sec	v_l m/sec	v m/sec	D_o microns	D_p microns
11	53	40	22.5	19.0	.00162	309.5	2.81	306.69	114.12	14.5
12	70	40	23	20.28	.001735	309.5	3.0	306.5	111.4	15.6
13	123	40	24	22.88	.00195	309.5	3.38	306.12	90.3	15.2
14	158	40	23.5	22.0	.00187	309.5	3.25	306.25	80.8	18.3

TABLE XIV

LIGNOSOL-VARIATION OF VOLUMETRIC RATE OF DRYING AIR

Trial No.	V cfm.	T_F °F	P_a psig.	P_L psig.	W lb/hr	Q_l/Q_a ratio	v_a m/sec	v_l m/sec	v m/sec	D_o microns	D_p microns
15	308	65	40	22.5	19	.00162	309.5	2.81	306.69	100.75	14.5
16	262	65	40	20	15	.00128	309.5	2.22	307.28	73.22	14.4
17	208	65	40	18	11.5	.000984	309.5	1.70	307.8	54.06	16.1
18	176	65	40	17	9.51	.000815	309.5	1.41	307.09	44.75	18.9

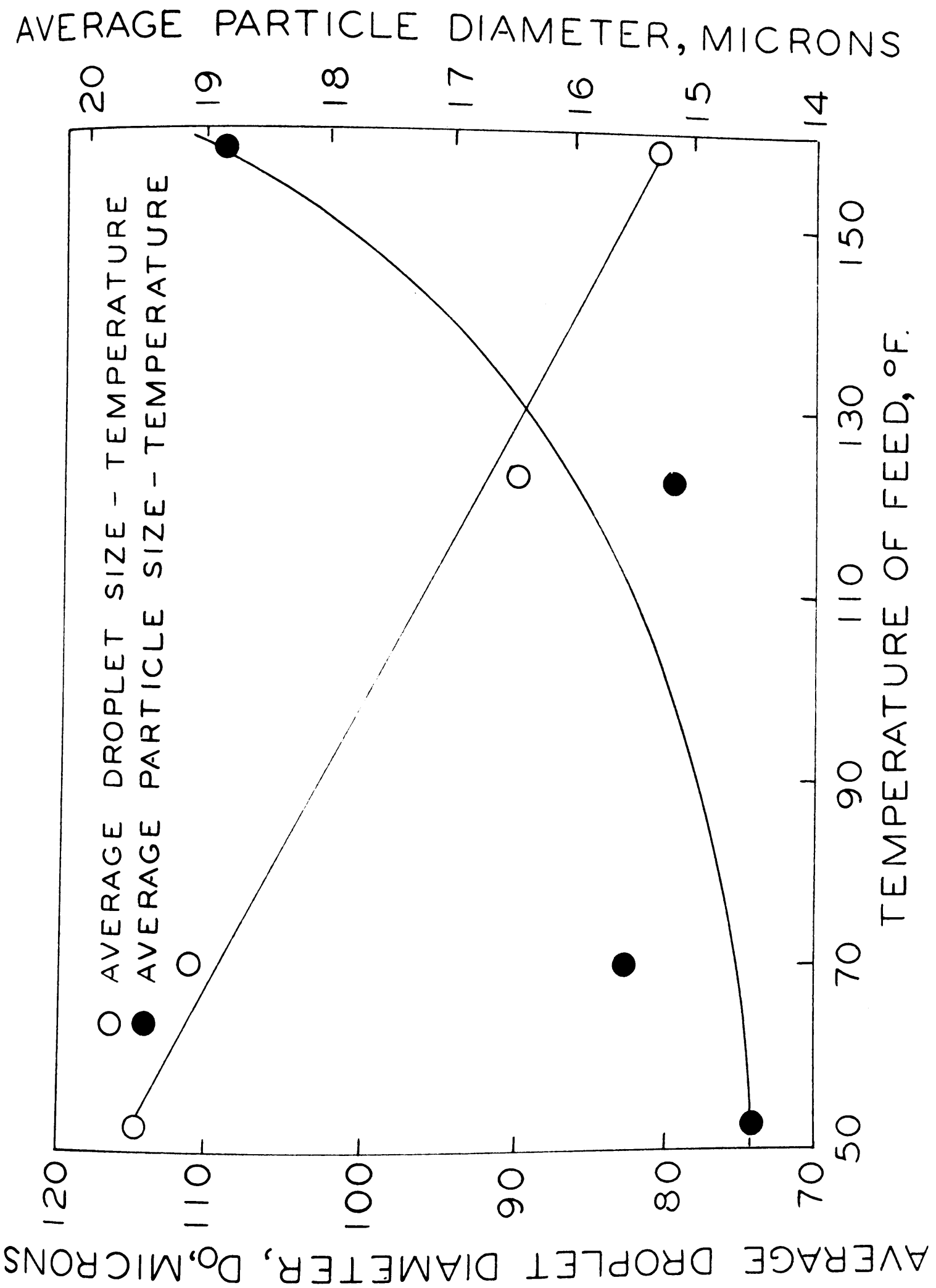

FIG. 21

LIGNOSOL-VARIATION OF INLET FEED TEMPERATURE

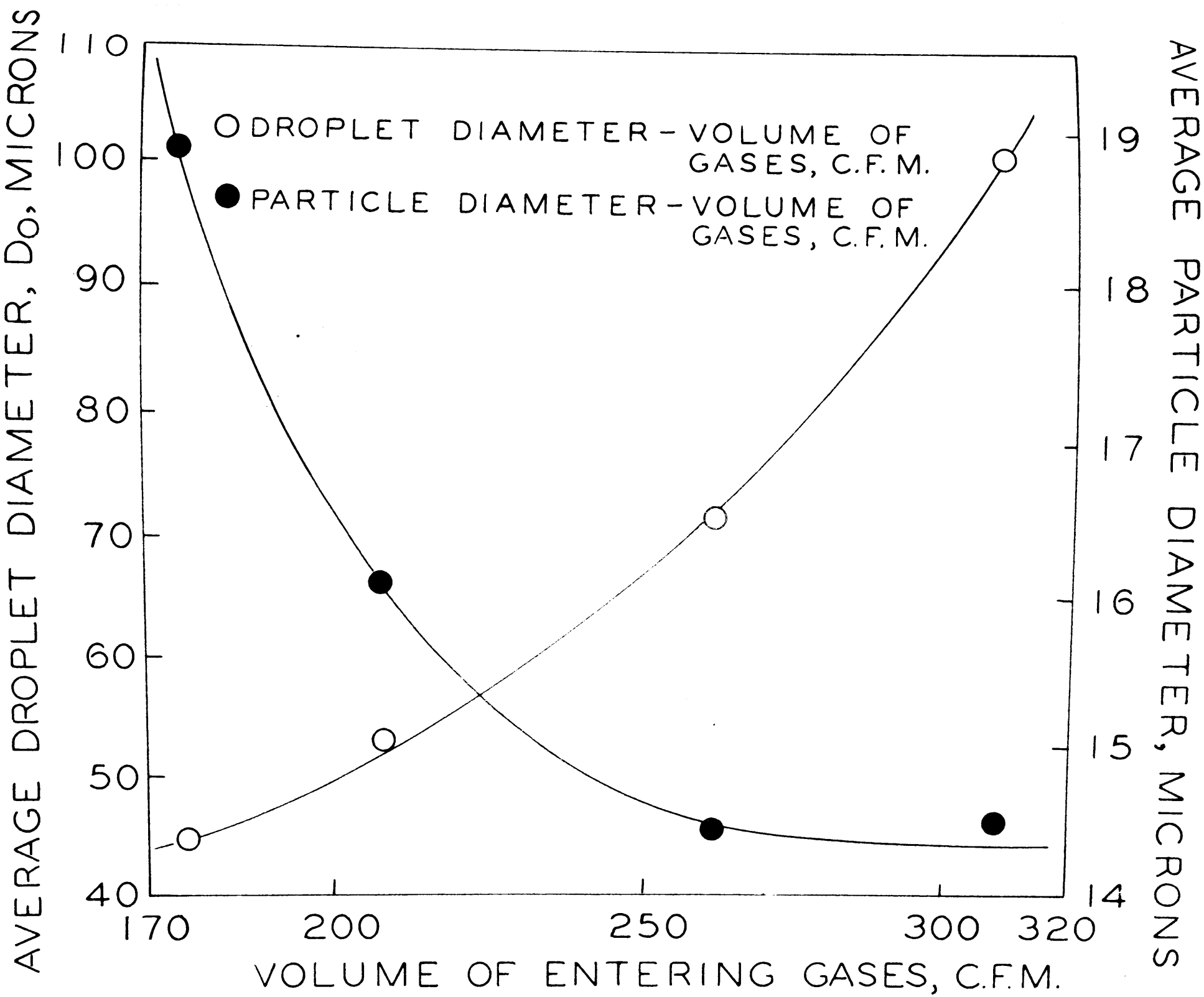

FIG. 22

LIGNOSOL-VARIATION OF VOLUMETRIC RATE

III PHYSICAL PROPERTIES OF FEED AND SPRAY-DRIED PRODUCT

1. APPARATUS AND PROCEDURE

The properties of the 10% Lignosol solution necessary for the calculation of D_o (see previous section), namely surface tension, density and viscosity, were not available from any known source and thus had to be determined experimentally. These properties were obtained by standard analytical methods: the surface tension by the capillary-rise method using a small cathetometer; the density on a chainomatic hydrometer balance; and the viscosity with an Ostwald-Cannon-Fenske Viscometer. The pH of initial and reformed solutions were determined with a standard pH meter.

The absolute density of the powder was determined with a Weld pycnometer, benzene being used as the suspension medium. Bulk density comparisons were made by utilizing a calibrated weighing bottle as a standard volume, and standardizing the packing technique. The powder was also examined microscopically.

The sedimentation-rate method of particle size distribution (27, 48, 79) was selected after a thorough study had been made of comparative methods (16, 18, 28, 50, 76, 89, 118, 137). An excellent article reviewing and estimating the relative values of a number of existing techniques is provided by Hawksley (73). A decision was finally made to use the sedimentation-rate method, in conjunction with a Joly balance, as results could be obtained with reasonable accuracy and rapidity.

Upon thorough investigation, benzene was chosen as the suspension medium, since both its density and wetting power gave satisfactory settling rates with the Lignosol powder. A slight variation was introduced in the standard technique. In order to minimize any initial velocity imparted to the particles when transferring them to the suspension tube, a shallow spoon was held just under the surface of the benzene column. The particles, which had been previously wetted and dispersed in a small amount of benzene, were quickly poured from a shallow dish into the suspension tube, withdrawing the spoon just before impact.

2. METHODS OF CALCULATION AND TABLE NOMENCLATURE

The physical properties of the Lignosol solution were calculated by the standard relations applying to the apparatus utilized for their determination.

Particle size distributions were obtained by plotting the weight settled against time, after first calibrating the spring scale on the Joly balance. The sedimentation-rates taken from this curve were then applied to the well-known Stokes law equation:

$$D = 20{,}000\sqrt{\frac{9}{2}\mu\frac{dx/dt}{(\rho_p-\rho_m)980}} \qquad (21)$$

giving particle diameters, D, in microns, for various size limits. Tangents are drawn to the sedimentation-rate curve, the intercepts of any two on the ordinate corresponding to the weight per cent of the material in the size interval at whose limits the tangents are constructed.

The definition of the average particle diameter, D_p, is identical to that of the average droplet diameter, D_o, namely, that diameter of a single particle with the same ratio of surface to volume as the

total sum of particles. This diameter was then determined from the experimental data by a graphical integration of the following equation, corresponding to the definition:

$$D_p = \frac{D^3 dn}{D^2 dn} \qquad (22)$$

A typical drop-size distribution is illustrated in the following table (representing trial 5, in Table XI, page 94). The viscosity of the benzene was 0.00638 poise, density 0.879 gm./cu.cm., and absolute density of the particle, 1.80 gm./cu.cm. The diameters, D, were calculated by equation (21).

Time sec.	dx/dt cm/sec	$dx/dt)^{\frac{1}{2}}$ $(cm/sec)^{\frac{1}{2}}$	D microns	corresponding weight gm.	corresponding weight %	D_p microns
0						
60	0.3285	0.5720	69.96	0.015	1.96	
225	0.0876	0.2959	36.16	0.05	6.54	
285	0.0692	0.2635	30.9	0.095	12.41	
540	0.0365	0.1910	23.36	0.095	12.41	
975	0.0202	0.1420	17.4	0.12	15.7	15.3
1305	0.01510	0.1229	15.04	0.045	5.88	
1950	0.0101	0.1008	12.34	0.13	16.99	
2930	0.00810	0.090	11.0	0.11	14.38	
3180	0.00620	0.0786	9.62	0.105	13.73	

For the purpose of comparison, it is important to note that the trial numbers indicated in Table XVI correspond to those shown in the Atomization section of Lignosol runs, page 98 and 102.

The following system of table nomenclature, which also applies to the symbols used in equations (21) and (22), is presented:

dx/dt = sedimentation rate, cm./sec.

ρ_p = density of particle, gm./cu.cm.

ρ_m = density of suspension medium, gm./cu.cm.

ρ_w = density of water, gm./cu.cm.

ρ_l = density of Lignosol solution, gm./cu.cm.

ρ_b = bulk density of powder, lb./cu.ft.

D = particle diameter for a given range, microns

D_p = average particle diameter, microns

μ = viscosity of suspension medium, poise

μ_w = viscosity of water, poise

μ_l = viscosity of 10% Lignosol solution, poise

σ_w = surface tension of water, dynes/cm.

σ_l = surface tension of Lignosol solutions, dynes/cm.

pH = hydrogen ion concentration of reformed solution

T_l = temperature of inlet drying air, ^oF

T_F = temperature of inlet feed, ^oF

Pa = pressure of air at the nozzle, psig.

V = volumetric rate of drying gas, C.F.M.

3. EXPERIMENTAL RESULTS

a) Physical Properties of Liquid Feeds

The physical properties of the liquid feeds are indicated in Table XV.

b) Physical Properties of Spray Dried Product

For the purpose of convenience, the physical properties of the dried material collected during the trials made in the Atomization Section are presented in Table XVI. Only relevant operating conditions

TABLE XV

PHYSICAL PROPERTIES OF LIQUID FEEDS

Water				Lignosol			
T_F °F	ρ_w gm./cu.cm.	σ_w dyne/cm.	μ_w poise	T_F °F	ρ_l gm./cu.cm.	σ_l dyne/cm.	μ_l poise
53	0.99975	74.2	.013098	53	1.0526	62.5	.0285
70	0.9982	72.7	.009608	70	1.0523	60.18	.0220
123	0.9880	67.8	.00545	123	1.0510	55.55	.0093
126	0.987	67.5	.00532	126	1.0505	55.0	.0085
158	0.9778	64.42	.004071	158	1.049	54.9	.0061

TABLE XVI

PHYSICAL PROPERTIES OF SPRAY DRIED PRODUCT

Trial No.	T_l °F	T_F °F	V cfm.	P_a psig.	D_p microns	ρ_b lb/cu.ft.	pH
1	365	65	308	3	24.2	6.89	
2	365	65	308	6	17.8	7.5	
3	365	65	308	12	16.25	8.1	
4	365	65	308	30	14.6	9.14	
5	365	65	308	40	15.3	9.3	
6	365	65	308	50	14.5	9.35	
7	282	65	308	40	13.1	9.4	8.02
8	365	65	308	40	14.5	9.06	7.98
9	420	65	308	40	15.4	7.3	7.93
10	482	65	308	40	19.0	5.82	7.88
11	365	53	308	40	14.5	8.1	
12	365	70	308	40	15.6	9.3	
13	365	123	308	40	15.2	9.35	
14	365	158	308	40	18.3	8.73	
15	365	65	308	40	14.5	8.53	
16	365	65	262	40	14.4	6.84	
17	365	65	208	40	16.1	6.35	
18	365	65	176	40	18.9	6.21	

have been indicated but more complete particulars can be obtained by reference to this section.

A discussion of the particle diameter, D_p, in reference to atomization conditions, has already been given in the previous section. Its relationship to bulk density appears to be rather well defined in any given set of experimental runs, but no overall dependence of bulk density, on average particle size alone, can be established. Particularly striking are the pronounced effects of inlet air temperatures on the bulk density, higher temperatures corresponding to very light materials. In a very general way the bulk density increases as the average particle diameter decreases.

In connection with the pH measurements, it is interesting to note that, while the original pH of the 10% Lignosol feed is 4.25, considerably higher values were obtained for the reformed solutions. Moreover, a very specific dependence appears to exist between pH of reformed solution and temperature of drying air, the pH decreasing with an increase in air temperatures. A possible chemical change at higher temperatures appears to be indicated. In support of this, it should be pointed out that a marked darkening of the otherwise white powder occurred at the high temperatures.

c) Microscopic Studies

Microscopic studies established that the particles were mainly spherical in shape, transparent and hollow. This latter fact was discovered when some of the particles were crushed and then examined, the egg-shell shapes attesting to their hollow form. The range of sizes was estimated as comparable to those established in particle size distributions.

The above results are well illustrated in the micrographs shown in figures 23, 24 and 25. In every case the magnification is 700 diameters. Figure 23, showing a sample of dispersed spherules, gives some indication as to shape, size and transparency. In figure 24, the microscope had been focused to show interference rings in light reflected from inside and outside top surfaces of the particle, while figure 25 illustrates the fragments formed by crushing the spherules between glass microscope slides. These latter figures support the contention that the particles are mainly hollow.

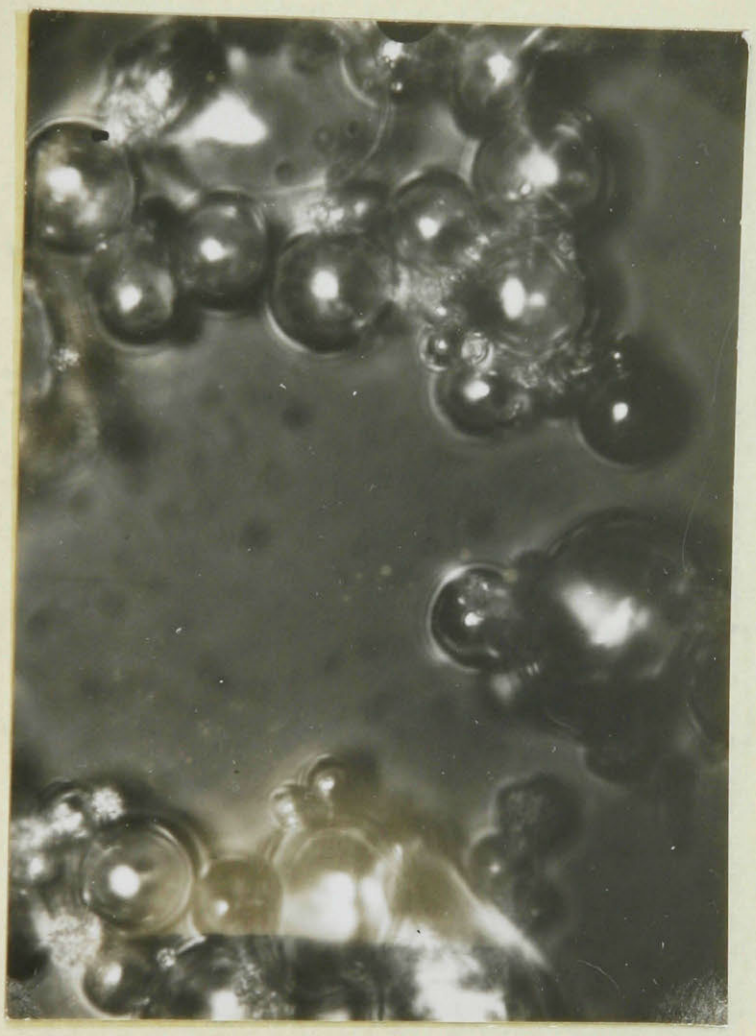

FIG. 23

MICROGRAPH - SHAPE AND SIZE OF DISPERSED SPHERULES

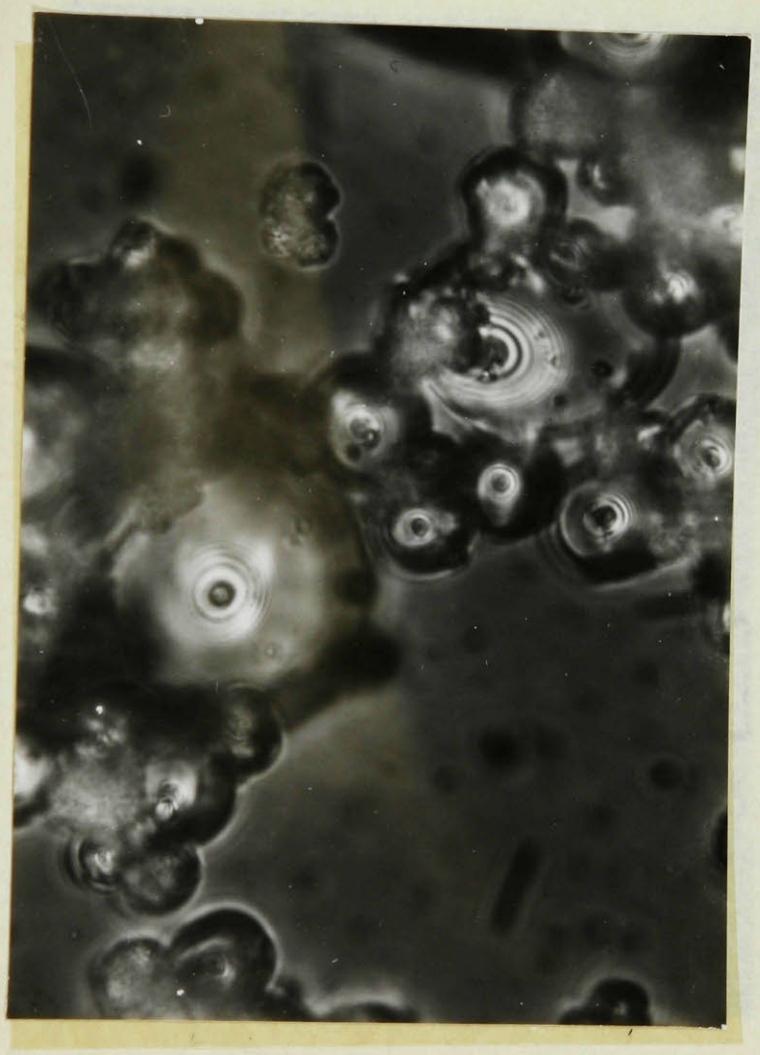

FIG. 24

MICROGRAPH - INTERFERENCE RINGS IN LIGHT REFLECTION FROM OUTSIDE TOP SURFACES

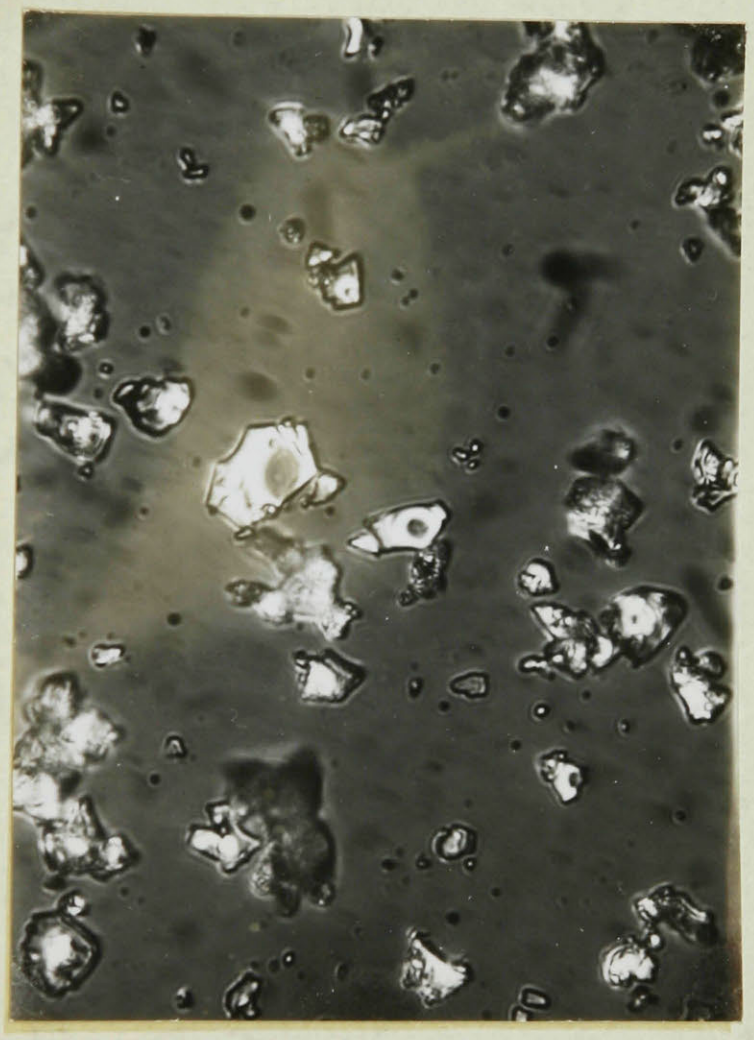

FIG. 25

MICROGRAPH - CRUSHED FRAGMENTS OF HOLLOW PARTICLES

CONCLUSIONS

A large amount of experimental data have been presented. Owing to the great number of factors involved, it is at first sight impossible to establish clearly the inter-relationships which undoubtedly exist. However, careful analysis reveals the existence of a few fundamental principles which appear to dominate the whole range of phenomena and give it a surprising degree of continuity.

As all rate processes, spray drying is governed by the concept of driving force and resistance. More specifically, spray drying is a diffusional process, and as such, the driving force is measured by a partial pressure or humidity difference while the resistance can be recognized as that of an interphase film. In the light of this concept, any variable which will influence these two factors will affect the rate of spray drying.

The major variable affecting the driving force is the inlet temperature of the drying air. It has already been pointed out that the temperature assumed by the droplet during the drying process is the wet-bulb temperature of the air. The higher the temperature of the air, the higher its wet-bulb, and hence the higher the vapor pressure of the water droplet corresponding to it. In the case of solutions, a reduced vapor pressure results in a reduced driving force. The humidity of the entering air is of lesser importance although in direct heaters it may be affected to a certain extent by the hydrogen content of the fuel.

The two main variables affecting the film resistance are the relative velocity of particle and air stream, and turbulence in the

latter, as shown by Maisel and Sherwood (108, 109). The first effect, in its simpler aspects, is governed by the laws of particle motion in turbulent air streams and by the degree of atomization. As for the second effect, there is no simple way of assessing its magnitude at the present stage of development.

It is obvious that all factors affecting the drying rate will also affect the capacity which is a direct function of it. In addition, however, capacity also depends on atomization because the latter governs the particle size and therefore the total transfer area. Moreover, atomization will set a definite limit to the capacity beyond which, on the basis of the criterion adopted in this investigation, the largest droplets will begin to hit the walls.

Efficiency, on the other hand, will be a function of both capacity and heat losses. While increased capacities can be expected at higher inlet air temperatures, all other conditions being constant, higher heat losses by radiation and convection will limit the efficiency.

On the basis of the principles thus established it is now possible to examine the experimental results obtained. The discussion will always be based on the drying of the largest particles present in the spray, as it has already been pointed out that they exert a controlling influence on all the rate processes involved. When the inlet drying air temperature is increased, the capacity increases, owing to an increase in driving force. A maximum capacity is reached, however, beyond which the heat losses exert a predominating influence and the capacity decreases. The same general behavior is followed, whether water or Lignosol is the feed. Comparison between Tables I

and V shows that the chamber has a much greater capacity in the case of water. This general effect occurs whenever comparable operating conditions are maintained and can be explained by a number of facts. The drying rate of a water droplet remains constant until it has totally evaporated, while in the case of a Lignosol solution the drying rate will decrease as the water vapor pressure decreases. This will generally not occur until the falling-rate period is reached for a colloidal solution, but will take place much sooner when a true solution is being dried. Of equal importance is the fact that a droplet of solution will still possess an appreciable size after bulk evaporation. As it is by that time in a lower region of the chamber, its radius of gyration will be correspondingly shorter and the centrifugal forces acting on it will be greater. Owing to the nature of the criterion adopted, this will effectively decrease the capacity of the chamber.

The critical influence of turbulence and relative velocity is most strikingly illustrated in the relation between nozzle depth and capacity, figure 9 for water, and figure 14 for Lignosol. If it can be assumed, as proposed by Edeling (44, 45), that the turbulent gas stream has no influence on the atomized spray until the droplets approach their terminal velocity, it can be readily demonstrated that an optimum nozzle position must exist. When the nozzle is located close to the top of the chamber, the terminal velocity of the spray is reached at a point where the velocity of the air stream, being measured in the cylindrical part of the chamber, is relatively small. As the nozzle depth is increased, the point of terminal velocity occurs

in regions of increasing gas velocities, due to the narrowing diameter of the chamber. On the other hand, if the location of the nozzle is too low, the droplets will hit the walls before reaching their terminal velocities. Thus an optimum position must exist between the two extremes. It is interesting to note that this optimum location is lower in the case of Lignosol solutions. It might be expected that, owing to the lower driving forces and correspondingly lower drying rates, the most favorable relation between the point of terminal velocity and gas velocity would be altered, and would probably occur in a region of higher gas velocities.

Figure 10 reveals that an optimum gas velocity and hence an optimum relative particle velocity definitely exists. As the velocity of the gas stream past the droplet increases, the laminar or stagnant diffusion film surrounding the latter gets thinner and the capacity is thereby increased. Beyond an optimum gas rate, increased centrifugal effects and shorter available drying times preponderate, resulting in decreased capacities. No such optimum volumetric rate was obtained in the case of the corresponding Lignosol trial, figure 15, but the shape of the two curves indicates that a similar behavior is followed. The lower capacities observed in this case, compared with those with water, have already been explained.

By combining the optimum conditions previously discussed, greatly increased capacities were obtained, as shown in figure 11. But, no such corresponding increases in efficiency were obtained. As a matter of fact the largest efficiency ever determined (92% in run 28, page 69) corresponded to a fairly low evaporative capacity.

The large effects exerted by the inlet feed temperature on the capacity were certainly unexpected. To account for them, it must be postulated that an appreciable element of time, at least when the total time available is considered, must be involved in the attainment of the wet-bulb temperature by the droplet. It must be remembered that Fogler and Kleinschmidt (57) stressed the marked cooling effects that accompany the expansion of the streams in a gas-atomizing nozzle. Increasing the feed temperature will probably overcome this detrimental factor to some extent. The decrease in average droplet and particle size at higher feed temperatures will undoubtedly contribute to the higher drying rates.

It was not the purpose of the experimental investigation on atomization to vindicate the validity of the Nukiyama and Tanasawa equations. There exists a distinct possibility that they do not accurately represent the absolute variations in droplet size with the operating conditions. As a matter of fact, such discrepancies appear to be indicated by the disparity between the average droplet diameter, D_o, and the corresponding particle diameter, D_p. However, in view of the supporting work of Smith and co-workers (101), the general trends of behavior seem to be correctly followed. This is further supported by inspection of figures 17 and 18, which show the variation of D_o with the compressed air pressure and the inlet feed temperature. The results merely confirm the well-known fact that in two-fluid nozzles increased air pressures and increased temperatures will cause finer atomization. Of greater interest, however, is the fact that working at a fixed feed rate, maximum capacity was consistently exceeded until

a definite pressure was reached, in spite of the fact that the average droplet diameter, D_o, had reached a minimum at lower pressures, where wetting of the walls was still observed. This is clearly indicated by the values shown in Table IX, page 94. This highlights the essential weakness of conclusions based on the value of the average diameter alone, and indicates that the distribution of the various droplet sizes about this average is of prime importance. This fact was implied in Edeling's work (44, 45), which showed that, beyond a certain point, an increase in air pressure merely narrowed the distribution and did not further decrease the average diameter.

Atomization of Lignosol solutions showed identical behavior as far as the droplet diameter is concerned. That the rate of liquid feed - keeping the air rate to the nozzle constant - also exerts an influence on the droplet, is shown by the results on D_o, in Tables XII and XIV. In addition, figure 19 indicates that under identical spray drying conditions, the larger initial droplet will give the larger dried particle. Two important conclusions can be deduced from this fact: under identical drying conditions, variations in particle diameters will closely reflect variations in droplet diameters; secondly, everything else being constant, perturbances in the formation of the dried particles such as surface checking, shrinking, case-hardening, expansion, bursting, etc. will occur to the same extent, irrespective of the initial droplet diameter. This is no longer the case where any of the operating conditions are varied, as shown by figures 20, 21 and 22. Since all these perturbances occur solely in the falling-rate period, prediction of the final value of the average particle diameter, D_p, can only be made if a knowledge

of the specific processes taking place during this brief period has been previously obtained. It is logical to assume that such knowledge is largely empirical. For example, according to figure 20, parallel increases in particle and droplet sizes are observed with an increased drying air temperature up to a point, beyond which the droplet size decreases but the particle size continues to expand. In figure 21, progressive expansion of the dried particle occurs as the inlet feed temperature is increased, while in figure 22 a progressive shrinking is observed at higher volumetric drying air rates.

For convenience of presentation, the particle size, which is really the most important single physical property of a spray dried product, was discussed with atomization. The next most important physical property is undoubtedly the bulk density. From theoretical considerations, bulk density should be a function of both particle size and effective particle density. The same element of uncertainty, which was previously observed in the prediction of particle size from droplet size owing to perturbances occurring during the falling rate period, is again experienced when an attempt is made to predict bulk density from particle size, and very probably due to the same reasons. It is quite apparent from the results in Table XVI, that when a single operating condition is varied, a decrease in particle diameter invariably results in an increased bulk density. However, such an absolute relationship is not exhibited when results from various sets of runs are compared. It is evident that the second factor affecting bulk density, namely the effective particle density, comes into play in this case, depending on whether shrinking or expanding occurs.

Throughout this investigation, calculations of efficiency were based on equation (19) page 43, which defines the Drying Thermal Efficiency. Use could, of course, have been made of equation (20), page 44, which defines the Heat Economy of the Drying Chamber, but comparison between the two equations shows that, although the absolute values would differ, the trends would be identical. An attempt was made to compare the efficiency of the unit used in the present investigation with published performance data whenever the necessary information was available. Recalculated on the basis of the Heat Economy equation, Fogler and Kleinschmidt (57) report values ranging from 45.6 to 58.7% on water sprayed at 212°F, and from 38.3 to 45.8% for a 10% solution of an organic material. Woodcock and Tessier (154) report a Heat Economy of 53.4%. These figures can be compared with corresponding values of 74.3% for water and 34.6% for Lignosol, obtained under similar conditions in this investigation.

On the basis of the experimental evidence presented, it is difficult to derive the mathematical relations necessary for the formulation of a fundamental theory of design. Although a step in the right direction has probably been taken, further work appears to be definitely needed.

BIBLIOGRAPHY

1. Alford, E. C., Chem. and Met. Eng., 41: No. 12, 634-6, 1934
2. American Dry Milk Institute Inc., Bull. 911, No. 6, 1948
3. Anon., Chem. Eng., 55: No. 3, 127-34, 1948
4. Anon., Chem. and Met. Eng., 33: 157-9, 1926
5. Anon., Chem. Inds., 62: 759, 1948
6. Anon., Ry. Mech. Engrs., 123: No. 8, 458-60, 1949
7. Antoni., A., Ge'nie Civil, 110: 417-20, 433-7, 1937
8. Antoni., A., Chem. Eng. Congr. World Power Conf., 1936
9. Avery, J. M. and Evans, R. F., Chem. and Met. Eng., 52: No. 4, 94-6, 1945
10. Beeton, F. E. and Trufood Ltd., British, 169,471, 1921
11. Bergh, F. P., Loebinger, H. J., Neuberger, H. C., U.S. 997,950, 1911
12. Bergolits, M. Kh., Farmatsiya, 8: No. 3, 15-8, 1945
13. Bergsfi, C., Mfg. Chemist, 20: 72-75, 1949
14. Berti, C., Soap Sanit. Chemicals, 23: No. 5, 38-40, 1947
15. Bevenot, P., British, 28: 767, 1906
16. Biddle, S. B. and Klein, A., Proc. Am. Soc. Testing Mats., Vol. 36: Part II, pp. 310-311, 1934
17. Blaine, R. L., A.S.T.M. Bull., No. 108, 1941
18. Blake, L. D., J. Soc. Chem. Ind., 68: 138, 1949
19. Booth, H. C., Baker, J. L. and Solac Ltd., British 109,471, 1917
20. Bowen, W. S., Ind.Eng. Chem., 30: 1001, 1938
21. Bowen, W. S., U.S. 2,081,909, 1934
22. Bradley, C. E. and Coffin, J. G., U.S. 1,428,526, 1927
23. Buhler, C. R., Seifensieder Ztg. 69, 90-2, 1942
24. Bullock, K. and Lightbran, J. N., Quart. J. Pharm., 16: 213-21, 1943

25. Burkhart, W. H. and Marceau, E. T., U.S. 2,152,788, 1939

26. Burton, W. G., J. Soc. Chem. Ind., 63, 213-15, 1949

27. Calbeck, J. H. and Hainer, H. R., Ind. Eng. Chem., 19: 58, 1927

28. Carman, P. C., J. Chem. Soc. S. Afr., 40: 142, 1940

29. Carr, O., U.S. 1,321,362, 1919

30. Ibid., 1,405,756, 1922

31. Carr, R. H. and Schild, G., Food Industries, 16: 809-14, 1944

32. Castleman, R. A., Jr., Bur. Standards J. Research, 6: 369, 1931

33. Chilton, T. H. and Colburn, A. P., Ind. Eng. Chem., 26: 1183, 1934

34. Crane, Technical Paper, No. M-409, 1942

35. D'Ans, Paul, Chem. App., 28: 49-52, 1941

36. D'Ans, Paul, Fette U Seifen, 545-8, 1940

37. Datin, R. C., U.S. 2,280,895, Apr. 28, 1942

38. De Haas, T. K., Chem. Weekbl., 45: 330-333, 1949

39. Denton, A., et al, J. Nutrition, 28: 421-6, 1944

40. Diamond, G. B., Unpublished Thesis, Some Factors Affecting the Capacity and Efficiency of a Spray Drying Unit, M. Eng., McGill University, 1948

41. Dickerson, W. H., U.S. 1,396,028; 1,397,039, 1921

42. Ibid., U.S. 1,600,503, 1926

43. Douthitt, F. H. and Gray, C. E., U.S. 1,797,055, 1931

44. Edeling, C., Angew Chem. Beihefte, 57: 1-54, 1949

45. Edeling, C., Chem. Ing. Tech., 21: 137-8, 1949

46. Edeling, C., Milchwissen Schaft 1/2, 88-95, 1947

47. Edgerton, L. B., U.S. 1,198,203, 1916

48. Enoksson, B., Nature, 61: 934, 1948

49. Faber, H. A., U.S. 2,237,482, 1941

50. Fairs, G. L., Trans. Soc. Chem. Ind., 62: 374, 1943

51. Farmer, E. H. and Six, C. G., Mfg. Chemist, XVIII-2, 67, 1947

52. Ferris, C. R. and Carte, E. T., U.S. 2,187,877, 1940

53. Fisher, N. C., U.S. 2,292,512, 1942

54. Fleisher, W. L., U.S. 1,497,168, 1,512,461, 1924

55. Fleming, R. S., U.S. 1,361,238-9, 1920

56. Fleuriel, P. M., U.S. 2,356,758, 1944

57. Fogler, B. B. and Kleinschmidt, R. V., Ind. Eng. Chem., 30: 1372, 1938

58. Friedman, S. J., Ind. Eng. Chem., 42: 1950

59. Ibid., Ind. Eng. Chem., 41: 1949

60. Ibid., Ind. Eng. Chem., 40: 1948

61. Ibid., Ind. Eng. Chem., 39: 1947

62. Ibid., Ind. Eng. Chem., 38: 1946

63. Gere, W. B., U.S. 1,188,755, 1916

64. Gensecke, W. and Ebner, K., Ger. 722,282, 1942

65. Gordon, C., Chem. Eng. Progress, 45: 477-481, 1949

66. Gerhold, C. G. and Mekler, L. A., U.S. 2,467,470, 1949

67. Gray, C. E. and Jensen, A., U.S. 1,078,848, 1913

68. Gray, C. E., U.S. 1,107,784, 1914

69. Greene, J. W., et al, Chem. Eng. Progress, 44: 591-60, 1948

70. Gruber, M. F., U.S. 2,235,459, 1944

71. Hall, J. M., U.S. 2,469,553, 1949

72. Ibid., U.S. 2,361,940, 1944

73. Hawksley, P. G. W., Brit. Coal Utilization Research Assoc. Bull., 245-57, 1944

74. Hemig, F. J., U.S. 1,214,160, 1917

75. Herman, A., Iszak, J. A. and Bercuson, N., Can. Chem. Process Inds., 33: 211-12, 1949

76. Hinkley, W. O., Ind. Eng. Chem., (Anal. Ed.) 14: 10, 1942

77. Hinze, J. O., Milborn, H., Am. Soc. Mech. Engrs. Meeting, San Francisco, Calif., June 27-30, 1949

78. Holliday, R. L., U.S. 1,621,506, 1927

79. Holmes, H. N., Laboratory Manual of Colloid Chemistry, 2nd. ed., John Wiley and Sons, New York

80. Houghton, H. G., in J. H. Perry's Chem. Eng. Hbk., 2nd. ed., pp. 1984-1993, N.Y., McGraw-Hill Book Co., 1941

81. Hunkel, L., Chem. App., 24: 197-9, 1937

82. Ingram, J. C., U.S. 1,472,472-3, 1923

83. Jebson, G. and Finkenhagen, C., U.S. 1,074,264, 1913

84. Johnstone, Trans. Am. Inst. Chem. Eng., 37: 95-133, 1941

85. Jones, A. B., U.S. 2,249,960, 1942

86. Kesper, J. F., Chem. App., 26: 353, 1939

87. Kleinschmidt, R. V., Chem. and Met. Eng., 46: 487, 1939

88. Kleinschmidt, R. V., in J. H. Perry's Chem. Eng. Hbk., 2nd ed., pp. 1983-4, New York, McGraw-Hill Book Co., 1941

89. Knapp, R. T., Ind. Eng. Chem. (Anal. Ed.) 6: 66, 1934

90. Komline, T. K., Sewage Works J., 19: 806-810, 1947

91. Kording, F., Schwen, G., Ulrich, H., Ger. 696,674, Aug. 29, 1940

92. Ladisch, R., Chem. Ztg., 156-9, 1942

93. Lamont, C. A., U.S. 51,263, 1865

94. Lamont, O. R., U.S. 1,734,260, 1929

95. Lapple, C. E., Heating, Piping, Air Conditioning, 16: 578-81, 1944

96. Lawrence, W. J. and Dreshfield, A. C., U.S. 2,215,183, 1940

97. Lee, D. W., Natl. Advisory Comm. Aeronaut., Rept. 425, 1932

98. Leo, H. T. and Taylor, C. C., U.S. 2,367,789, 1945

99. Lewis, H., Ind. Chemist, 10: 439-41, 499-501, 1934

100. Ibid., Ind. Chemist, 11: 77-75, 1935

101. Lewis, H. D., Edwards, D. G., et al, Ind. Eng. Chem., 40: 67, 1948

102. Luring, W., U.S. 890,078, 1908

103. Ibid., U.S. 940,398, 1909

104. MacLachlan, J. C., U.S. 1,301,288, 1919

105. Ibid., U.S. 1,394,035, 1921

106. MacTaggart, E. F., Trans. Inst. Chem. Engrs. (London), 117, 1949

107. Mailatt, C. D. and Dickerson, W. H., U.S. 1,678,505, 1929

108. Maisel, D. S. and Sherwood, T. K., M.I.T., unpublished paper, "Evaporation of Liquids into Turbulent Gas Streams", 1949

109. Ibid., "The Effect of Air Turbulence on the Rate of Evaporation of Water", 1949

110. McLaughlin, W. B., U.S. 1,090,740, 1913

111. Meinesz, Age, Dutch 51,332, 1941

112. Merrell, I. S. and Merrell, O. E., U.S. 1,183,393, 1916

113. Merrell, L. C., Merrell, I. S., Gere, W. B., U.S. 860,929, 1907

114. Mertens, A., U.S. 2,308,992, 1943

115. Moon, C. B. O., Soap Perfumery and Cosmetics 20: 573-5, 1947

116. Mosher, P. R., U.S. 2,376,497, 1945

117. Murdock, S. B., U.S. 1,484,271, 1924

118. Myers, S. L., Rock Products, 44: 56, 1941

119. Natuss-Andreev, V. A., U.S.S.R., 68: 537, 1947

120. Nukiyama, S. and Tanasawa, Y., Trans. Soc. Mech. Engrs. (Japan) 4: No. 14, 86, 1938

121. Ibid., 4: No. 15, 138, 1938

122. Ibid., 5: No. 18, 63, 68, 1939

123. Ibid., 6: No. 22, II-7, 1940

124. Ibid., 6: No. 23, II-8, 1940

125. Nyrop, J. G., Austria, 109,733, 1940

126. Osborne, W. S., U.S. 962,781, 1910

127. Peebles, D. P., U.S. 1,914,895, 1933

128. Percy, S., U.S. 125,406, 1872

129. Perry, J. H., Chemical Engineers Handbook, 2nd ed., McGraw-Hill Book Co., N.Y., 1941

130. Philip, T. B., Trans. Inst. Chem. Engrs. (London), 13: 107-20, 1935

131. Power, Chem. Eng. Mining Review, 20: 201, 1928

132. Prokofiev, P. and Solonauts O., Farmatsiya 14: No. 8, 22, 1941

133. Reavell, B. N., Soap Perfumery Cosmetics 17: 816-18, 1944

134. Reavell, J. A., Chem. and Ind., 618-21, 1937

135. Reavell, J. A., J. Soc. Chem. Ind., 46: 925-51, 1927

136. Reavell, J. A., British 503,737, 1939

137. Richardson, E. G., J. Phys. Soc., 55: 48, 1943

138. Ridgway, J. W., Baldyge, W. V., Scarba, M., Proc. 3rd, Ind. Waste Conf. Purdue Univ. Eng. Bull. Ext. Ser. No. 64, 128-37, 1947

139. Romer, J. B., Proc. A.S.T.M. 41: 1152, 1941

140. Sauter, J., Forschungs Arbeiten auf dem Gebiete des Ingenieurwesens, No. 313, 1928

141. Sauter, J., Forsch. Gebiete Ingenieurw, No. 297, 1926

142. Ibid., No. 312, 1928

143. Schambra, W. P., Trans. Am. Inst. Chem. Engrs., 41: 35-50, 1945

144. Six, G. J. and Six, C. J., British 565,476, 1944

145. Smith, D. A., Meeting Am. Inst. Chem. Engrs., Montreal, Oct. 1949

146. Smola, A., Ost Chem. Ztg., 49: 198-205, 1948

147. Stauf, R., U.S. 666,711, 1901

148. Stewart, E. S., Chem. and Met. Eng., 35: 470-72, 1928

149. Stutzke, R. W. G., U.S. 1,215,889, 1917

150. Torsten, R., U.S. 2,343,027, 1944

151. Waite, R., Chem. and Ind., 659-61, 1940

152. Walton, W. H. andPrewett, W. C., Proc. Phys. Soc. 62B, No. 354, PT 6, 341-50, 1949

153. Williams, C. G., Sc.D. Thesis in Chem. Eng., Mass. Inst. Tech., 1949

154. Woodcock and Tessier, Can. J. Research, 21A: 75-8, 1943

155. Zenzes, A. M. and Schloessinger, Wm., U.S. 2,432,222, 1947

156. Ziginia, P. T. and McKenna, T. L., U.S. 2,154,000, 1939